Removal and Recovery of Nutrients by Ion Exchange from Water and Wastewater

By

Monami Das Gupta

A thesis submitted to fulfilment
of the requirements for the degree of
Master of Engineering

University of Technology, Sydney
Faculty of Engineering

June, 2011

CERTIFICATE

I certify that this thesis has not already been submitted for any degree and is not being submitted as part of candidature for any other degree.

I also certify that the thesis has been written by me and that any help that I have received in preparing this thesis, and all sources used, have been acknowledged in this thesis.

Signature of Candidate

.....

Monami Das Gupta
June 2011

Acknowledgement

Ashim Das Gupta, Mala Das Gupta, and Monica Das Gupta for their unconditional love and support (forever and always)

Prof. Vigneswaran and Prof. Loga for all their guidance

Melanie, Bryan, Christine, Johir, Chinu, Megha, Mimi N., Ben, Karan, Ahad, Mahesh, Arjun, Melissa, Phil B., Phil vH, Dean, Belinda, Lipola, Cristein, Stephanus, Linh, Thamer, Yousef, Thanh, Wendy, Suk, Sherub, Javeed, Ganesh, Prof. Hao, Dr. Shon and Van for their endless support and encouragement

My extended family, for always being there for me and supporting my dreams and ambitions

Thank you

for making this journey a very memorable and enjoyable one

Table of Contents

List of Tables

Table of Figures

Nomenclature

BPR = biological phosphate removal

BV = bed volumes

Cl^- = chloride

CO_3^{2-} = carbonate

COD = chemical oxygen demand

CR = chemical reduction

Fe^{3+} = iron (III)

g/L = gram per litre

$H_2PO_4^-$ = dihydrogen phosphate ion

HAIX = hybrid anion exchanger

HCl = hydrochloric acid

HCO_3^- = bicarbonate

HFO = hydrated ferric oxide

HPO_4^{2-} = monohydrogen phosphate ion

hr = hours

LDHs = layered double hydroxides

MBR = membrane bioreactor

mg N/L = milligram nitrogen per litre

mg NO_3^- / L = mg nitrate per litre

mg P/L = milligram phosphorus per litre

mg PO_4^{3-} / g = mg phosphate per gram

mg/L = milligram per litre

min = minutes

mL/min = millilitre per minute

mM = milli Molar

N = nitrogen

NaCl = sodium chloride

NaOH = sodium hydroxide

Nitrate-N = N in the form of nitrate

Nitrite-N= N in the form of nitrite

nm = nanometre

NO_3^- = nitrate

oyster-zeolite = resin with crushed oyster shells

P = phosphorus

pH = measure of the acidity or basicity of an aqueous solution

ppm = parts per million

Purolite (A500PS) = used in the decolourisation of sugar syrups

Purolite (A520E) =Purolite (nitrate selective)

SO_4^{2-} = sulphate

Ti^{4+} = titanium (IV)

TiO_2 = titanium dioxide

U = uranium

U(IV) = uranium (IV)

UCT = University of Cape Town-type process

VFA = volatile fatty acids

zeolite = an aluminosilicate mineral

Zr^{4+} = zirconium (IV)

Abstract

In this study, a fixed bed ion exchange system for nutrient removal and recovery for water and waste water was developed and tested for nitrate and phosphate. A post-treatment consisting of a fixed bed bed ion-exchange system with a Purolite and an HFO column in series and individually was used to remove and recover nitrate and phosphate from synthetic water and wastewater. The efficiency of the ion exchange materials incorporated into the anthracite matrix at 1, 3, 5 and 10%, in their ability to remove and recover these nutrients was investigated. Another ion exchange material, HAIX, was also investigated for the removal and recovery of nitrate and phosphate. Also, the study considered regeneration and reuse of the ion exchange media in order to see how long the system can effectively remove and recover nitrate and phosphate before saturation. Purolite was found to exhibit a higher capacity for the removal of nitrate than for phosphate. HFO was found to exhibit a higher capacity for the removal of phosphate than for nitrate. Both these media were required in series to remove both nitrate and phosphate. Increase in dose of the two ion exchange materials incurred an increased in removal efficiency of nitrate and phosphate. However, the selectivity of Purolite for nitrate and HFO for phosphate decreased with increase percentage by mass of the ion exchanger in the anthracite matrix. Regeneration was undertaken using a distilled water wash as well as 3% NaCl wash. It was found that NaCl successfully regenerated the exhausted media for reuse. Distilled water wash was not a successful medium for regeneration. A column experiment was also conducted with MBR effluent to investigate the possibility of removing the nitrate and phosphate. Both N and P in the MBR effluent were found in different forms (as NH_4 – N, organic N, inorganic and organic phosphorus). Other competing anions like Cl^- and SO_4^{2-} were also present in the feed. Despite the different forms of N and P as well as competing anions, the Purolite and HFO in series system still had a removal efficiency of 87-100%. The column was able to remove almost 100% of nitrate and phosphate in the effluent. The Langmuir, Freundlich and Sips isotherm models were used to model the equilibrium isotherm of nitrate and phosphate removal by Purolite (A500PS), HAIX and HFO. The results show that the experimental data satisfactorily fitted to all three models. The kinetic data for the adsorption of both nitrate and phosphate were satisfactorily described by the Ho model. The fit for phosphate on HFO was less satisfactory than the other adsorbents.

1. Introduction

Throughout recent decades, the wastewater treatment industry has identified the discharge of nutrients, especially nitrates and phosphates, into waterways as a risk to natural environments due to their serious effects on eutrophication.

Nutrients are derived from point sources and non-point (or diffuse) sources. Point-sources of nutrients are more important in areas with large population densities or with significant coastal tourism, and may include:

- industrial outfalls (including those from sewage treatment works);
- wastes from aquaculture production; and
- effluents from ships, yachts & boats (OzCoasts 2010).

Non-point sources of nutrients are usually of greater concern than point sources because they tend to be larger and more difficult to control. Important nonpoint sources of nutrients include:

- runoff from agricultural areas; and
- urban stormwater (OzCoasts 2010).

Eutrophication is a major national and international problem because it can lead to:

- an increase in the frequency of harmful algal blooms, shellfish contamination, anoxic and hypoxic events and fish kills;
- a loss of ecosystem integrity, aquaculture production, fish stocks and amenity value; and
- changes in biodiversity (OzCoasts 2010).

Contamination of ground water with nitrate is a serious problem in many places throughout the world. Nitrate is potentially harmful to human health, causing conditions such as blue-baby syndrome, and is considered a carcinogen (Wang, Kmiya & Okuhara 2007). The removal of nitrate is essential for water contaminated with nitrate before being utilised since a large amount of nitrate in drinking water often causes a disease called methemoglobinemia and other health disorders such as hypertension, increased infant mortality, goiter, stomach cancer, thyroid disorder, cytogenetic defects and birth defects (Ayyasamy et al. 2007).

Consequently, new tertiary treatment processes have developed, commonly

utilising physico–chemical and biological methods to remove nutrients from secondary wastewaters (Blaney, Cinar & SenGupta 2007). The traditional method used for nitrate removal is biological treatment (nitrification/denitrification). This process is very effective for the removal of nitrate; however it may fail to obtain the required effluent quality when exposed to peak and variable organic loads. The disadvantages of such methods include larger reactor volumes, high operating costs, and waste sludge production. Furthermore, complete nutrient removal is not feasible due to thermodynamic and kinetic limitations. Another major problem in biological methods used for nitrate removal from water is that secondary treatment is still required for bacterial removal (Ayyasamy et al. 2007).

Physical and chemical processes such as reverse osmosis, electrodialysis and chemical denitrification have been developed for nitrate removal from water. Although these techniques are effective in removing nitrate from contaminated water, they are very expensive for pilot scale operation with a limited potential application (Ayyasamy et al. 2007).

Phosphorus is a key nutrient that stimulates the growth of algae and other photosynthetic microorganisms such as toxic cyanobacteria (blue-green algae), and must be removed from wastewater to avoid eutrophication in aquatic water systems (Conley et al. 2009). The risk of adverse effects to the plant and animal communities in waterways declines as phosphate concentrations approach background levels. Around the world, there has been a growing awareness of the need to control phosphorus emissions. This is reflected in many countries adopting increasingly stringent regulations, which made phosphorus removal more widely employed in wastewater treatment (Oehmen et al. 2007).

Currently, there are a variety of techniques recommended for phosphate removal, which can be basically classified as chemical precipitation by using ferric or aluminium salts (Sherwood & Qualls 2001; Clark, Stephenson & Pearce 1997), biological removal (Oehmen et al. 2007; Van Loosdrecht et al. 1997), and adsorption (Oehmen et al. 2007; de Vicente et al. 2008). Although biological process is environmentally friendly, it is not capable of removing phosphorus below a particular concentration if there is a lack of easily biodegradable organic carbon present in the

wastewater. Chemical precipitation and biological processes have been widely used for phosphate removal from industrial effluents (Wang et al. 2005). However, it is still technically difficult and economically impractical for both techniques to enhance phosphate removal in order to meet increasingly strict regulations on phosphate discharge (Pan et al. 2009). In addition, the precipitation and biological treatment techniques are sensitive to seasonal and diurnal variations in temperature and changes in feed concentrations (Onyango et al. 2007).

Nitrate and phosphate can both be successfully removed by physico-chemical processes such as ion exchange (Blaney, Cinar & SenGupta 2007; Onyango et al. 2007). This method offers various advantages, including the ability to handle shock loadings and operate over a wider range of temperatures as well as operation simplicity and low operation cost. Ion exchange/sorption processes using selective ion exchange media is ideal for the reduction of nitrates and phosphates to near-zero levels provided that the adsorbent is nitrate and/or phosphate selective, cost effective and amenable to efficient regeneration and reuse (Blaney, Cinar & SenGupta 2007).

1.1. Aim and Scope of Study

The objective of this research was to develop a fixed bed ion exchange system for nutrient removal and recovery, mainly nitrate and phosphate from wastewater. In order to achieve this, a post-treatment consisting of a fixed bed ion-exchange system with two ion exchange media individually and in series was used to remove nitrate and phosphate. The study investigated the efficiency of the ion exchange materials in their ability to remove nitrate and phosphate. Also, the investigation considered regeneration and reuse of the ion exchange media in order to see how long the system can effectively remove and recover nitrate and phosphate before saturation.

The scope of this research entailed utilising three ion exchange media, hydrated ferric oxide (HFO), Purolite and hybrid anion exchanger (HAIX), to remove and recover nitrate and phosphate from synthetic wastewater with concentrations 50 mg N/L and 15 mg P/L, respectively. Purolite was selected because of its affinity for nitrate removal. HFO was selected because of its selectivity for phosphate removal. Batch equilibrium and kinetics studies were undertaken with all three ion exchange media to

determine the exchange capacity and rates of exchange. Modelling of experimental data was undertaken using Langmuir, Freundlich and Sips isotherm for equilibrium data as well as the Ho model for kinetics data. Removal efficiency of nutrients from a MBR effluent containing lower concentration of nutrients (10 - 13 mg N/L and 5 - 6 mg P/L) was also investigated.

2. Literature Review

The presence of trace amounts of nitrate and phosphate in the treated wastewater from municipalities and industries is often responsible for eutrophication. Eutrophication is the excess of nutrients (mainly nitrates and phosphates) and associated effects such as rapid growth of blue-green algae and hyacinth-like plants, which leads to short and long term environmental and aesthetic problems in lakes, coastal areas, and other confined water bodies (Zhao & Sengupta 1998). Consequently, new tertiary treatment processes have been developed to remove nutrients from water and wastewater.

Phosphorus is a primary ingredient in fertilisers used in agriculture to increase productivity. It is also found in detergents and pesticides. All these sources increase phosphorus concentrations in the aqueous environment and lead to the production of algal bloom. This is caused by phosphorus enriched conditions, allowing greater nitrogen uptake which brings about an increase of algae growth. Concerns regarding eutrophication led to the development of technologies for phosphorus removal in the 1950s (Streat, Hellgardt & Newton 2008b).

Furthermore, estimates of phosphate resources predict that they may be exhausted in as little as several decades (Martin, Parsons & Jefferson 2009). The substantial rise in the price of phosphorus based fertiliser in 2008, signifying that sustainable use of this valuable and finite resource is becoming increasingly critical. An ideal solution to this problem would therefore be a technique that can both remove phosphorus from wastewater streams and recover it as a useful product, such as a fertiliser (Martin, Parsons & Jefferson 2009).

Nitrate contamination of surface and groundwater is an increasingly important problem worldwide. Although nitrate is found in most of the natural waters at moderate concentrations, elevated levels in ground water mainly result from human and animal wastes, and excessive use of chemical fertilisers (Samatya et al. 2006a). The other most widespread sources of nitrate are uncontrolled on-land discharges of municipal and industrial wastewaters, run off septic tanks, processed food, dairy and meat products and decomposition of decaying organic matter buried into ground (Samatya et al. 2006a). These fertilisers and wastes are sources of nitrogen-containing compounds which are converted to nitrates in the soil. Nitrates are extremely soluble in water and can move easily through soil into the drinking water supply (Samatya et al. 2006a).

Excess of nitrate can cause several environmental problems and because of this the Australian Drinking Water Guideline has stipulated a limit of 50 mg nitrate/L in drinking water (National Health and Medical Research Council, Australian Government 2009). The effect of nitrate itself is described as primary toxicity. Its high intake causes abdominal pains, vomiting, diarrhoea, hypertension, increased infant mortality, central nervous system birth defects, spontaneous abortions, diabetes, respiratory tract infections, and changes to the immune system (Lohumi et al. 2004). Secondary toxicity of nitrate arises from microbial reductions of nitrate to the reactive nitrite ion by intestinal bacteria. Nitrate has been implicated in methemoglobinemia, especially to infants under six month of age (Lohumi et al. 2004). Methemoglobin (MetHb) is formed when nitrite (formed from the endogenous bacterial conversion of nitrate from drinking water) oxidises the ferrous iron in hemoglobin to the ferric form. MetHb cannot bind oxygen, and the condition of methemoglobinemia is characterised by cyanosis, stupor, and cerebral anoxia. Symptoms include an unusual bluish gray or brownish gray skin colour, irritability, and excessive crying in children with moderate MetHb levels and drowsiness and lethargy at higher levels (Fewtrell 2004). Therefore, it is vital to develop a system to remove and recover nitrate from wastewater due to the harmful environmental and physiological effects it possesses.

The following sections will describe the different treatment options available for nutrient removal, mainly nitrate and phosphate. These options will be discussed in full detail and comparisons made with ion exchange as a viable option for nutrient recovery.

2.1. Biological Nutrient Removal

The traditional method used for nitrogen and phosphorus removal is biological treatment (nitrification/denitrification). Although this process is very effective for the removal of nitrogen, it may fail to achieve the required effluent quality when exposed to peak and variable organic loads (Van Loosdrecht et al. 1997). Other disadvantages are the need for larger reactor volumes, higher operating costs, and waste sludge production when phosphorus removal is achieved by chemical precipitation (Morse et al. 1998). Phosphorus can also be removed by biological processes and although this process is environmentally friendly, one cannot remove phosphorus below a particular concentration if there is a lack of easily biodegradable organic carbon present in the wastewater (Van Loosdrecht et al. 1997).

2.1.1. Biological nitrate removal

Biological denitrification is an efficient process for nitrogen removal from wastewater in which heterotrophic bacteria in the absence of oxygen (anaerobic conditions) convert nitrate-N and nitrite-N to nitrogen gas (Prosnansky, Sakakibara & Kuroda 2002; van Rijn, Tal & Schreier 2006). The process requires sufficient organic carbon as an electron donor for complete nitrate removal (Cambardella et al. 1999; Greenan et al. 2006; Healy, Rodgers & Mulqueen 2006). Methanol, ethanol, and acetic acid are commonly used as organic carbon sources for denitrification processes to enhance denitrification activity in organic carbon-limited wastewaters (Menasveta et al. 2001; Killingstad, Widdowson & Smith 2002; Suzuki et al. 2003). The optimum C/N ratio required for complete nitrate reduction to nitrogen gas by denitrifying bacteria depends on the nature of the carbon source and the bacterial species present (van Rijn, Tal & Schreier 2006; Chiu & Chung 2003).

The availability of the organic carbon for denitrification is an important factor that controls the denitrification performance (Tan & Ng 2008). A wide range of chemical oxygen demand (NO_3^-) values have been reported in the literature for complete denitrification (Carucci et al. 1996; Tseng, Potter & Koopman 1998). Tam et al. (1994) reported an optimal biological oxygen demand ratio of 2.48 for denitrification using methanol and acetic acid as the carbon source. The cost of these carbon sources is a major part of total treatment cost. Thus, waste carbon sources such as industrial effluents have been suggested as alternatives (Sage, Daufin & Gésan-Guiziou 2006). However, low carbon availability in some industrial effluents has led to incomplete denitrification and accumulation of denitrification intermediates such as nitrite, nitric oxide and nitrous oxide (Chiu & Chung 2003; Kim et al. 2002).

Nitrate removal rates reported by researchers depend on operational parameters, such as system configuration, types of organic carbon source, redox states of the reactors and the ambient nitrate concentration at which the various reactors were operated (van Rijn, Tal & Schreier 2006; Park, Craggs & Sukias 2008).

2.1.2. Biological phosphate removal

In biological phosphate removal (BPR) processes, certain types of bacteria are

used to remove phosphates from water and store them in bacteria cells. This is dependent on the accumulation of bacteria that are capable of storing large amounts of polyphosphate in their cells (Marais, Loewenthal & Siebritz 1983). These organisms can accumulate about 12% phosphorus on a dry-weight basis, compared to 1% to 3% for normal bacteria. This signifies that the efficiency of the process is directly tied to the formation of polyphosphate-accumulating bacteria. Therefore, for effluent BPR processes, the incoming wastewater needs to be mixed with the sludge in a true anaerobic zone, which entails that no oxygen or nitrate is present (Van Loosdrecht et al. 1997). This zone includes a layer of sludge, which forms from the solids that settle out of the wastewater. Here, wastewater is treated by anaerobic bacteria, microscopic organisms, such as certain protozoa, and sludge worms, all of which thrive in anaerobic conditions. The oxygen in the aerobic zone makes conditions favourable for aerobic bacteria. Both aerobic and anaerobic bacteria are very important to the wastewater treatment process and to each other. Bacteria treat wastewater by converting it into other substances. Aerobic bacteria convert wastes into carbon dioxide, ammonia, and phosphates, which, in turn, are used by the algae as food. Anaerobic bacteria convert substances in wastewater to gases, such as hydrogen sulphide, ammonia, and methane. Many of these by-products are then used as food by both the aerobic bacteria and algae.

In the anaerobic zone, volatile fatty acids (VFA) present in the wastewater, or formed by fermentation processes, can be accumulated by polyphosphate-accumulating bacteria. With a lot of VFA for food and low levels of dissolved oxygen and nitrite, phosphorus accumulating bacteria release phosphate from their cells so they can take up more food (Sydney Water 2010).

In several cases the ratio of chemical oxygen demand to phosphate in the influent is too low to produce enough biomass for polyphosphate storage. The biomass production is frequently lowered because sludge age (low growth rate and thus low net biomass yield) is prolonged to support the growth of nitrifying bacteria (Van Loosdrecht et al. 1997).

An adequate design of the anaerobic phase is therefore essential for an efficient BPR process and will depend greatly on the characteristics of the wastewater. Sewage from anaerobic sewers will already be partially fermented into VFA, thus small anaerobic reactors can be applied. With aerobic sewers, for example, the wastewater does not contain VFA and the anaerobic phase has to be based on the slower

fermentation process. This requires a larger anaerobic reactor. The length of the aerobic phase in the treatment process will usually be limited by the nitrification, as a result of the slower growth rate of nitrifying bacteria. It is not usually limited by the phosphate uptake by the nitrifying bacteria (Van Loosdrecht et al. 1997).

There are various BPR process configurations. A basic scheme for a biological phosphate removal process is shown in Figure 2-1 (Van Loosdrecht et al. 1997).

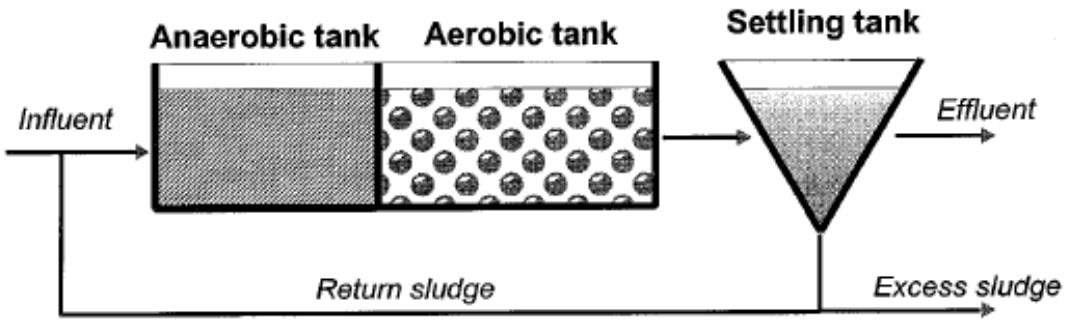

Figure 2-1: A schematic representation of a BPR process (Van Loosdrecht et al. 1997)

2.1.3. Combined biological phosphate and nitrogen removal

Biological phosphate and nitrogen removal requires unfavourable conditions with respect to sludge age (Van Loosdrecht et al. 1997). The biomass production is frequently lowered because sludge age (low growth rate and thus low net biomass yield) is prolonged to support the growth of nitrifying bacteria (Van Loosdrecht et al. 1997). Furthermore, it is usually assumed that denitrification and phosphate-removal processes compete for the same substrate. This assumption is based on the observations that, if nitrate is introduced into the anaerobic tank, the biological phosphate removal process deteriorates (Hascoet & Florentz 1985). In order to prevent the presence of nitrate in the anaerobic tank, UCT (University of Cape Town)-type processes are used, as illustrated in Figure 2-2. Here the nitrate-containing return sludge is first introduced into a denitrification reactor (shown in Figure 2-2 as the anoxic tank), after which the nitrate-free sludge/water mixture is partly recycled to the anaerobic tank.

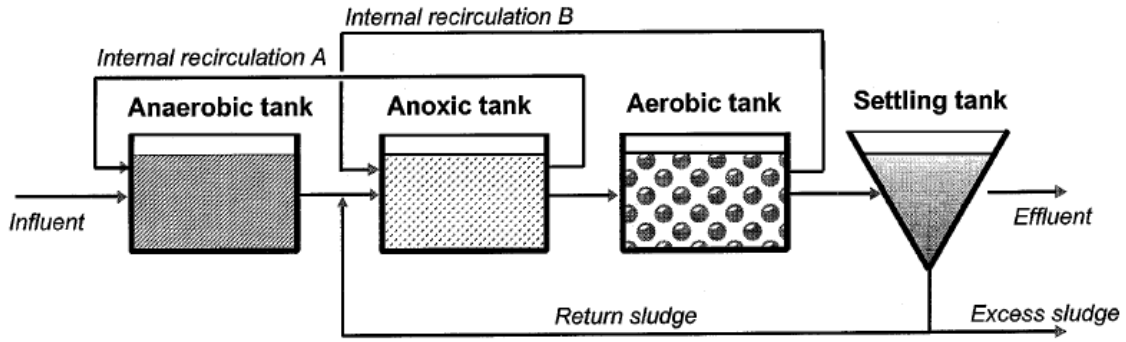

Figure 2-2: Schematic representation of a University of Cape Town-(UCT)-type process (Van Loosdrecht et al. 1997)

The negative effect of nitrate on phosphate release is attributable to direct substrate competition between heterotrophic denitrifiers and polyphosphate-accumulating bacteria. In this competition, the denitrifiers dominate (Van Loosdrecht et al. 1997). This observation along with the fact that the bacterial group responsible, Acinetobacter, cannot denitrify, produced a common interpretation that phosphate and nitrate removal are competing processes.

2.2. Chemical Nutrient Removal

2.2.1. Chemical phosphate removal

Nutrients can also be removed chemically and the main chemical process of removal is by precipitation of nutrients followed by sedimentation. The widespread use of chemical precipitation for phosphorus removal in wastewater treatment started in Switzerland during the 1950s, in response to the growing problem of eutrophication. This simple technology is now strongly established in many countries around the world (Morse et al. 1998).

Chemical precipitation is fundamentally a physico-chemical process, comprising the addition of a divalent or trivalent metal salt to wastewater, causing precipitation of an insoluble metal phosphate that is settled out by sedimentation. The most suitable metals are iron and aluminium, added as chlorides or sulphates. Lime may also be used to precipitate calcium phosphate. Anionic polymers may be used to assist solid separation (Morse et al. 1998).

Salt addition can achieve 80–95% total phosphorus removal. This results in the phosphorus reacting and precipitating with the metal salt and its disposal as sludge, to

be potentially reused in the agricultural industry.

Chemical precipitation is a very flexible approach to phosphorus removal and can be applied at several stages during wastewater treatment (Morse et al. 1998). Primary precipitation is where the chemical is dosed before primary sedimentation and phosphorus removed in primary sludge (Morse et al. 1998). Secondary (or simultaneous) precipitation is where the chemical is dosed directly to the aeration tank of an activated sludge process and phosphate removed in secondary sludge (Morse et al. 1998). Tertiary treatment is where dosing follows secondary treatment and although a high-quality effluent can be produced, this approach is not generally favoured because of high chemical costs and the creation of an additional, chemical, tertiary sludge (Morse et al. 1998).

Chemical precipitation typically produces phosphorus metal salts within the wasted sludge. When disposed to agricultural lands, it therefore has potential value as a phosphorus fertiliser, although research on their bioavailability is inconclusive (Morse et al. 1998). This uncertainty has contributed to the desire to develop alternative technologies that potentially offer a more valuable and consistent product for recycling phosphorus to agriculture and industry.

Addition of chemicals should be kept to a minimum in water treatment since there are numerous negative aspects of this practice. The counterion of the salts, usually chloride, remains in water, causing an increased salinity of surface waters. The chemical precipitate accumulates in the sludge, resulting in extra costs for treatment of the excess sludge. Furthermore, the sludge content in a treatment system is restricted to a maximum amount, which requires large treatment reactors (Van Loosdrecht et al. 1997).

2.2.2. Chemical nitrate removal

Chemical reduction (CR) of nitrate can be conducted by using various compounds, mainly hydrogen, iron, formic acid and aluminium (Della Rocca, Belgiorno & Meriç 2007). The main disadvantage of CR of nitrate is the production of ammonia, which must be removed using an additional treatment (Della Rocca, Belgiorno & Meriç 2007). Nevertheless, catalytic hydrogen reduction can be set, via a bimetallic catalyst, to produce nitrogen gas as shown in Figure 2-3.

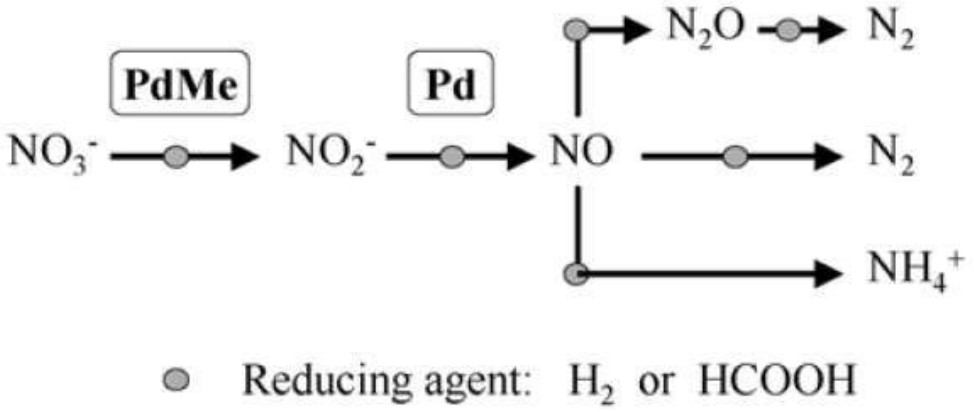

Figure 2-3: Scheme of the catalytic nitrate reduction (Della Rocca, Belgiorno & Meriç 2007)

2.3. Combination of Biological and Chemical Phosphate Removal

Removal of phosphate can be initially achieved by chemical precipitation (Fytianos, Voudrias & Raikos 1998), followed by biological methods and this combination is the usual method used to remove phosphorus at full-scale (Seida & Nakano 2002).

Removal of phosphate by chemical and biological methods requires a well-controlled addition of chemicals. If the addition of chemicals is too high, the phosphate will be fixed as a precipitate and not be available for the biological removal by the bacteria to form polyphosphate. If this polyphosphate is absent the polyphosphate-accumulating bacteria cannot accumulate the substrate under anaerobic conditions and thereby lose their competitive advantage over normal heterotrophic bacteria (Van Loosdrecht et al. 1997).

Combination of chemical and biological phosphate removal has the advantage that the biological process is highly selective. If low effluent phosphate concentrations have to be achieved a large overdose of chemicals is required. The bacteria have a very high affinity for phosphate and therefore a phosphate concentration below 0.1 mg P/L can easily be attained (Van Loosdrecht et al. 1997). However, the addition of a large dose of chemicals will result in an increased salinity of surface waters as mentioned before (Van Loosdrecht et al. 1997) and this can be toxic to most polyphosphate accumulating bacteria.

Traditional biological nutrient removal is incapable of achieving an effluent

stream of 0.1 mg P/L (Blaney, Cinar & SenGupta 2007). However, it is possible to increase chemical dose to attain this concentration, but the additional cost, sludge production, and the water industry's desire to move towards chemical free treatment makes it an undesirable option (Martin, Parsons & Jefferson 2009). An investigation into new techniques is therefore required, to enable the water industry to comply with the tighter consent limits and so protect the ecology of surface waters.

2.4. Adsorption / Ion Exchange

Nitrate and phosphate can both be effectively removed by physico-chemical processes such as ion exchange. This treatment option offers a number of advantages, which include the ability to handle shock loadings and the ability to operate over a wider range of temperatures. Ion exchange/adsorption processes using selective ion exchangers are ideal candidates for the reduction of nitrate and phosphate to near-zero levels provided that the adsorbent is nitrate and/or phosphate selective, cost effective and amenable to efficient regeneration and reuse.

Adsorption is a robust and effective technique used in water and wastewater treatments. The success of an adsorption technology depends on the selection of an appropriate adsorbent. Whilst selecting an adsorbent, the criteria commonly considered are adsorption capacity, reuse, local availability, compatibility, kinetics, and cost. Given that no single adsorbent can be isolated to meet all the required criteria, a lot of attention has thus been devoted to the development of several potential adsorbents that may suit given local conditions (Onyango et al. 2007).

The primary advantages of adsorption are that unlike chemical precipitation, no additional sludge is produced, and that no reagents are required to adjust the pH. For phosphate removal, adsorbents such as activated alumina, activated red mud (Pradhan et al. 1998) and iron oxide coated filter medium (Ayoub, Koopman & Pandya 2001) have been investigated (Streat, Hellgardt & Newton 2008b).

Ion-exchange technology has been widely used for the removal of nitrate in water (Della Rocca, Belgiorno & Meriç 2007). Ion exchange is defined as the reversible interchange of ions between a solid phase (the ion exchanger) and a solution phase (Martin, Parsons & Jefferson 2009). The ion-exchange mechanism is generally known as a result of simple electrostatic interaction, although factors such as the size, charge and nature of counterions, their hydration energy of the ions in solution, and the types of

functional groups on the ion exchanger surfaces contribute to the mechanisms. These factors significantly impact on the thermodynamics and kinetics of the exchange reactions (Gu et al. 2000). The optimal design and operation of an ion-exchange system thus require accurate knowledge of the thermodynamics and equilibria of the exchange reactions among various ions and counterions in the system. Typical approaches for acquiring these data include the measurement of multicomponent ion exchange equilibria and the development of thermodynamic models which, based on multicomponent equilibrium data, can predict multicomponent exchange reactions (Gu, Ku & Jardine 2004).

Since phosphorus occurs in final effluent wastewater streams predominantly as phosphate anions and appreciable amounts of N occurring as nitrate anion and ammonium cation, using an ion exchange process could achieve the twin aims of removal and recovery of these nutrients. The affinity of an exchange material for a particular ion is proportional to the valence and concentration of the ion. Even though phosphate species have relatively high valency, the phosphate concentration in wastewaters is low in comparison to other anions. This means that in a conventional ion exchange process, removal of phosphate is not very efficient as the exchanger reaches capacity very quickly because all the exchange sites are occupied with the competing anions. The lack of phosphate selectivity and the high operating cost due to the frequent application of regeneration chemicals were cited as major shortcomings affecting the overall viability of the fixed bed process (Zhao & Sengupta 1998). Therefore, an ion exchange system in which both nitrate and phosphate can be effectively removed has to be developed. In addition, the ion exchange media has to be amenable to regeneration and reuse.

2.4.1. Application of ion exchange with membrane bioreactor (MBR)

Ion exchange/adsorption processes can be developed for applications downstream of the MBR owing to the very high degree of solid removal already achieved by MBR. However, the influence of salts like SO_4^{2-}, HCO_3^-, Cl^-, CO_3^{2-} and residual COD that may be present in the MBR effluent need to be studied on account of their ability to inhibit the ion exchange of nutrients such as nitrate and phosphate.

2.4.2. Ion exchangers with affinity for nitrate removal

The ion exchange process seems to be the most suitable for small water suppliers contaminated by nitrate because of its simplicity, effectiveness, selectivity, recovery and relatively low cost (Bae et al. 2002). Recently several nitrate selective resins have been developed. Nitrate specific resins have been proven to have affinity for the following ions in decreasing order; $NO_3^- > SO_4^{2-} > Cl^- > HCO_3^-$ (Samatya et al. 2006a). The ion exchange process involves passage of nitrate loaded water through a resin bed containing strong base anion exchange resins on which nitrate ions are exchanged for another anion adsorbed on the resin until the resin's exchange capacity is exhausted. The exhausted resin is regenerated using a concentrated solution of sodium chloride (Samatya et al. 2006a) where the adsorbed nitrate is exchanged by chloride in the sodium chloride.

Several research projects were conducted on the removal of nitrate in drinking water by adsorbing nitrate by exchange resins; on macroporous resins type such as IMAC HP-555 and on freezing resins type such as Dowex SBRP (Clifford & Liu 1993; Liang et al. 1999). Resins whose selectivity is better for nitrates than for sulphates (Duolite A 196, Amberlite IRA 996) were developed in 1985 (Yamaguchi et al. 1999) with the specific resin Purolite A520E (Bae et al. 2002). Both the benzyltrimethyl ammonium type and the benzyldimethylethanol ammonium type resins have a significantly stronger affinity for nitrate over either chloride or bicarbonate but a lower affinity for nitrate as compared to sulphate at ionic concentrations typical of potable waters. This lower affinity for nitrate over sulphate leads to two difficulties in effective removal of nitrate. One difficulty is a limited useful capacity as the sulphate to nitrate ratio grows above about 0.25. The second difficulty is commonly referred to as "Nitrate Dumping", where the sulphate ions desorb previously adsorbed nitrate causing an increase in concentration of nitrate above the feed nitrate concentration (Samatya et al. 2006a).

When nitrate dumping occurs, the concentration of nitrates in the treated water can approach the sum of the concentrations of both the sulphates and nitrates in the raw water. For example, in water containing 80 ppm nitrate and 85 ppm sulphate, overrunning the unit will cause nitrate levels to rise until they approach 165 ppm. Nitrate selective resins prevent this nitrate concentration rise from occurring (Water Quality Products April 2003).

It has been demonstrated that clinoptilite is very effective as an ion exchanger for the removal of ammonium ions from wastewater (Baykal & Guven 1997) because clinoptilite is a cation exchanger and ammonium is a cation. Jorgensen & Weatherley (2003) reported that the performance loss of the clinoptilite was observed to be less than 10% even after 10 cycles of regular operation and regeneration. They also found that this medium was successful for the removal of nitrogen at low nitrogen loading rates. At higher rates, the removal efficiency decreased significantly. Furthermore, in the presence of protein, the ammonia uptake by clinoptilite was much lower than when proteins were absent.

Other exchangers with a high affinity for ammonium ion are naturally occurring zeolite, polymeric exchangers such as Doxex (50w-x8) and Purolite (Jorgensen & Weatherley 2003; Beler-Baykal, Oldenburg & Sekoulov 1996). Polymeric ion exchangers are reported to have high macroporosity. Macroporosity refers to the areal or volumetric proportion of macropores in ion exchangers. The term “macropore” conveys connotations of rapid pathways for the movement of water and chemicals in ion exchangers (Gimenez 2006). Higher macroporosity enhances the adsorption capacity of the ion exchanger. Although, Doxex (50w-x8) does not possess significant porosity, ammonium uptake by Doxex was not affected by the presence of any other ions in the system compared to Purolite and clinoptilite (Jorgensen & Weatherley 2003).

Della Rocca et al. (2007) reported that the following materials can be used for nitrate adsorption:

- ion-exchange resins (Amberlite IRA 900, Duolite A 126, Amberlite IRA 996, Purolite A 520 E, etc.)
- phosphonic acid ester type
- Sepiolite and HCl activated (a kind of fibroussilicate clay mineral formed as both tetrahedral and octahedral sheets)
- activated carbon
- bamboo powder charcoal
- amine-modified coconut coir

All these materials (natural and synthetic) have in common a great external surface. External surface is the main property of adsorbent materials because adsorption is an interface process between water and solid material (Della Rocca, Belgiorno & Meriç 2007).

2.4.3. Ion exchangers with affinity for phosphate removal

A variety of adsorbents have been developed for phosphate removal, such as aluminium oxide, iron oxide, zirconium oxide, ion exchange resin, and hydrotalcite (Terry 2009). Terry (2009) used hydrotalcite, a clay mineral ion exchange medium. This type of medium can effectively remove phosphorus as well as nitrogen. However the pH requirement is in the strongly acidic range (2.0~2.1), which limits the applicability of the process.

Oxides of many polyvalent metals, namely, Fe^{3+}, Ti^{4+} and Zr^{4+} exhibit very favourable ligand sorption properties for phosphate through the formation of inner sphere complexes (Dutta et al. 2004). Similarly zirconium salts (Zr^{2+}) are also applied for phosphate recovery (Lee et al. 2007). Of all these, HFO is innocuous, inexpensive, readily available, and chemically stable over a wide pH range. The sizes of freshly precipitated amorphous HFO particles were found to vary between 10 and 100 nm.

Another medium for capture of nitrate and phosphate is a mixture of crushed oyster shells with zeolite. The oyster-zeolite media combined with membrane filtration achieved up to 90% and 53% removal efficiencies of nitrate and phosphate respectively from water containing 45 mg N/L and 6 mg P/L (Jung et al. 2006).

2.4.4. Layered double hydroxides

Layered double hydroxides (LDHs) are a class of synthetic anionic clays in which some of the divalent cations have been replaced by trivalent cations in the octahedral sheet of the clays so that the LDHs produce unbalanced positive charges which are capable of adsorbing anions from water (Lv et al. 2008). Figure 2-4 illustrates a schematic representation of the LDH structure. Liv et al. (2008) used calcined layer double hydroxide containing Ca, Mg and Al as an adsorbent for phosphate and found that Mg/Al molar ratio of 2:1 had the highest capacity to remove phosphate from aqueous solutions. The adsorbed phosphate can be easily desorbed by sodium carbonate (Na_2CO_3) solution and LDHs can be readily regenerated while achieving the recovery of valuable phosphate. A major disadvantage of the process is the interference of other ions for phosphate adsorption.

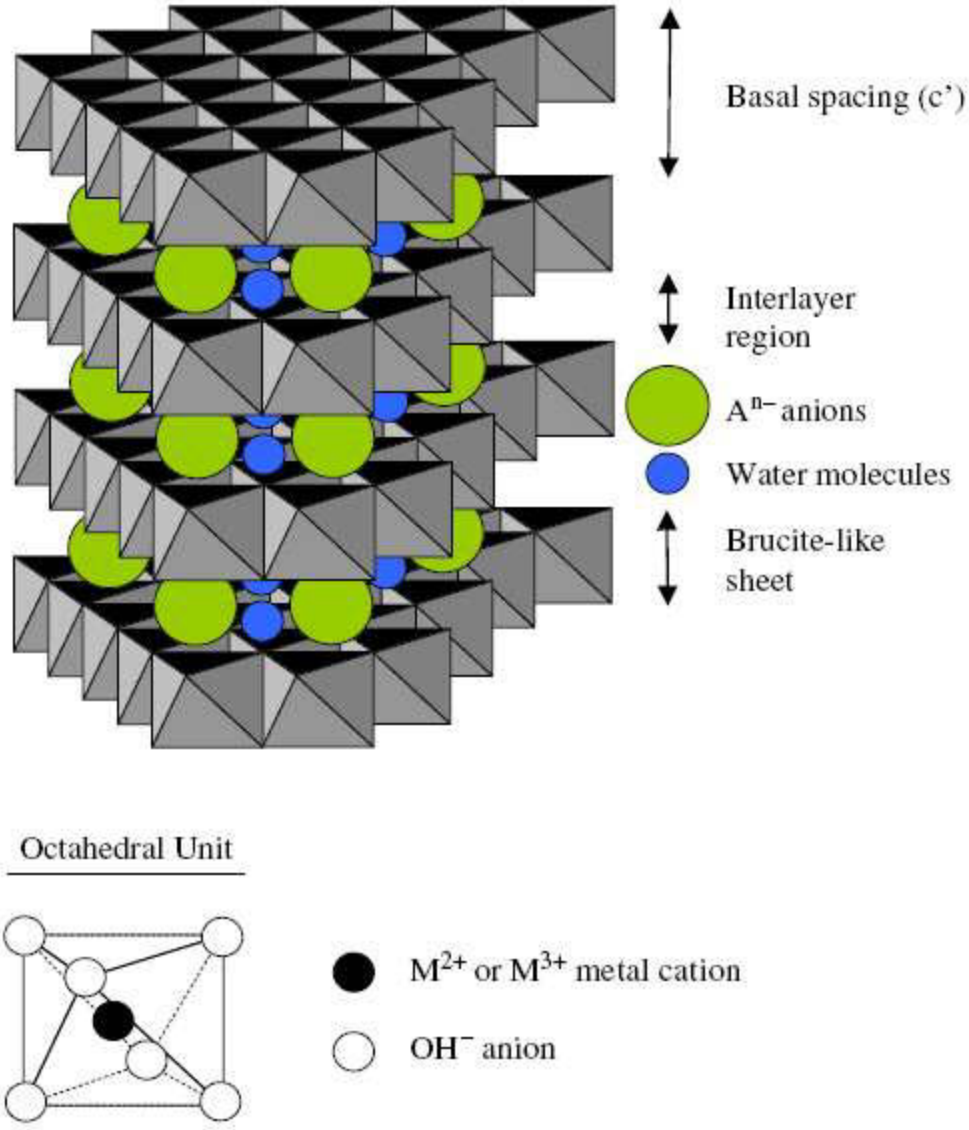

Figure 2-4: Schematic representation of the LDH structure (Goh, Lim & Dong 2008)

Seida and Nakano (2002) have developed double layered hydroxides containing iron. The release of the cations in the iron compounds, in addition to any hydroxide ions, act as coagulants in addition to adsorption to remove phosphate.

2.4.5. HAIX

A new type of hybrid anion exchanger (HAIX) media which is highly selective for phosphate, and can be easily regenerated has been investigated by Blaney et al. (2007), Martin et al. (2009) and Cumbal and Sengupta (2005). The media consisted of HFO nanoparticles dispersed irreversibly within the pore structures of polymeric anion exchanger beads (Blaney, Cinar & SenGupta 2007; Martin, Parsons & Jefferson 2009;

Cumbal & SenGupta 2005). Figure 2-5 gives a representation of an HAIX resin with quaternary ammonium functional groups irreversibly dispersed with HFO nanoparticles.

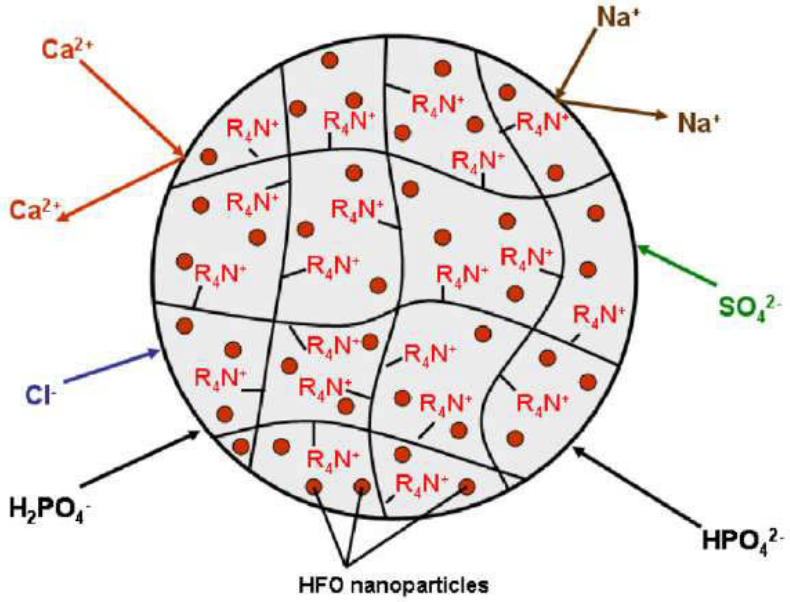

Figure 2-5: Representation of an HAIX resin with quaternary ammonium functional groups (R_4N^+) irreversibly dispersed with HFO nanoparticles (Blaney, Cinar & SenGupta 2007)

HAIX combines the durability and mechanical strength of polymeric anion exchange resins with the high sorption capacity of HFO for phosphate. The media was trialled in fixed bed mini column experiments with real final effluent from two UK sewage treatment works, one with treatment based on chemical precipitation with iron chloride salts into an activated sludge process, and one based on trickling filter treatment with no specific phosphorus removal process (Martin, Parsons & Jefferson 2009). Results showed that the media had high capacity for removing phosphate, reaching its maximum adsorption capacity at 4000 and 1300 bed volumes for the chemical precipitation and trickling filter works respectively, with performance greatly exceeding that of a standard anion exchanger, Amberlite IRA-410.

In addition, Martin et al. (2009) also trialled the media's ability to elute the phosphorus after breakthrough, with the aim of recovering and processing it into a useful product such as a fertiliser. A one step regenerative process using a single solution containing 4% NaOH and 2% NaCl was passed through the resin bed and the phosphorus concentration of each bed volume leaving the column analysed. 80% of the phosphorus was eluted in the first bed volume. Subsequent tests investigated the performance of the media after successive partial regenerations of one bed volume of the NaOH/NaCl solution. There was no loss of performance observed after ten

regeneration cycles, and levels of eluted phosphate were consistently high. These results suggest that the media has high potential for the removal and recovery of phosphate from wastewater streams. Additionally, the small volume of regenerant required translates to a very small operational footprint (Martin, Parsons & Jefferson 2009).

Blaney et al. (2007) conducted laboratory studies which showed that HAIX selectively removed phosphate from the background of much higher concentrations of competing sulphate, chloride and bicarbonate anions due to the combined presence of Coulombic and Lewis acid–base interactions. Experimental results demonstrated that HAIX's phosphate–sulphate separation factor was over two orders of magnitude greater than that of commercial ion exchange resins. Additionally, optimal HAIX performance occurred at typical secondary wastewater pH conditions, which was around 7.5.

HAIX is amenable to efficient regeneration and reuse with no noticeable loss in capacity. Also, HAIX can be used at natural pH levels to remove phosphorus, an advantage of this process. Although HAIX was used successfully with HFO, the combination of polymeric anion exchange with other metal oxides such as TiO_2 needs to be investigated to determine whether there is any added advantage because according to the study by Shon et al. (2007) TiO_2 appears to have a higher pollutants scavenging capacity than iron oxides.

Based on the work by Morel & Hering (1993) and Zhao & Sengupta (1998), immobilising particles of a transition metal cation onto a polymer base will enable it to act as an anion exchanger with a high affinity towards anions with strong ligand characteristics such as phosphate. The HAIX used in their study was made using such a process. The parent material was a standard polymeric strong base anion exchanger, into which hydrated ferric oxide (HFO) nanoparticles were dispersed. At above neutral pH the phosphate in wastewater streams exists primarily as the divalent anion HPO_4^{2-} (Zhao & Sengupta 1998), and its intermediate, the monovalent $H_2PO_4^-$ (Blaney, Cinar & SenGupta 2007). HPO_4^{2-} is a fairly strong bidentate ligand containing two oxygen donor atoms (Martin, Parsons & Jefferson 2009). Likewise, $H_2PO_4^-$ is a fairly strong monodentate ligand with one oxygen donor atom. The ligand strength of both forms (i.e. their ability to form inner sphere complexes with transition metal oxides - for e.g. ferric oxide) is much greater than the other inorganic anions commonly present in wastewater (Zhao & Sengupta 1998). This enables HAIX with HFO to act as a phosphate selective ion exchanger, and because it can be regenerated in the same manner as a conventional

exchange resin, the phosphate can be desorbed and recovered.

Similar to the parent resin of HAIX, Amberlite IRA-410 is a strongly basic anion exchange resin in the chloride form. It consists of a styrene-divinylbenzene gel matrix and has an ammonium functional group. Comparing the performance of the Amberlite with the HAIX resin will therefore quantify the effect of adding HFO nanoparticles to HAIX, and demonstrate the higher efficiency of HAIX over a standard exchange resin in removing phosphate from wastewater. Martin et al. (2009) aimed to provide an initial analysis of the performance of the HAIX material in terms of differing feed solutions in comparison with Amberlite; for phosphate removal and recovery, and to economically assess its potential for use by the water industry.

The experiment of Martin et al. (2009) showed that the HAIX resin was able to remove a significant proportion of the phosphate and eventually reached capacity after treating 1000 bed volumes (Figure 2-6). There was a gradual decline in removal rates as the exchange sites on the resin become associated with phosphate. During the run, the HAIX removed 23.55 mg PO_4^{3-}/g resin from the solution, from a starting concentration of 15.2 mg PO_4^{3-}/L. In contrast, the Amberlite's performance rapidly tailed off and after reaching capacity at around 170 bed volumes, started to elute the phosphate completely. This is due to the resin's preference for sulphate over phosphate which results in early breakthrough and chromatographic elution of phosphate (Zhao & Sengupta 1998). Sulphate concentration in the influent solution was 60 mg/L. The Amberlite removed only 0.99 mg PO_4^{3-}/g resin during its run, from an initial concentration of 16.2 mg/L. The low efficiency of phosphate removal by Amberlite was also reported by others (Blaney, Cinar & SenGupta 2007; Zhao & Sengupta 1998). The low performance was characterised by rapid breakthrough followed by phosphate elution, and a complete lack of removal thereafter. Amberlite is therefore not considered to be an efficient choice for phosphate removal, as its selectivity is poor due to the competition from much higher concentrations of sulphate found in wastewater. Additionally, the elution of phosphate from a column containing Amberlite is clearly an undesirable trait. The HAIX resin has a much higher capacity for phosphate in comparison, and there is no evidence to suggest that it exchanges other ions in preference to phosphate (Martin, Parsons & Jefferson 2009).

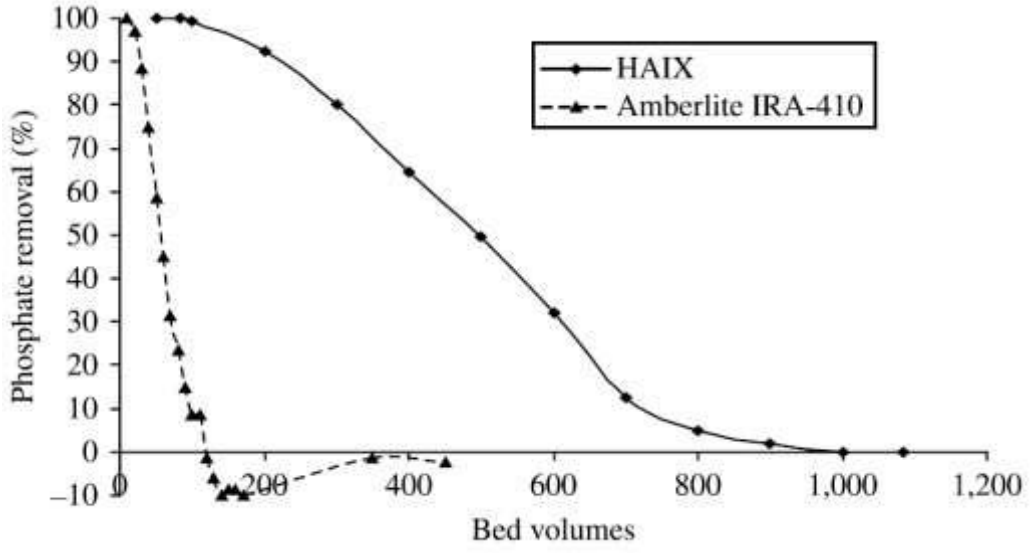

Figure 2-6: Performance comparison of Amberlite IRA-410 and HAIX (Martin, Parsons & Jefferson 2009)

2.4.6. Purolite

Purolite is an effective nitrate selective ion exchanger used by many to reduce nitrate concentration in wastewater (Samatya et al. 2006a; Gu, Ku & Jardine 2004; Bae et al. 2002; Jorgensen & Weatherley 2003; Samatya et al. 2006b).

Purolite A520E is a macroporous strong base anion resin which is specially designed for the removal of nitrates from water for potable processes. The macroporous matrix and the special ion exchange group functionality imparts ideal nitrate selectivity to Purolite A520E making this resin particularly suitable for nitrate removal even when moderate to high concentrations of sulphate are present. Hence this resin gives superior performance in nitrate removal applications when compared with standard exchange resins (Purolite 2010b).

Samatya et al. (2006a) investigated the removal of nitrate from aqueous solutions containing 100 mg NO_3^-/L by using nitrate selective anion exchange resin, Purolite A520E. The removal of nitrate increased with an increasing resin dose. The adsorption process obeyed the Langmuir adsorption isotherm giving a maximum adsorption capacity of 81.97 mg NO_3^-/g dry resin. This resin gave promising results for column-mode removal of nitrate from ground water containing 195 mg NO_3^-/L and other anion species such as bicarbonate, chloride and sulphate ions. The breakthrough point of nitrate was about half (229 BV) of that obtained with model aqueous solution (451 BV) due to the other ionic impurities, especially bicarbonate ions (482 mg/L) and

much higher concentration of nitrate in ground water (195 mg NO_3^-/L). As a result, ground water containing lower nitrate concentration than the permissible level for drinking water was produced by Purolite A520E. Elution of adsorbed nitrate increased with an increase in concentration of NaCl. A quantitative stripping of nitrate (about 100%) from the resin was obtained with 0.6 M NaCl solution. Based on the results of their experiments, Samatya et al. (2006a) suggested that ion exchange process using Purolite A520E can be applied more widely and economically in small-scale water suppliers for nitrate removal.

Gu et al. (2004) investigated competitive ion-exchange reactions among nitrate (NO_3^-), sulphate (SO_4^{2-}), chloride (Cl^-), and uranium (U) as part of remedial activities involving studies of the geochemistry and removal of U and NO_3^- from contaminated groundwater. Past waste disposal activities at the site have created a mixed-waste plume of contamination in the underlying unconsolidated residuum and competent shale bedrock. The contaminated groundwater contained high levels of NO_3^- (137.6 mM), SO_4^{2-} (10.6 mM), and U(VI) (~0.2 mM), and a highly buffered low pH (~3.8). The ion-exchange technology using the synthetic anion-exchange resins Purolite A520E and Dowex 1-X8 was evaluated as a means of removing NO_3^- and U to minimize or prevent the off-site migration of the contaminated groundwater to a nearby creek.

Both the resins are Type-I strong-base anion exchange resins with a chloromethylstyrene backbone and 5-8% divinylbenzene cross-linking. The total anion exchange capacities of the Purolite A520E and Dowex 1-X8 resins were ~2.8 and 3.2 mmol(-)/g, respectively, on a dry weight basis (Gu, Ku & Jardine 2004).

Gu et al. (2004) conducted sorption experiments to evaluate the effectiveness of the Purolite A520E resin to remove nitrate from simulated groundwater solutions containing varying concentrations of NO_3^- to SO_4^{2-} (molar ratios of NO_3^-/SO_4^{2-} in the test solution were ~0.5 and 2.8 and the initial NO_3^- concentration ranged from 0-4.3 mM). They found that the sorption of NO_3^- and SO_4^{2-} appeared to follow the Freundlich sorption isotherm; the sorption increased rapidly at low NO_3^- or SO_4^{2-} concentrations and slowed significantly as the sorption capacity of the resin was approached. However, NO_3^- was preferentially removed over SO_4^{2-}, and the resin sorbed much more NO_3^- than SO_4^{2-} at any given equilibrium concentration and at different NO_3^- to SO_4^{2-} ratios. Most NO_3^- in solution was sorbed (~0.2 mmol/g) despite the fact the NO_3^- to SO_4^{2-} molar ratios varied from 0.5 to ~2.8 in initial reactant solutions. The pH had very little

influence on the sorption of NO_3^- and SO_4^{2-} at a pH range of 4 - 7.

To further evaluate the sorption selectivity of the major anions (NO_3^-, SO_4^{2-}, and Cl^-), Gu et al. (2004) performed binary exchange reactions by varying the equivalent ionic fractions (X_i) of these anions in reactant solutions but maintaining a constant total equivalent ionic concentration of 0.16 mol(-)/L. A plot of the ionic (or molar) fractions of NO_3^- and Cl^- sorbed on resin against those in solution phase clearly indicates that NO_3^- was selectively sorbed (Figure 2-7a). Nearly 90% of the exchange sites were sorbed with NO_3^- when the ionic fraction of NO_3^- or Cl^- in solution was about 50%; only about 10% of the exchange sites were sorbed with Cl^-. A plot of the separation factors suggests that nitrate was more selectively sorbed than Cl^- by a factor of about 40-60 (Figure 2-7b). The separation factor of NO_3^- over Cl^- was about 6-10 and remained relatively constant over a range of NO_3^- concentrations (or different ionic fractions). On the other hand, the separation factor of Cl^- over NO_3^- was only about 0.1-0.15.

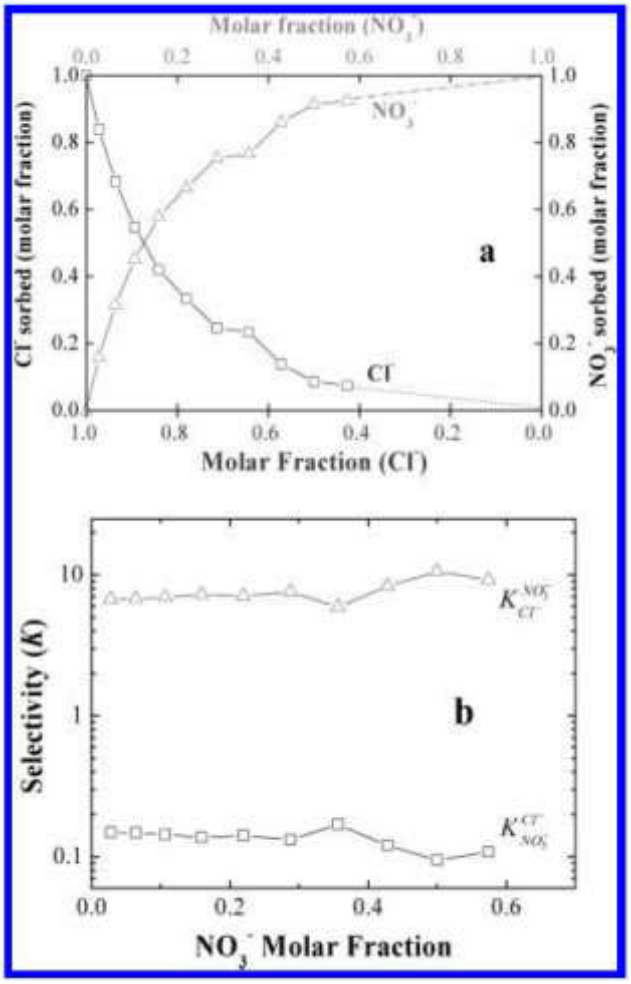

Figure 2-7: (a) Plot of the molar (or equivalent) ionic fractions of chloride and nitrate sorbed on the A-520E resin against those in the solution phase. (b) Calculated separation factors of nitrate and chloride. The total equivalent ionic concentration was 0.16 mol(-)/L (Gu, Ku & Jardine 2004)

Similarly, for the binary exchange reactions between NO_3^- and SO_4^{2-}, nitrate was more selectively sorbed than SO_4^{2-}, by a factor of nearly 100 (Figure 2-8a). More than 95% of the exchange sites were sorbed with NO_3^- when the equivalent ionic fraction of NO_3^- in solution was about 50%, and only 5% of the exchange sites were sorbed with SO_4^{2-}. At the NO_3^- ionic fraction of 0.2, nearly 75% of the exchange sites were sorbed with NO_3^-. These results suggest that SO_4^{2-} anions are less competitive than Cl^- with regard to sorption on the A520E resin. Indeed, analysis of the binary exchange reactions between SO_4^{2-} and Cl^- revealed that Cl^- was more selectively sorbed than SO_4^{2-} by a factor of about 5-10 (Figure 2-8b). The separation factor of Cl^- over SO_4^{2-} was about 2.5 and remained relatively constant over a range of Cl^- or SO_4^{2-} ionic concentrations. The separation factor of SO_4^{2-} over Cl^- was only ~0.4. At the equivalent ionic fraction of 0.5, about 70% of the exchange sites were sorbed with Cl^- as compared with only ~30% of

the exchange sites sorbed with SO_4^{2-}. The selectivity of these three anions on the Purolite A-520E resin followed the order of $NO_3^- > Cl^- > SO_4^{2-}$.

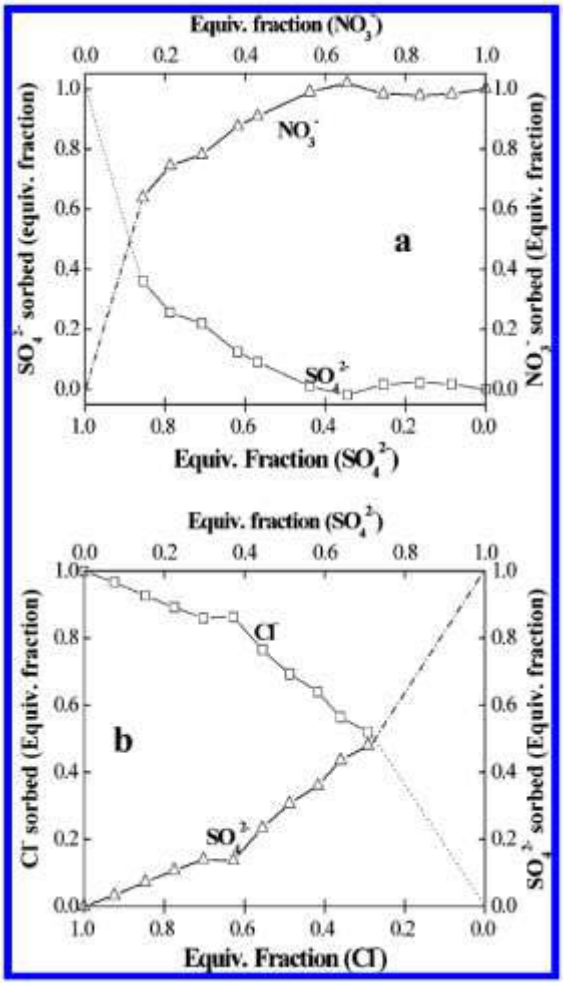

Figure 2-8: Plot of the equivalent ionic fractions of (a) sulphate and nitrate and (b) chloride and sulphate sorbed on the A-520E resin against those in the solution phase. The total equivalent ionic concentration was 0.16 mol(-)/L (Gu, Ku & Jardine 2004)

2.4.7. Hydrated ferric oxide (HFO)

It is well known that HFO has a high capacity to specifically adsorb phosphate both at positively charged surface sites as well as on neutral sites (Blaney, Cinar & SenGupta 2007; Streat, Hellgardt & Newton 2008b; Zeng, Li & Liu 2004; Genz, Kornmüller & Jekel 2004). This property of HFO is beneficially used in removing phosphate from water (Streat, Hellgardt & Newton 2008b; Zeng, Li & Liu 2004; Genz, Kornmüller & Jekel 2004).

Streat et.al (2008b) have carried out adsorption experiments in both batch and column modes utilising hydrous ferric oxide, which they have developed using the

freeze/thaw dewatering method (Streat, Hellgardt & Newton 2008a).

Three samples of synthetic granular ferric hydroxide were prepared in the laboratory:

- Akageneite prepared by partial neutralization of ferric chloride
- Granular ferric hydroxide dewatered by freeze/thaw technique
- Granular ferric hydroxide dewatered at ambient temperature

Single ion uptake capacities had been determined for all three granular ferric hydroxide materials studied. For the anionic species studied (arsenate, phosphate and fluoride), adsorption increased with decreasing pH, in the range 4–9. The highest uptake capacity for all anionic species occurred at pH 4, due to the iron oxide surface possessing the highest positive charge at this pH, hence strongly attracting the negatively charged species (Streat, Hellgardt & Newton 2008b).

Conversely for the cationic species studied (cadmium), the uptake capacity increased with increasing pH, in the range 4–9. The highest uptake was at pH 9, where the surface is most negative, hence the attractive forces towards a positively charged cationic species is the strongest (Streat, Hellgardt & Newton 2008b).

Fluoride possessed the highest adsorption capacity (1.8 mmol/g), followed by arsenate (0.9–1 mmol/g) and phosphate (0.65–0.75 mmol/g). Arsenate is a larger ligand interacting more strongly with the iron oxide surface and therefore is preferred over phosphate. Cadmium uptake capacity was less than fluoride but greater than arsenate and phosphate, indicating that both negative and positive surface sites are present on granular ferric hydroxide depending on the system pH. This agrees with an isoelectric point of 7–8. It is suggested that there is a combination of bidentate and monodentate species, dependent on pH and surface loading. It is probable that there is a higher quantity of mondentate complexes, hence increasing the available surface sites for adsorption compared to both arsenate and phosphate (Streat, Hellgardt & Newton 2008b).

The competition of other anions on arsenic uptake capacity was determined in column experiments. The same experimental conditions were maintained to enable comparisons of breakthrough capacities for a single ion system (arsenate) with binary and ternary systems containing phosphate and fluoride.

The ternary system (arsenate–phosphate–fluoride) produced a surprising result, since the presence of both phosphate and fluoride caused the affinity of arsenate and

phosphate to be almost equal, with phosphate slightly preferred over arsenate. This could be evidence of the faster kinetics of phosphate adsorption over arsenate. It is also observed that some partial desorption of phosphate and arsenate occurs, as the competing effects for surface sites is accentuated by the presence of fluoride (Streat, Hellgardt & Newton 2008b).

Elution in each column experiment was carried out by the addition of 0.1 M sodium hydroxide. All three anions were successfully desorbed from granular ferric hydroxide, with efficiencies in the range 85–100% (Streat, Hellgardt & Newton 2008b).

Zeng et al. (2004) explored the feasibility of utilising industrial waste iron oxide tailings for phosphate removal in laboratory experiments. The experimental work emphasised on the evaluation of phosphate adsorption and desorption characteristics of the tailing material, which contained more than 30% iron oxides. The major findings of the study of Zeng et al. (2004) were:

- The isotherm data were well fitted with five adsorption isotherm models by non-linear regression. The three parameter equations (Redlich–Peterson and Langmuir– Freundlich) provided better fitting than the two-parameter equations (Freundlich, Langmuir and Temkin). The applicability of the two-parameter isotherm models to explain the phosphate adsorption data approximately followed the order: Temkin ≈ Freundlich > Langmuir.
- The initial phosphate adsorption on the tailings was rapid and the adsorption rate was slightly higher at a higher temperature between 5ºC and 35ºC.
- The phosphate adsorption on the tailings tended to decrease with an increase of pH, from 8.6 mg P/g at pH 3.2 to 4.6 mg P/g at pH 9.5 with an initial load of 10 mg P/g tailings. This trend was likely attributable to an increased repulsion between the negatively charged PO_4^{3-} species and negatively charged iron oxide surface sites at a higher pH.
- A phosphate desorbability of approximately 13–14% was observed. The low desorbability likely resulted from a strong bonding between the adsorbed PO_4^{3-} and iron oxides in the tailings. Thus, the adsorbed PO_4^{3-} on the tailings is relatively difficult to be desorbed.
- The strong ability of phosphate removal by the tailings was also confirmed by column flow-through adsorption tests using both synthetic phosphate solution and liquid hog manure.

- It was demonstrated that the iron oxide tailings were an effective adsorbent for phosphate removal. Due to their low cost and high capability of phosphate adsorption, the iron oxide tailings have the potential to be utilised for cost effective removal of phosphate from wastewater.

Genz et al. (2004) studied the advanced phosphate removal by adsorption process for its suitability as a post-treatment step for membrane bioreactor (MBR) effluents low in phosphate concentration and particle content. Granulated ferric hydroxide (GFH) and activated aluminium oxide (AA) were studied in batch tests and lab-scale filter tests for adsorption of phosphate in MBR filtrates. GFH showed a higher maximum capacity for phosphate and a higher affinity at low phosphate concentrations compared to AA. Competition by inorganic ions was negligible for both adsorbents at the original pH (8.2). Dissolved organic carbon appeared to be the strongest competitor for adsorption sites. When equilibrium phosphorus concentrations exceeded 2 mg/L in the spiked MBR filtrates, a precipitation of calcium phosphates occurred in addition to adsorption. During column studies the effluent criteria of 50 µg P/L was reached after a throughput of 8000 bed volumes for GFH and 4000 for AA. A partial regeneration and reloading of both adsorbents could be achieved by the use of sodium hydroxide (Genz, Kornmüller & Jekel 2004).

2.4.8. Selection of adsorbents for nitrate and phosphate removal

Based on the literature review it appears that to remove nitrate an ion exchange resin column such as Purolite is necessary and for phosphate an HFO column is necessary. Therefore, in this study, these two materials were investigated for their ability to remove and recover nitrate and phosphate. HAIX has both HFO and ion exchange resin and therefore this media was also tested for removal and recovery of nitrate and phosphate.

3. Experimental Materials and Methods

The following sections present the experimental materials utilised as well as the methods undertaken for this study. Batch adsorption equilibrium, batch adsorption kinetics and column adsorption experiments were conducted to develop an ion exchange system that can efficiently remove and recycle nitrate and phosphate from wastewater.

3.1. Materials

The materials utilised during the study include:

- Two 60-cm columns
- Anthracite (sieved with particle sizing between 600 μm and 1.18 mm)
- HFO (50-80 mesh)
- Purolite (PURA500PS, PURA520E with varied particle sizes)
- HAIX
- dihydrogen phosphate (KH_2PO_4) and potassium nitrate (KNO_3) for the preparation of synthetic feed
- Pump and various piping with valves
- Milli-q water/distilled water and tap water
- MBR effluent
- Shaker
- Beakers, sample bottles, funnels and bucket

The ion exchange media used in this research consists of Purolite (A500PS and A520E) and HFO as well as HAIX.

Purolite was obtained from PUROLITE (USA). The following tables summarise the physical and chemical characteristics of the two types of Purolite media used.

Table 3-1: Typical physical and chemical characteristics of Purolite (A500PS) (Purolite 2010a)

Polymer Structure	Macroporous polystyrene crosslinked with divinylbenzene
Appearance	Spherical beads
Functional Group	$R\text{-}(Me)_3N^+$
Ionic Form – as shipped	Chloride – Cl^-
Total Capacity (Cl^- Form)	0.8 eq/l minimum

Moisture Retention (Cl^- Form)	63-70%
Bead Size Range (microns)	+1200 <2%, -420 <2%
Screen Size Range (U.S. Standard)	16-40 mesh
Reversible Swelling ($Cl^- \rightarrow OH^-$)	20% max
Specific Gravity (Cl^- Form)	1.04
Shipping Weight	655-685 kg/m^3 (41-43 lb/ft^3)
Temperature Limit (Cl^- Form)	100ºC (212ºF)
Temperature Limit (OH^- Form)	65ºC (150ºF)
pH Limits (Stability, Cl^- Form)	0-14

Table 3-2: Typical physical and chemical characteristics of Purolite (A520E) (Purolite 2010b)

Polymer Matrix Structure	Macroporous styrene-divinylbenzene
Physical Form and Appearance	Opaque cream spherical beads
Whole Bead Count	95% min.
Functional Groups	Quaternary Ammonium
Ionic Form, as shipped	Chloride – Cl^-
Total Exchange Capacity (Cl^- Form)	
Wet, volumetric	0.9 meq/ml minimum
Dry, weight	2.8 meq/g minimum
Moisture Retention (Cl^- Form)	50-56%
Particle Size Range	+1200 mm <5%, -300 mm <1%
Screen Size Range (U.S. Standard Screen)	16-50 mesh, wet
Reversible Swelling ($Cl^- \rightarrow SO_4/NO_3$)	negligible
Shipping Weight (approx.)	680 g/l (42.5 lb/ft^3)
Operating Temperature, Cl^- Form	100ºC (212ºF) max.
pH Range, Stability	0-14
pH Range, Operating	4.5 – 8.

A hydrous ferric oxide (HFO) (30-80 mesh) with the chemical formula of FeOOH obtained from Sigma Aldrich (USA) was used. X-ray diffraction analysis indicated that the HFO was amorphous with the presence of some nano-size iron oxides as reported for other HFO materials (Davis & Leckie 1978; Trivedi & Axe 2000).

HAIX is supplied by SolmeteX (USA). Figure 3-1 shows the salient properties of the commercially available cation exchanger and anion exchanger used for preparation of the HAIX. However, no endorsement is implied; similar exchangers are also available from other manufacturers (Cumbal & SenGupta 2005).

Anion and Cation Resin	Purolite A-400 and IRA-900	Purolite C-100
Structure (Repeating Unit)	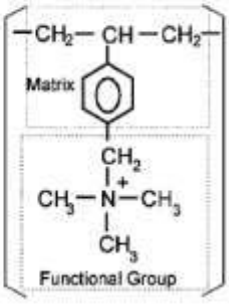	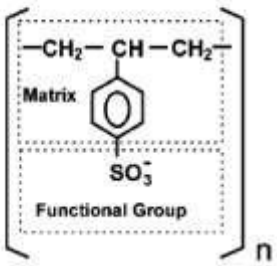
Functional Group	Quaternary ammonium	Sulfonic acid
Matrix	Polystyrene	Polystyrene
Capacity (meq/g resin)	3.6	4.0 (Dry) 2.5 (Wet)
Manufacturer	Purolite Inc. and Rohm and Haas Co., Philadelphia	Purolite Inc., Philadelphia

Figure 3-1: Polymeric ion exchangers as host materials for preparation of HAIX (Cumbal & SenGupta 2005)

The preparation of the HAIX consisted of the following three steps: first, loading of Fe(III) onto the sulfonic acid sites of the cation exchanger by passing 4% $FeCl_3$ solution at an approximate pH of 2; second, desorption of Fe(III) and simultaneous precipitation of iron(III) hydroxides within the gel phase of the exchanger through passage of a solution containing both NaCl and NaOH, each at 5% w/v concentration; and third, rinsing and washing with a 50/50 ethanol-water solution followed by a mild thermal treatment (50 - 60°C) for 60 min (Cumbal & SenGupta 2005).

Figure 3-2 depicts the major steps of the process. Hybrid anion exchangers were prepared through a slightly modified proprietary technique. Total iron contents of the hybrid exchangers were determined following 24 hr digestion in two successive steps with 10% sulphuric acid (Cumbal & SenGupta 2005).

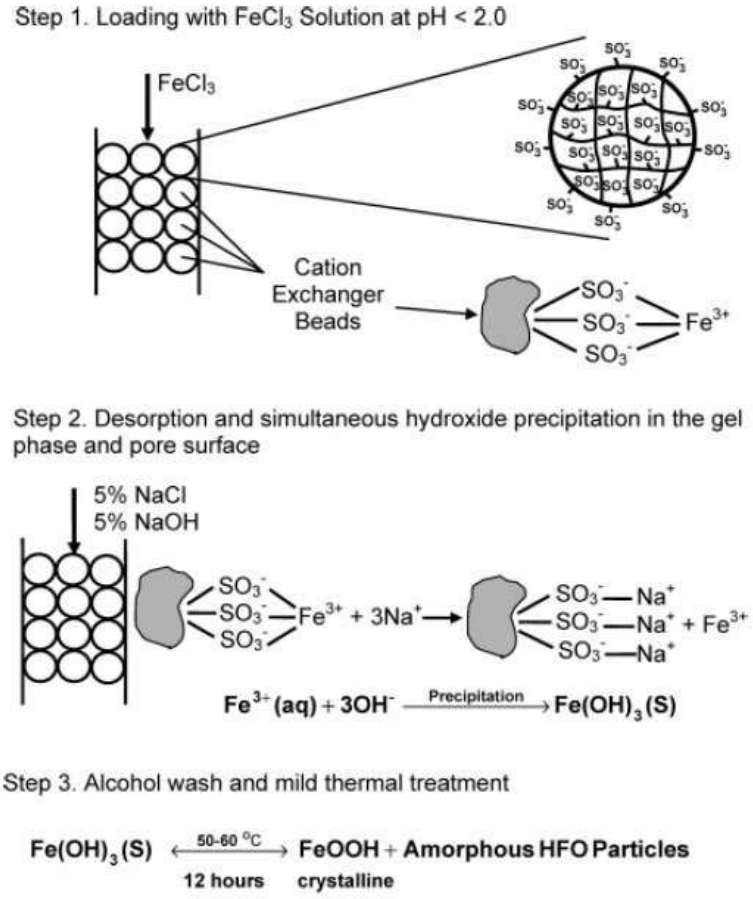

Figure 3-2: Illustration of the three-step procedure to disperse HFO nanoparticles inside spherical polymer beads (Cumbal & SenGupta 2005)

3.2. Methods

3.2.1. Batch (kinetics and equilibrium) studies

Batch (kinetics, equilibrium) experiments were carried out using synthetic feed. A synthetic inorganic solution of nitrogen and phosphorus prepared using potassium dihydrogen phosphate (KH_2PO_4) and potassium nitrate (KNO_3) in tap water, with concentrations 15 mg P/L and 50 mg N/L respectively was used in each beaker. Purolite (A500PS), HFO and HAIX were used in varying doses during these experiments. Beakers were filled with 150 mL of synthetic feed with varying dose of adsorbent and shaken for up to 72 hr on a laboratory shaker. Samples were taken periodically from the supernatant liquid and analysed for nitrate and phosphate using ion chromatograph.

For Purolite (A500PS) and HFO, the doses used were 0.5 g/L, 1 g/L, 3 g/L, 5 g/L and 10 g/L (0.075 g, 0.15 g, 0.45 g, 0.75 g and 1.5 g, respectively in 150 mL

synthetic feed). For HAIX, the doses used were 1 g/L, 3 g/L, 5 g/L, 7 g/L, 10 g/L, 15 g/L and 20 g/L (0.15 g, 0.45 g, 0.75 g, 1.05 g, 1.5 g, 2.25 g and 3.0 g, respectively in 150 mL synthetic feed). All experiments were undertaken at room temperature (25ºC).

In addition, a kinetics study was carried out using a higher concentrated synthetic feed of nitrate and phosphate (100 mg N/L and 50 mg P/L, respectively) at room temperature (25ºC). This study was conducted using Purolite (A500PS) and HAIX at 5 g/L dose. Beakers were filled with 150 mL of synthetic feed and 0.75 g of adsorbent and shaken for up to 6 hr on a laboratory shaker. Samples were taken periodically from the supernatant liquid and analysed for nitrate and phosphate using ion chromatograph.

3.2.2. Purolite and anthracite column adsorption study

Adsorption column experiments were performed using glass columns with an internal diameter of 2 cm and height of 60 cm, constant-flow stainless steel pumps (at 1 m/hr) and fraction collectors. A column was packed with 120 g of anthracite (particle sizing between 600 μm – 1.18 mm) and varying percentage (1%, 3%, 5% and 10%) by mass of Purolite (A500PS, 300 - 420 μm). This particular type of Purolite was selected as the first media to be tested for nitrate and phosphate removal efficiency as it was readily available and could be ground and sieved to obtain the particle sizes between 300 - 420 μm. The anthracite and Purolite were properly mixed in a bucket prior to packing the column. Anthracite alone does not remove nitrate and phosphate.

A synthetic inorganic solution of nitrogen and phosphorus prepared using potassium dihydrogen phosphate (KH_2PO_4) and potassium nitrate (KNO_3) in tap water, with concentrations 15 mg P/L and 50 mg N/L respectively, was fed into the columns with an upward directional flow. This solution was made fresh prior to running each of the experiments. Samples (~10 mL) were taken periodically for a total of 6 hr; every 30 min for the first 2 hr and then every hour. Samples were analysed for nitrate and phosphate using ion chromatograph.

For the 10% Purolite run, the experiment was broken up into several days, with samples collected at every half hour intervals after 360 min.

3.2.3. Purolite column adsorption study

Column experiments were performed with Purolite only using glass columns with an internal diameter of 2 cm, constant-flow stainless steel pumps and fraction collectors. Varying bed heights (3 cm, 6 cm and 12 cm) with a constant flow rate of 2 m/hr (10.5 mL/min) were used to test the effect of bed height on nitrate and phosphate removal. Purolite (A520E) was utilised in this phase of research. Manufacturers have stated that this type of Purolite is nitrate selective and is very efficient in removing anionic nutrients from water (Purolite 2010b). Experiments were carried out for lengthy periods (up to 2 - 3 days) to investigate the time-wise trends for nitrate and phosphate removal.

In addition, a column adsorption study was carried out using a higher concentrated synthetic feed of nitrate and phosphate (100 mg N/L and 50 mg P/L, respectively). This study was conducted using Purolite (A500PS) at 6 cm bed height (24 g) and 2 m/hr (10.5 mL/min). The experiment was conducted for 8 hr with samples taken at 30 min then every hour and analysed for nitrate and phosphate using ion chromatograph.

3.2.4. HAIX column adsorption study

Column experiments were performed with HAIX using glass columns with an internal diameter of 2 cm, constant-flow stainless steel pumps and fraction collectors. Bed height of 6 cm (24 g) with a constant flow rate of 2 m/hr (10.5 mL/min) was used to test the removal efficiency of nitrate and phosphate. The experiment was carried out for a lengthy period (up to 28 hr) to investigate the time-wise trends for nitrate and phosphate removal.

In addition, a column adsorption study was carried out using a higher concentrated synthetic feed of nitrate and phosphate (100 mg N/L and 50 mg P/L, respectively). This study was conducted using HAIX at 6 cm bed height (24 g) and 2 m/hr (10.5 mL/min). The experiment was conducted for 8 hr with samples taken at 30 min then every hour and analysed for nitrate and phosphate using ion chromatograph.

3.2.5. Purolite and HFO with anthracite columns in series adsorption study

Adsorption column experiments were performed with Purolite and HFO in series using glass/perspex columns, constant-flow stainless steel pumps, and fraction collectors. Two columns with internal diameter of 2 cm and height of 60 cm were packed with 120 g of anthracite (particle sizing between 600 μm – 1.18 mm), one with Purolite (A500PS, 300 - 420 μm) and the other with HFO (50-80 mesh). The percentage by mass of Purolite and HFO was varied (1%, 3%, 5% and 10%) in each experimental run to investigate the effect of the amount of media on the removal of nutrients. The anthracite and ion exchangers were properly mixed in a bucket prior to packing the columns.

A synthetic inorganic solution of nitrogen and phosphorus containing potassium dihydrogen phosphate (KH_2PO_4) and potassium nitrate (KNO_3), with concentrations 15 mg P/L and 50 mg N/L respectively, was fed into the columns with an upward directional flow. This solution was made fresh prior to running the experiments. Samples (~10 mL) were taken periodically for a total of 6 hr; every 30 min for the first 2 hr and then every hour and analysed for nitrate and phosphate using ion chromatograph. Samples were taken at two points; one after the solution passed through the Purolite column but before going through the HFO column and the second sample collected after the solution went through the HFO column. The flow rate was kept constant at 1 m/hr (5 mL/min). Distilled water was fed through the columns as a wash before starting the experiment.

For the 10% Purolite and HFO run, the experiment was broken up into several days, with samples collected at every half hour intervals after 360 min.

Particle size was a significant factor in these experiments as the packing in the column is required to be ideally mixed and able to withstand an upward directional flow. Anthracite was sieved prior to every experimental run to gather particles which were in between the 600 μm – 1.18 mm size range. In addition, the media used in each column had to be the proper sizing as well so that the column packing stays intact while the solution is passed up the columns. Therefore, the particle sizes of 300 – 420 μm for Purolite (A500PS) and 50-80 mesh for HFO were selected as the particle size large

enough to be ideally packed with the anthracite in the columns.

The experimental set up is illustrated in Figure 3-3. The set up consisted of a 15-litre feed tank, a constant-flow pump, two 60-cm glass/Perspex columns, and two sampling points. Column 1 was packed with anthracite and Purolite. Column 2 was packed with anthracite and HFO.

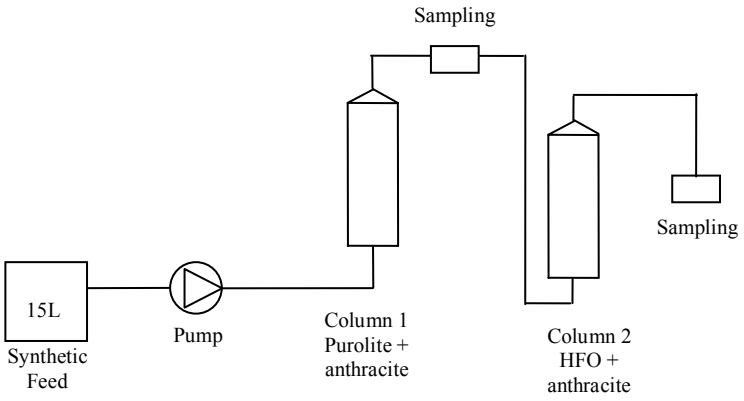

Figure 3-3: Schematic illustration of the experimental set up

3.2.6. Regeneration study

Regeneration studies were conducted using distilled water and 3% NaCl solution washes. These studies were undertaken to see if exhausted media can be regenerated for reuse. For the distilled water wash, columns were washed for 5 min at 1 m/hr (5 mL/min) flow rate and samples were collected for analysis to determine the amounts of nitrate and phosphate desorbed by this wash. For the 3% NaCl wash, columns were washed for 40 min at 10 m/hr (52.5 mL/min) flow rate to desorb as much nutrients as possible before the next experimental run. These columns were left overnight standing (about 16 hours) with the respective wash solutions and then used for another experimental run the following day.

3.2.7. MBR effluent as feed for column adsorption studies

In this experiment, effluent from a MBR experiment was collected and then subjected to ion exchange column as post treatment to remove nutrients (nitrate and phosphate).

The schematic diagram of laboratory scale membrane bioreactor (MBR) used in this study is presented in Figure 3-4. A flat sheet membrane module with an area of 0.2 m^2 made of polyvinylidene fluoride was used in this study. The average pore size of the membrane was 0.14 µm. Air flow rate in the range of 0.8-1.0 $m^3/m^2.h$ membrane area was applied to produce shear stress on the membrane surface. The effective volume of the reactor was 10 L.

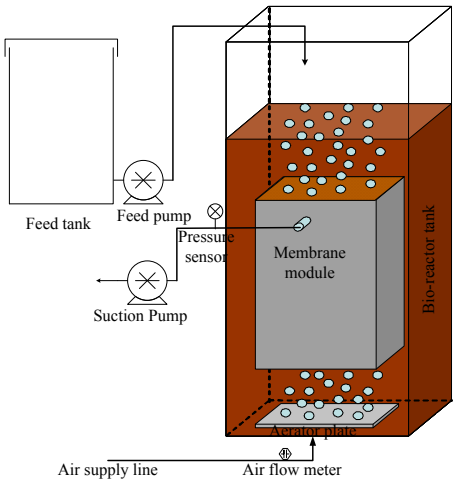

Figure 3-4: Laboratory scale membrane bioreactor

At the beginning, 10 L MBR was seeded with 3 L of sludge obtained from a domestic sewage treatment plant. After seeding, the bioreactor was continuously fed with a synthetic feed consisting of ethanol (as an organic source) and mineral salts containing nitrogen and phosphorus (as nutrients) in the ratio of COD:N:P ratio equal to 150:5:1 with an organic load of 1.5 kg COD/m^3.day. This COD: N: P ratio represents that of domestic wastewater. The average sludge retention time was 20 days. The mix liquor suspended solid (MLSS) and mix liquor volatile suspended solid concentration was in the range of 5-5.5 g/L and 4.3-4.5 g/L, respectively. MLSS concentration was maintained by wasting excess sludge (5% v/v) daily and diluting it by adding similar amount of water. The pH of the mixed liquor was kept between 6.5 and 8.

The effluent collected from the MBR was passed through the Purolite - anthracite column (2.5 and 5%) followed by the HFO - anthracite column (2.5 and 5%) and samples were collected as described for synthetic feed experiments in Section 3.2.5. Two experiments were undertaken, one with 2.5% by mass of the two media and the

next experiment with 5% by mass of the two media. The characteristics of the MBR effluents used in this study are presented in Table 3-3. The MBR experiments were done with the flux of 20 L/m^2.h (represented in Table 3-3 as Effluent 1) and 30 L/m^2.h (represented in Table 3-3 as Effluent 2).

Table 3-3: Characteristics of MBR effluents

Parameters	Effluent 1	Effluent 2
NO_3-N (mg/L)	12.9	10.6
PO_4-P (mg/L)	5.9	5.2

3.3. Analytical Methods

3.3.1. Ion chromatography

The samples collected were analysed using ion chromatography (IC) to determine the concentration of nitrate and phosphate in the effluent. The concentrations of nitrate and phosphate were determined from a standard curve prepared using known concentrations of nitrate and phosphate and IC readings.

The mobile phase solution for the ion chromatograph was made using 285.6 mg of sodium bicarbonate and 381.6 mg of sodium carbonate in 2 L of milli-Q water. This solution was stirred for 15 min then filtered using a microfilter. In addition, a 20 mM solution of sulphuric acid was made for the analysis. Milli-Q water was filtered using a microfilter and then 1.1mL of 98% H_2SO_4 was added to 1 L of filtered water. The final solution required was filtered milli-Q water. These solutions were freshly made prior to each analysis.

Samples were diluted by 20 times with milli-Q water prior to analysis due to the high chloride content present in tap water and the high nitrate and phosphate concentrations present in the synthetic feed.

3.3.2. Photometric analysis

A manual chemical analysis was undertaken with samples containing high chloride concentration because high chloride concentration affects the sensitivity of nitrate and phosphate measurements by the ion chromatograph. High chloride solutions

have a tendency of saturating the IC column being utilised currently for anions.

Samples collected from the MBR effluent as feed experiments were subjected to nutrient (phosphate and nitrate) analysis using manual method with the help of a Spectroquant MERCK Nutrient analysis kit. The measurement of NO_3^--N and PO_4-P was carried out using the cell test method (Spectroquant, Merck) and a photometer (NOVA 60, Merck).

For the NO_3-N analysis, 4 mL of NO_3-1 (Cat No. 1.14776.0002) was injected into a test tube and 0.5 mL of the effluent sample was added. Into the same test tube, 0.5 mL of NO_3-2(Cat No.1.14776.0002) was also added and mixed well. After a reaction time of 10 min, the nitrate value was measured in the device. The nitrate ions react with 2,6-Dimethyl (DMP) to form 4 Nitro-2,6-Dimethylphenol which was determined photometrically.

The standard method for the phosphate analysis (determination of orthophosphate) is the photometric, PMB method. The spectroquant MERCK Cat. No. 114848 reagents were used for the analysis. Initially 5 mL of sample was injected into a test tube and five drops of PO_4-1 solution was added and mixed well. To this solution, 1 level of blue microspoon of PO_4-2 was also added and shaken vigorously to dissolve the solid substances. Then after a reaction time of 5 min, the solution was placed in a cell and PO_4-P concentration was measured in the device.

4. Results and Discussion

In the first phase of the study, batch kinetics and equilibrium studies were undertaken to determine the adsorption rate and capacity of the three media tested using synthetic water. The data were modelled using the Langmuir, Freundlich, and Sips isotherm models and Ho's kinetic model. In the second phase of the study, Purolite (A500PS) and anthracite was used as adsorption media for nitrate and phosphate removal from synthetic water in column experiments. In the third phase of the study, Purolite (A520E) only as well as HAIX were used as adsorption media for nitrate and phosphate removal from synthetic water. This phase of study was undertaken to investigate whether the nitrate and phosphate removal efficiency could be increased by using only the ion exchange media without the inert anthracite material so that the weight of ion exchange media in the column can be increased. Instead of using ion exchange resin and HFO mixture as the adsorption media as tested in HAIX, the two media can be used separately in two columns in series to removal nitrate and phosphate. This method was used in the fourth phase of the study, where Purolite (A500PS) and HFO with anthracite in series were used as adsorption media for nitrate and phosphate removal from synthetic water. The fifth phase of the study incorporated regeneration tests for the media tested. In the final phase of the study, the column experiments were undertaken using MBR effluent as feed.

4.1. Batch Kinetics and Equilibrium Studies

4.1.1. Purolite adsorbent

Batch studies were conducted to determine the rate of adsorption and maximum adsorption capacity of nitrate and phosphate in the synthetic feed on Purolite (A500PS). Varied doses of Purolite at 0.5 g/L, 1 g/L, 3 g/L, 5 g/L and 10 g/L (0.075 g, 0.15 g, 0.45 g, 0.75 g and 1.5 g, respectively in 150 mL) with synthetic feed were used in the studies.

Figure 4-1 shows that with increase in time up to approximately 1680 min for 1, 3, 5 and 10 g/L dose of Purolite the adsorption of nitrate and phosphate increased and beyond these times, they reached equilibrium. For 0.5 g/L dose of Purolite, from 300 min onwards adsorption of both nitrate and phosphate did not change.

As the dose of Purolite increased from 0.5 to 10 g/L, there was a significant

increase in removal efficiency of both nitrate and phosphate. This is expected as a higher dose of Purolite increases the number of adsorptions sites. The nitrate and phosphate concentrations at equilibrium with 0.5 g/L Purolite (A500PS) was 40 mg N/L and 13 mg P/L, respectively. These equilibrium concentrations drastically decreased at 10 g/L dose (5.4 mg N/L and 3.2 mg P/L). This study showed that as the Purolite dose increased the equilibrium concentration of nitrate and phosphate decreased confirming that at higher doses of the media, there was better removal efficiency (Figure 4-1).

Furthermore, this study confirmed that Purolite (A500PS) is nitrate selective. Table 4-1 summarises the nitrate and phosphate removal efficiencies at equilibrium with the varied dose of Purolite used. The results showed that at every dose of Purolite used, the nitrate removal efficiency is higher than the phosphate removal efficiency. The removal efficiency difference became narrow as the dose of Purolite increased because there were more sites for adsorption at high doses and this decreased the competition for adsorption.

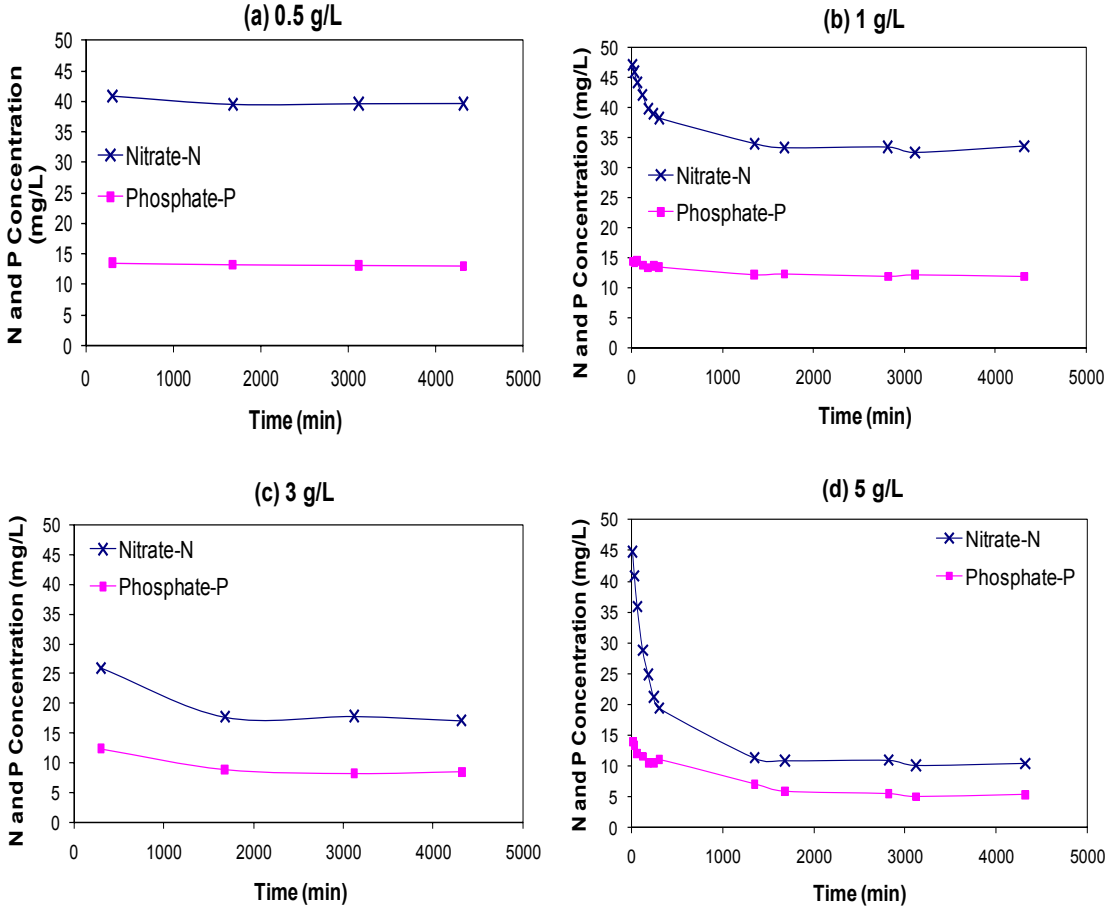

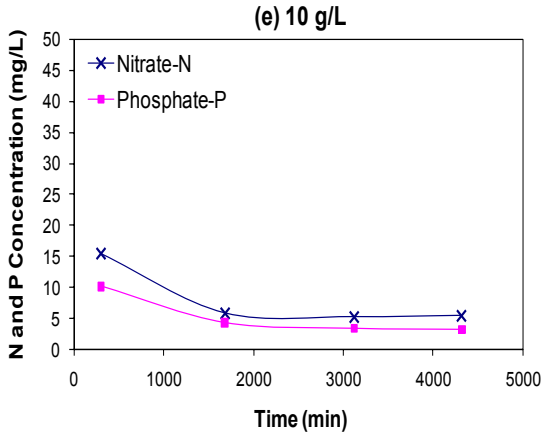

Figure 4-1: Batch kinetics of adsorption of nitrate and phosphate on Purolite (A500PS) at different doses of Purolite (a) 0.5 g/L, (b) 1 g/L, (c) 3 g/L, (d) 5 g/L and (e) 10 g/L

Table 4-1: Nitrate and phosphate removal efficiencies (at equilibrium*) with varying dose of Purolite (A500PS) during batch equilibrium study

Purolite dose (g/L)	Nitrate Removal Efficiency at Equilibrium (%)	Phosphate Removal Efficiency at Equilibrium (%)
0.5	20.7	13.5
1	32.8	21.2
3	65.7	43.2
5	79.1	64.0
10	89.2	78.8

* Equilibrium time used was 4320 min.

Adsorption equilibrium is described as the relationship between the amounts of solute per unit adsorbent and the equilibrium concentration of the solute remaining in solution which is called the adsorption isotherm. The amount of adsorbate that can be adsorbed by an adsorbent can be determined with the help of adsorption equilibrium. Adsorption equilibrium is an important method for evaluating the adsorption capacity of an adsorbent as well as the amount of adsorbed substances for a given parameters of concentration and temperature (Suzuki 1990). This process starts as the adsorbents contacts with fluid and reaches an equilibrium condition in which the rate of both adsorption and desorption are equal. It is normally characterised by two parameters: solute concentration in the adsorbent (q_e) and solution concentration at equilibrium (Ce).

Adsorption Models

There are a number of isotherm models proposed by previous researchers that describe the adsorption process. Many mathematical models have been developed relating q_e and Ce.

Freundlich and Langmuir models are the most widely used due to their simplicity and proper fitting to experimental data. Both these isotherm models describe the single component adsorption whereas the ideal adsorbed solution theory has been used to describe the multicomponent adsorption (Crittenden et al. 1985; Matsui, Yuasa & Li 1998).

The Langmuir model is the simple theoretical model for monolayer adsorption. The Langmuir model is developed based on the following underlying assumptions (Cooney 1999; Faust & Aly 1987; Weber 1972):

- the molecules are adsorbed on definite sites on the surface of the adsorbent;
- each site can bind only one molecule of the adsorbing species (monolayer);
- the adsorption energy is the same at all sites; and
- there are no forces of interaction between adjacently adsorbed molecules.

The Langmuir isotherm is described as:

$$q_e = \frac{q_m b C_e}{1 + b C_e} \qquad (1)$$

where q_e is the amount adsorbed at equilibrium (mg/g), Ce is the equilibrium concentration (mg/L), b is a Langmuir constant related to the binding energy of adsorption (L/mg), and q_m is a Langmuir constant related to the saturated maximum monolayer adsorption capacity (mg/g).

The Freundlich isotherm is an empirical equation developed based on the assumption that the adsorbent has a heterogeneous surface composed of different classes of adsorption sites, and the adsorption process can be modelled by the following equation:

$$q_e = K_F . C_e^{\frac{1}{n}} \qquad (2)$$

where K_F is a Freundlich constant indicative of the adsorption capacity of the adsorbent, and n is an experimental constant indicative of the adsorption intensity of the adsorbent.

The Sips model (Chabani, Amrane & Bensmaili 2009) is a different empirical model representing equilibrium adsorption data. This isotherm model has the features of both the Langmuir and Freundlich isotherm models. As a combination of the Langmuir and Freundlich isotherm models, the Sips model contains three parameters, q_m, b and n, which can be evaluated by fitting the experimental data. For single solute equilibrium data, the Sips adsorption isotherm model can be written as follows:

$$q_e = \frac{q_m (bC_e)^{\frac{1}{n}}}{1 + (bC_e)^{\frac{1}{n}}} \qquad (3)$$

In adsorption studies, process kinetics describes the rate at which the species are transferred from the solution to the adsorbent surface or pores of an adsorbent. The rate of adsorption determines the time required to reach equilibrium condition.

Ho et al. (1996) presented a pseudo second-order reaction rate model to describe the adsorption kinetics of metals on peat, as shown below:

$$\frac{t}{q_t} = \frac{1}{2k_H q^2} + \frac{t}{q} \qquad (4)$$

where k_H is the Ho rate constant for adsorption and is a function of temperature (g/mg/min); q is the amount of adsorbate at equilibrium (mg/g); and q_t is the amount of adsorbate at any time t, (mg/g).

Ho's pseudo second order kinetic model was used to simulate a number of sorption systems (Azizian 2004). Ho's pseudo second order model presents the experimental kinetic data for the entire sorption period for most of the systems better than other models. This model has been used extensively by a lot of researchers as it could simulate excellent fit of the experimental kinetic data to the model for the entire sorption period (Kumar & Sivanesan 2006).

To fit the data obtained from the kinetic studies, the equation (4) can be rearranged as follows:

$$q_t = \frac{2k_H q^2 t}{1 + 2k_H q\ t} \qquad (5)$$

Modelling Experimental Data

The Langmuir, Freundlich and Sips isotherm models were used to model the equilibrium isotherm of nitrate and phosphate removal by Purolite (A500PS), given in Figure 4-2 and Figure 4-3, respectively.

From the Langmuir isotherm model, the experimental results indicated the maximum adsorption capacity (q_m) of 64 mg NO_3^- per g – dry resin and energy of adsorption value (b) of 0.012 L/mg (Table 4-2). In order to predict the adsorption efficiency of the adsorption process, a dimensionless equilibrium parameter was determined by using the following equation (Samatya et al. 2006a):

$$r = \frac{1}{1 + bC_o} \qquad (6)$$

Where C_o is the initial concentration and b is the Langmuir isotherm constant. Values of $r < 1$ represent favourable adsorption and values greater than 1.0 represent unfavourable adsorption. The value of r for the initial concentration of 50 mg/L nitrate was found to be 0.625 (Table 4-2). Therefore, the resin Purolite (A500PS) showed favourable adsorption.

From the Freundlich isotherm model, the experimental results indicated the value of K_F was 1.7 and n was 1.5. From the Sips isotherm model, the experiment results indicated that the value of q_m was 50, b was 0.012 and 1/n was 1.1. The model parameters for the data are presented in Table 4-2 and Table 4-3.

.

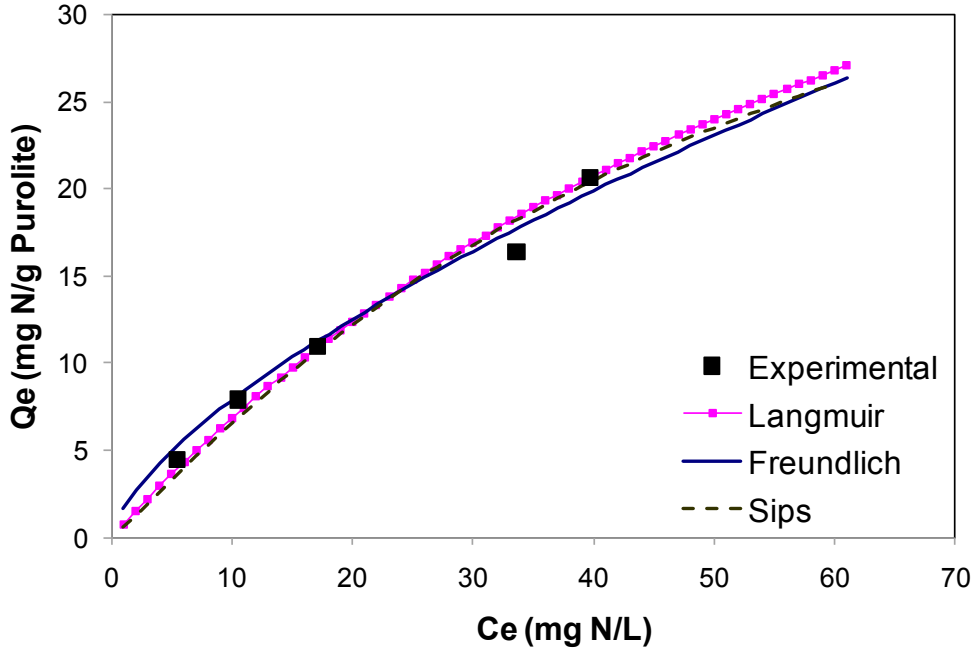

Figure 4-2: Equilibrium isotherm modelling plot for nitrate removal by Purolite (A500PS)

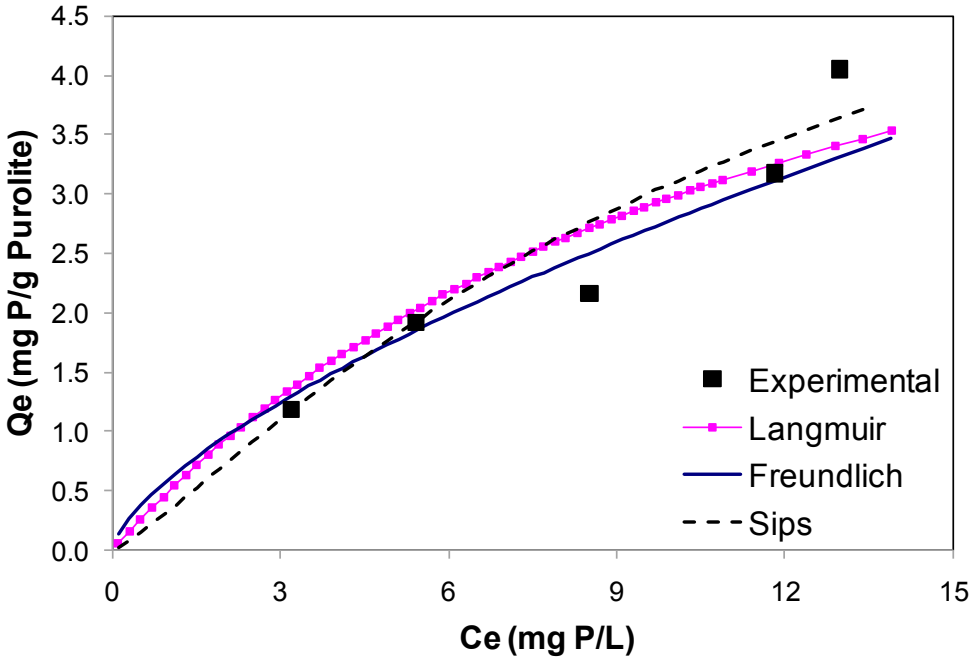

Figure 4-3: Equilibrium isotherm modelling plot for phosphate removal by Purolite (A500PS)

Table 4-2: The values of the parameters in the Langmuir and Freundlich equation and r values for nitrate and phosphate removal

Purolite (A500PS)	q_m (mg/g)	b (L/mg)	K_F (mg/g)	n	r
Nitrate - N	64	0.012	1.7	1.5	0.625
Phosphate - P	6.7	0.08	0.6	1.5	0.455

Table 4-3: The values of the parameters in the Sips equation for nitrate and phosphate removal

Purolite (A500PS)	q_m (mg/g)	b (L/mg)	1/n
Nitrate - N	50	0.012	1.1
Phosphate - P	7	0.05	1.2

The results show that the experimental data satisfactorily fitted to all three models. The model predicted Qe and experimentally measured Qe were compared using the regression equation y = mx where y is the model predicted Qe, x is the experimentally measured Qe, and m is the slope. The results showed that m and the coefficient of determination R^2 were approximately equal to 1in all cases confirming the satisfactory fit of the data to all three models (Figures 4-4 – 4-6, Tables 4-4 – 4-5). However, the R^2 values were lower for phosphate than for nitrate.

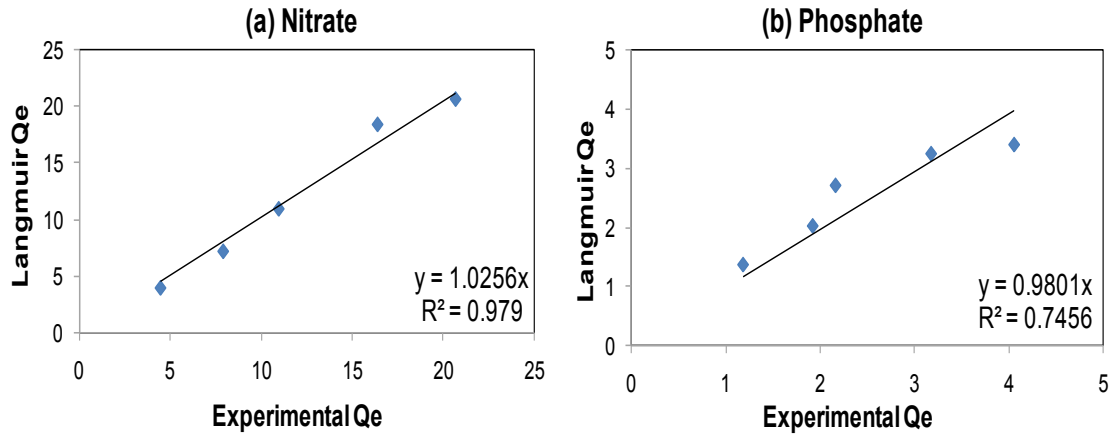

Figure 4-4: Langmuir model Qe compared with experimental Qe for (a) nitrate and (b) phosphate removal at varying dose of Purolite (A500PS)

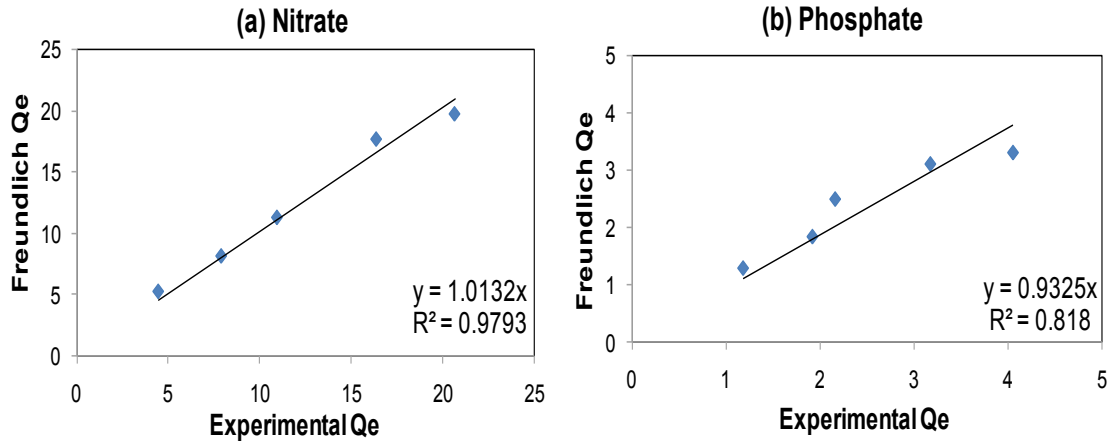

Figure 4-5: Freundlich model Qe compared with experimental Qe for (a) nitrate and (b) phosphate removal at varying dose of Purolite (A500PS)

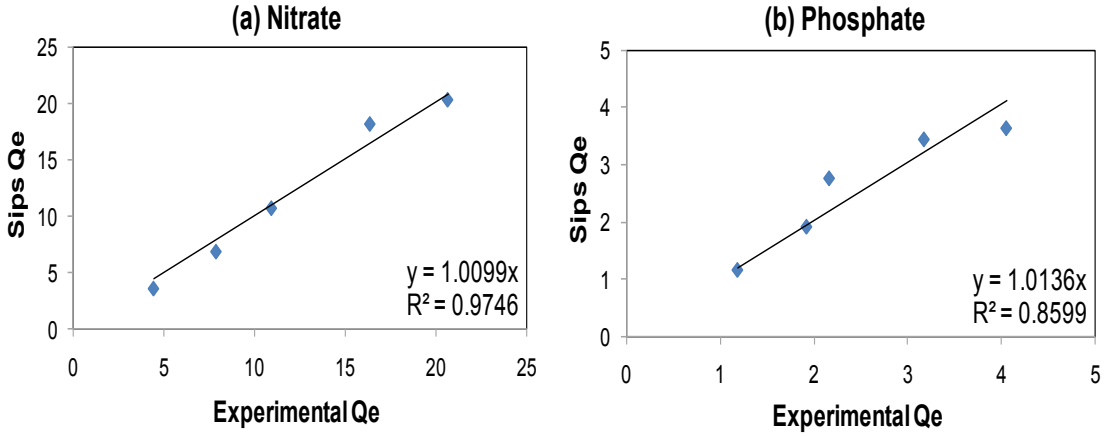

Figure 4-6: Sips model Qe compared with experimental Qe for (a) nitrate and (b) phosphate removal at varying dose of Purolite (A500PS)

Table 4-4: Comparison of experimental values of Qe with values obtained from isotherm models at different doses of Purolite (A500PS) for nitrate removal

Qe values	0.5 g/L	1 g/L	3 g/L	5 g/L	10 g/L	m	R^2
Experimental	20.68	16.39	10.96	7.91	4.46		
Langmuir	20.64	18.39	10.91	7.15	3.90	1.03	0.98
Freundlich	19.77	17.71	11.30	8.14	5.24	1.01	0.98
Sips	20.37	18.22	10.72	6.86	3.57	1.01	0.97

(R^2: coefficient of correlation; m is the slope of the regression line y = mx)

Table 4-5: Comparison of experimental values of Qe with values obtained from isotherm models at different doses of Purolite (A500PS) for phosphate removal

Qe values	0.5 g/L	1 g/L	3 g/L	5 g/L	10 g/L	m	R^2
Experimental	4.05	3.17	2.16	1.92	1.18		
Langmuir	3.41	3.26	2.72	2.02	1.36	0.98	0.75
Freundlich	3.31	3.11	2.50	1.85	1.30	0.93	0.82
Sips	3.64	3.45	2.77	1.92	1.17	1.01	0.86

(R^2: coefficient of correlation; m is the slope of the regression line y = mx)

The kinetic data for the adsorption of both nitrate (Figure 4-7) and phosphate (Figure 4-8) were satisfactorily described by the Ho model. The Ho model parameters for the adsorption kinetics data are presented in Table 4-6. K_H value was found to decrease with increase Purolite dose showing that the rate of adsorption increased with Purolite dose.

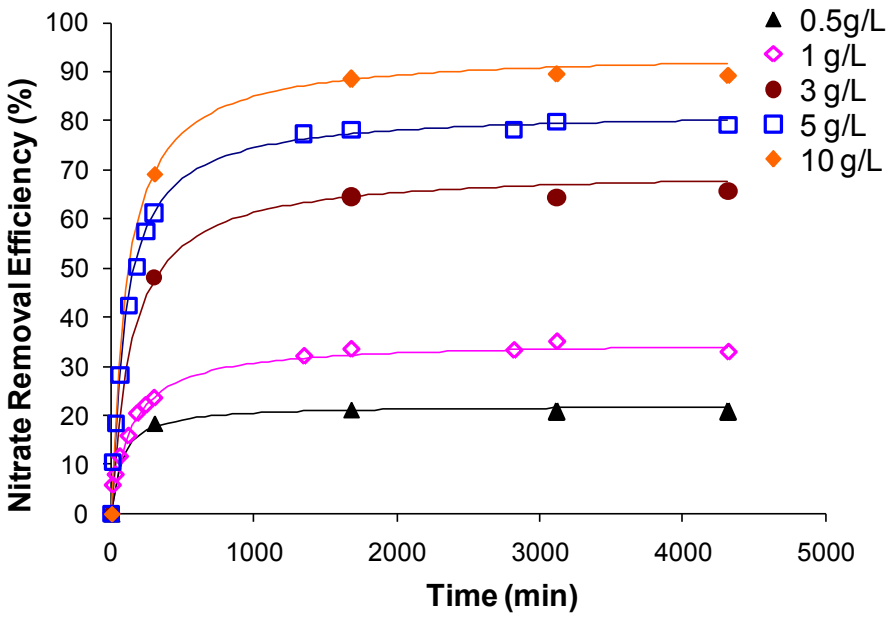

Figure 4-7: Kinetics modelling using Ho model for nitrate removal at varying dose of Purolite (A500PS)

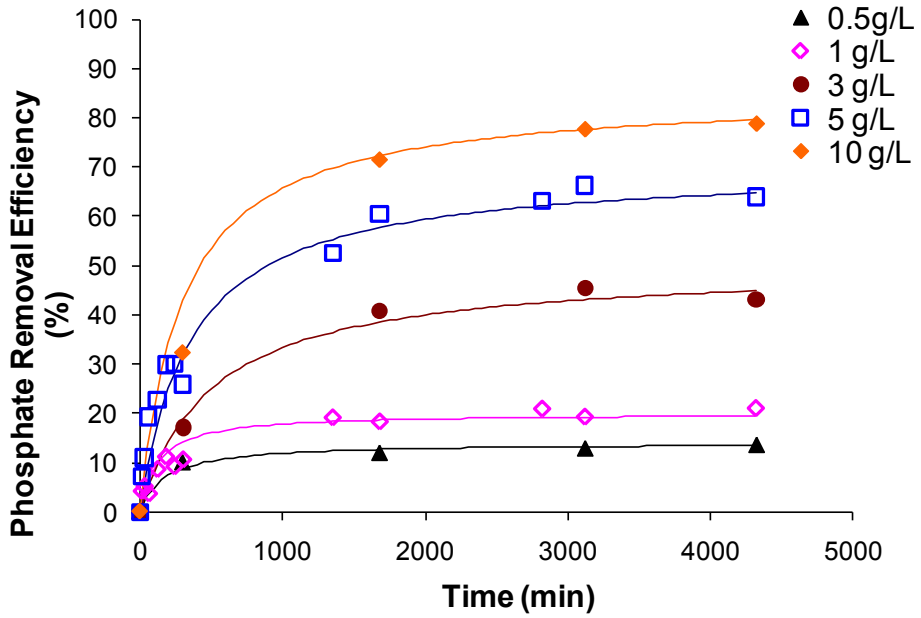

Figure 4-8: Kinetics modelling using Ho model for phosphate removal at varying dose of Purolite (A500PS)

Table 4-6: The values of the parameters in the Ho model for nitrate and phosphate removal at varying dose of Purolite (A500PS)

Purolite (A500PS)		0.5 g/L	1 g/L	3 g/L	5 g/L	10 g/L
Nitrate-N	q	22	35	70	82	94
	k_H	0.0003	0.0001	0.00005	0.00006	0.00005
Phosphate-P	q	14	20	50	70	85
	k_H	0.0002	0.0002	0.00002	0.00002	0.00002

Another kinetics study was carried out but using a highly concentrated synthetic feed of nitrate and phosphate (100 mg N/L and 50 mg P/L, respectively) with 5 g/L dose of Purolite (A500PS). Figure 4-9 shows the trend of nitrate and phosphate removal during this kinetics study. The concentration of nitrate-N and phosphate-P at 360 min was 48.63 mg/L and 41.31 mg/L, respectively. This further confirms that Purolite is nitrate selective as there was 51% removal efficiency for nitrate at 360 min, compared to 17% for phosphate.

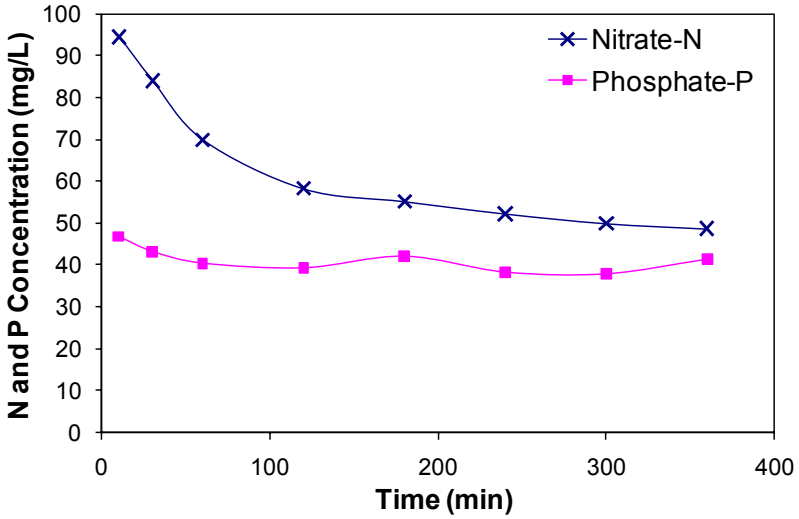

Figure 4-9: Kinetics of adsorption of nitrate and phosphate on Purolite (A500PS) at 5 g/L dose using initial concentrations of 100 mg N/L nitrate and 50 mg P/L phosphate

The Ho model was used to describe the adsorption kinetics with Purolite (A500PS) at 5 g/L using a higher concentrated synthetic feed of 100 mg N/L and 50 mg P/L. This model again satisfactorily explained the kinetics of adsorption of nitrate and phosphate on Purolite (Figure 4-10 and 4-11). The Ho model parameters for the data are presented in Table 4-7. The k_H values were higher than the value obtained for lower feed concentration of nitrate and phosphate presented in Table 4-6 for Purolite at the same dose of 5 g/L. This shows that an increase of feed concentration decreased the rate of adsorption.

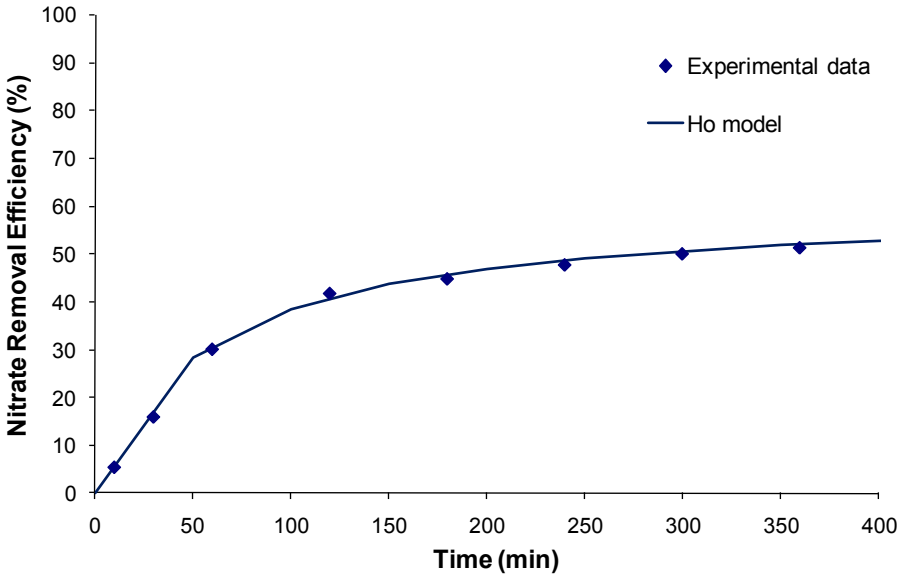

Figure 4-10: Kinetics modelling using Ho model for nitrate removal at 5 g/L of Purolite (A500PS) (nitrate concentration in feed was 100 mg/L)

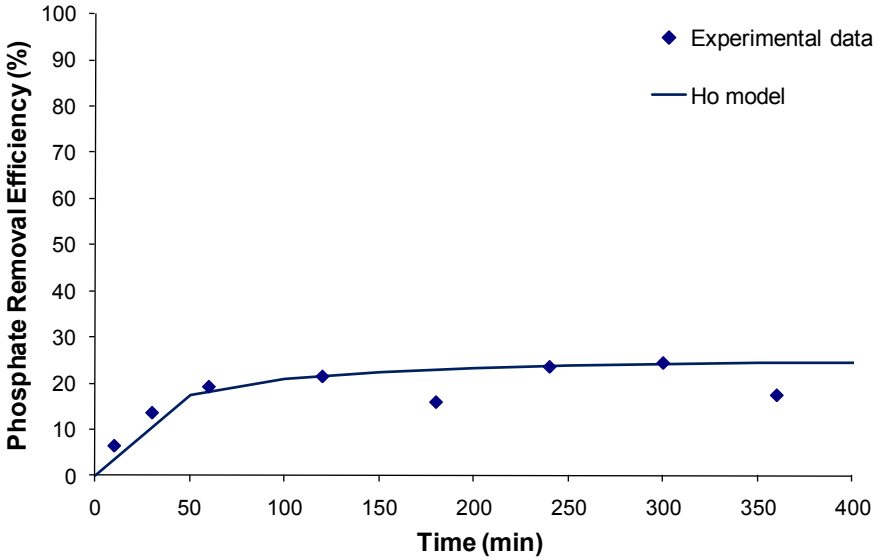

Figure 4-11: Kinetics modelling using Ho model for phosphate removal at 5 g/L of Purolite (A500PS) (phosphate concentration in feed was 50 mg/L)

Table 4-7: The values of the parameters in the Ho model for nitrate and phosphate removal at 5 g/L dose of Purolite (A500PS) (feed concentrations of 100 mg/L nitrate-N and 50 mg/L phosphate-P)

Purolite (A500PS)		5 g/L
Nitrate-N	q	60
	k_H	0.00015
Phosphate-P	q	26
	k_H	0.0008

4.1.2. HAIX adsorbent

Batch studies were conducted to determine the rate of adsorption and maximum adsorption capacity of nitrate and phosphate in the synthetic feed (50 mg/L nitrate-N and 15 mg/L phosphate-P) on HAIX. Varied doses of HAIX at 1 g/L, 3 g/L, 5 g/L, 7 g/L, 10 g/L, 15 g/L and 20 g/L (0.15 g, 0.45 g, 0.75 g, 1.05 g, 1.5 g, 2.25 g and 3.0 g, respectively in 150 mL) with synthetic feed were used in the studies.

Figure 4-12 shows the trend of nitrate and phosphate removal during the batch studies with HAIX. As the dose of HAIX increased, the removal efficiency of nitrate and phosphate significantly increased as observed for Purolite in Section 4.1.1. This is expected as a higher dose of HAIX increases the number of adsorptions sites. The nitrate and phosphate concentrations at equilibrium of 1 g/L HAIX were 47.6 mg N/L and 13.6 mg P/L, respectively. These equilibrium concentrations drastically decreased at 20 g/L dose (16.9 mg N/L and 0 mg P/L). This study showed that as the HAIX dose increased the equilibrium concentration of nitrate and phosphate decreased indicating that at higher doses of the media, there was better removal efficiency.

Furthermore, this study showed that HAIX is phosphate selective unlike Purolite (Section 4.1.1) which was nitrate selective. Table 4-8 summarises the nitrate and phosphate removal efficiencies at equilibrium with the varied dose of HAIX used. The results showed that at every dose of HAIX used, the phosphate removal efficiency is higher than the nitrate removal efficiency. At 10, 15 and 20 g/L, the phosphate removal efficiency at equilibrium was 100%, signifying that HAIX is phosphate selective.

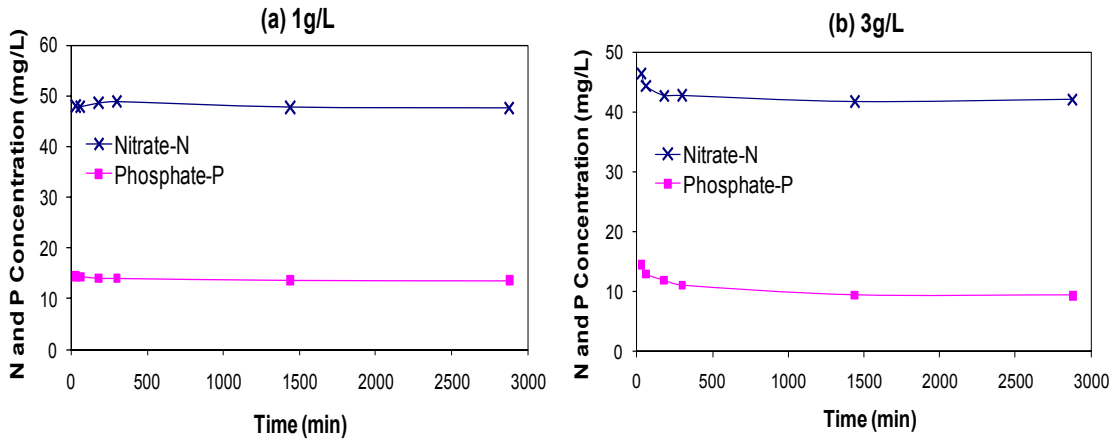

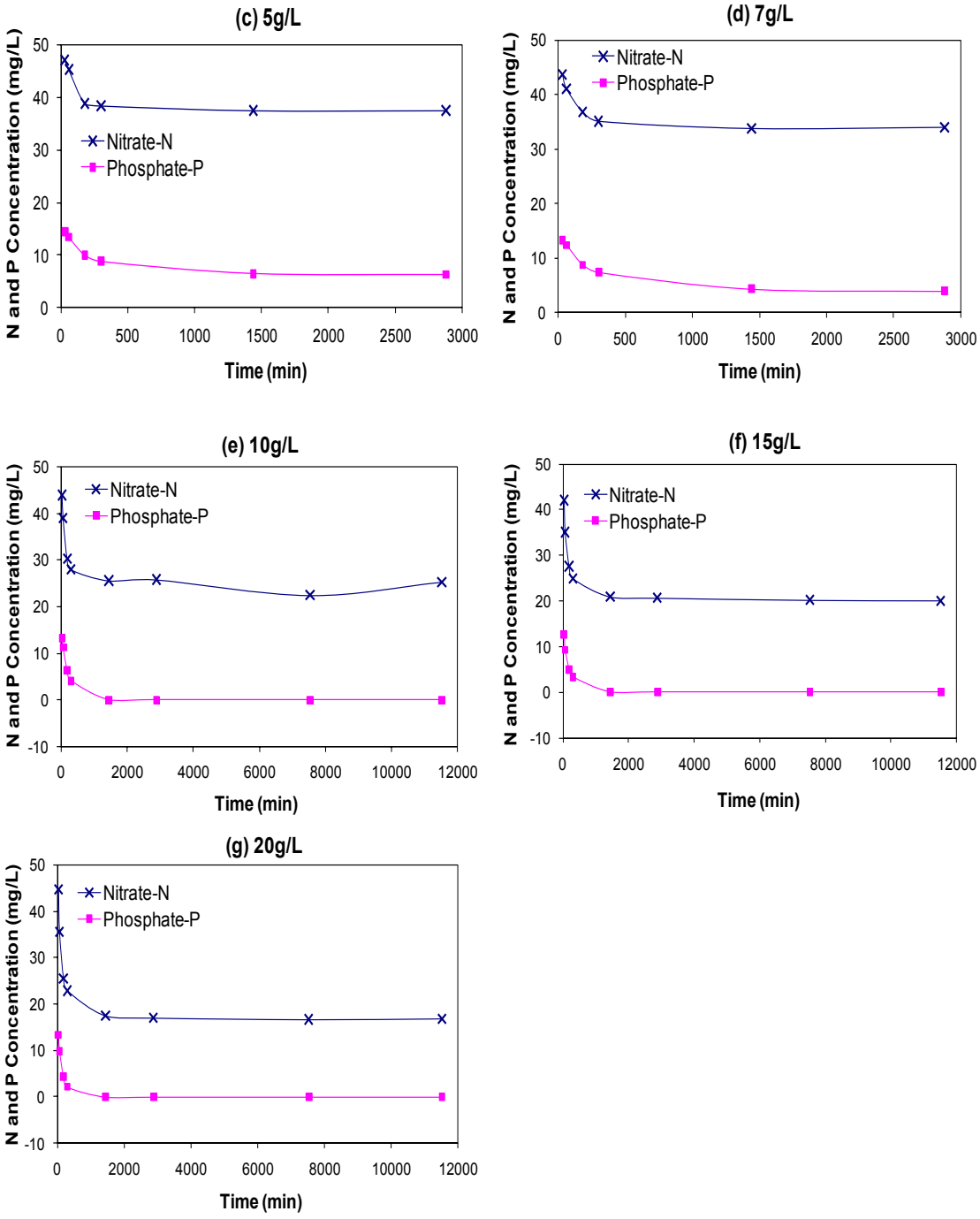

Figure 4-12: Kinetics of nitrate and phosphate adsorption on HAIX at different doses of HAIX (a) 1 g/L, (b) 3 g/L, (c) 5 g/L, (d) 7 g/L, (e) 10 g/L, (f) 15 g/L and (g) 20 g/L

Table 4-8: Nitrate and phosphate removal efficiencies (at equilibrium*) with varying dose of HAIX during batch adsorption study

HAIX dose (g/L)	Nitrate Removal Efficiency at Equilibrium (%)	Phosphate Removal Efficiency at Equilibrium (%)
1	4.9	9.1
3	15.8	37.7
5	24.9	58.0
7	32.0	73.7
10	49.3	100

* Equilibrium time used was 2880 min.

Modelling Experimental Data

The Langmuir, Freundlich and Sips isotherm models were used to model the equilibrium isotherm of nitrate and phosphate removal by HAIX. The results are presented in Figure 4-13 and Figure 4-14.

From the Langmuir isotherm model, the experimental results indicated the maximum adsorption capacity (q_m) of 25 mg NO_3^- per g – dry resin and energy of adsorption value (b) of 0.05 L/mg. The value of r for the initial concentration of 50 mg/L nitrate was found to be 0.57. Therefore, the resin HAIX showed favourable adsorption.

From the Freundlich isotherm model, the experimental results indicated the value of K_F was 5 and n was 3 for nitrate removal. From the Sips isotherm model, the experiment results indicated that the value of q_m was 38, b was 0.06 and 1/n was 0.7 for nitrate removal. The model parameters for the data are presented in Table 4-9 and Table 4-10.

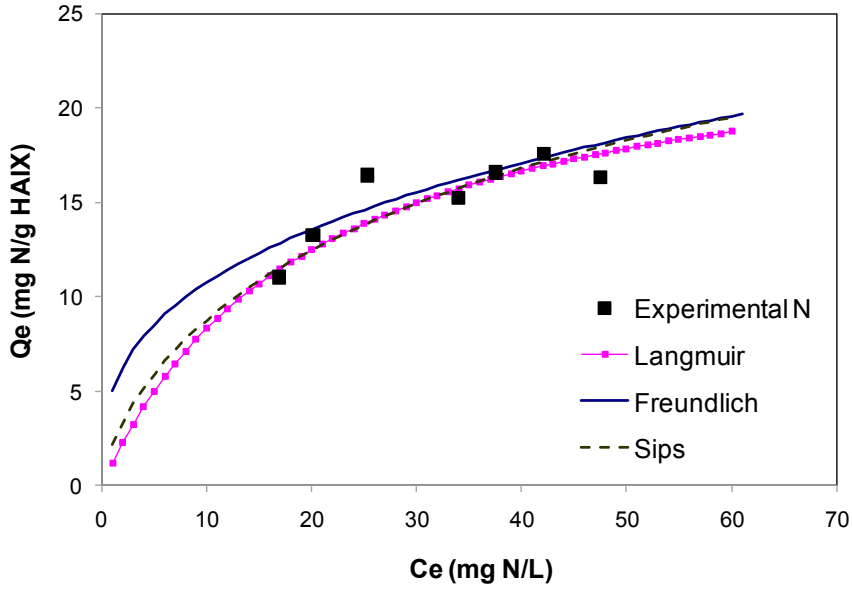

Figure 4-13: Equilibrium isotherm modelling plot for nitrate removal by HAIX

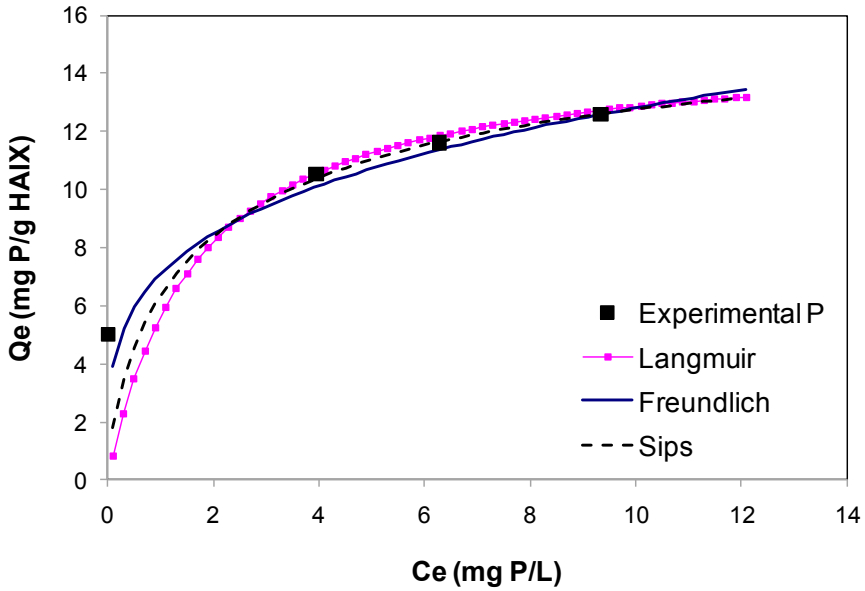

Figure 4-14: Equilibrium isotherm modelling plot for phosphate removal by HAIX

Table 4-9: The values of the parameters in the Langmuir and Freundlich equation and r values for nitrate and phosphate removal

HAIX	q_m (mg/g)	b (L/mg)	K_F (mg/g)	n	r
Nitrate-N	25	0.05	5	3	0.57
Phosphate-P	15	0.6	7.1	3.9	0.1

Table 4-10: The values of the parameters in the Sips equation for nitrate and phosphate removal

HAIX	q_m (mg/g)	b (L/mg)	1/n
Nitrate-N	38	0.06	0.7
Phosphate-P	17	0.6	0.7

The results show that the experimental data satisfactorily fitted to all three models. The model predicted Qe and experimentally measured Qe were compared using the regression equation y = mx where y is the model predicted Qe, x is the experimentally measured Qe, and m is the slope. The results showed that m and the coefficient of determination R^2 were approximately equal to 1in all cases confirming the satisfactory fit of the data to all three models (Figures 4-15 – 4-17, Tables 4-11 – 4-12). However, the R^2 values were lower for than nitrate for phosphate.

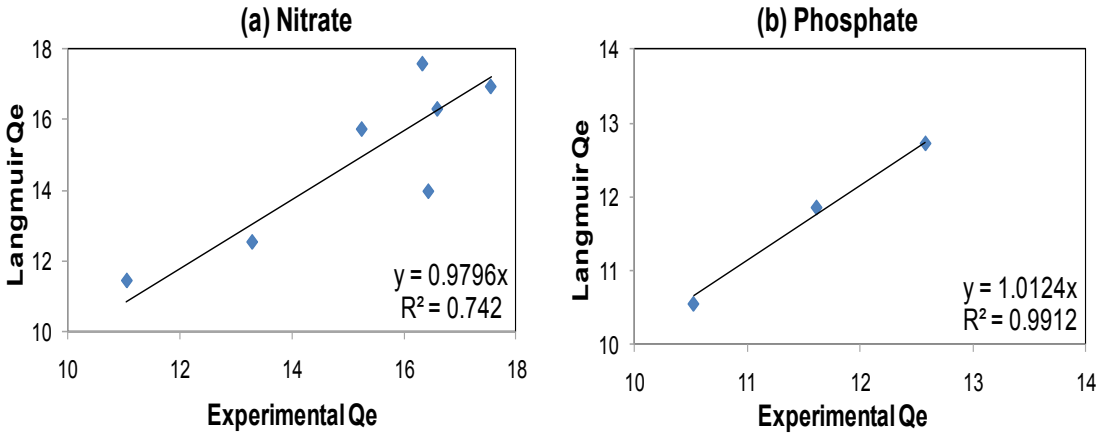

Figure 4-15: Langmuir model Qe compared with experimental Qe for (a) nitrate and (b) phosphate removal at varying dose of HAIX (outliers for phosphate have been removed)

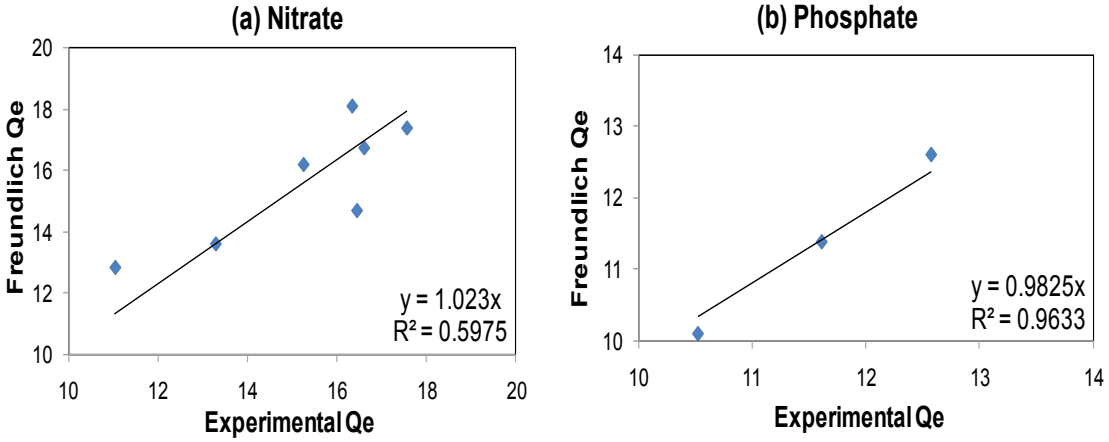

Figure 4-16: Freundlich model Qe compared with experimental Qe for (a) nitrate and (b) phosphate removal at varying dose of HAIX (outliers for phosphate have been removed)

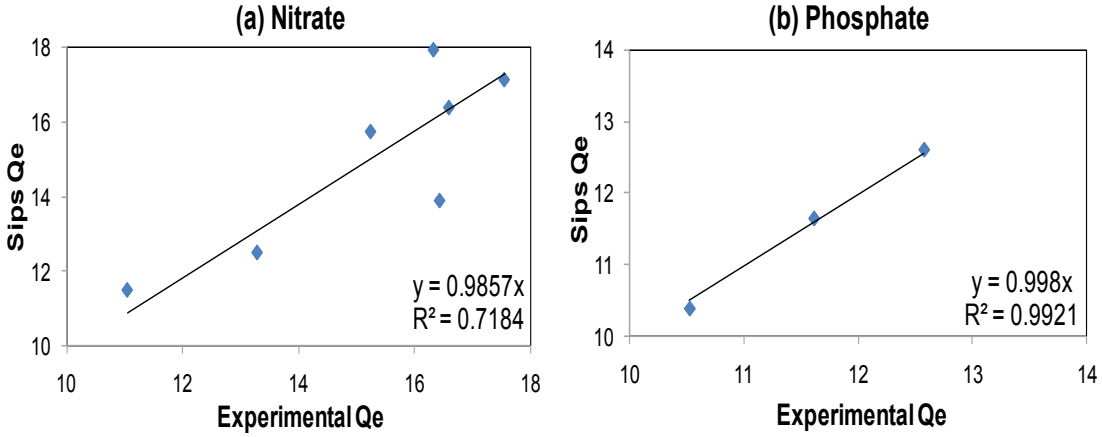

Figure 4-17: Sips model Qe compared with experimental Qe for (a) nitrate and (b) phosphate removal at varying dose of HAIX (outliers for phosphate have been removed)

Table 4-11: Comparison of experimental values of Qe with values obtained from isotherm models at different doses of HAIX for nitrate removal

Qe values	1 g/L	3 g/L	5 g/L	7 g/L	m	R^2
Experimental	16.33	17.56	16.60	15.25		
Langmuir	17.60	16.95	16.31	15.74	0.98	0.74
Freundlich	18.11	17.39	16.74	16.20	1.02	0.60
Sips	17.95	17.15	16.40	15.75	0.99	0.72

(R^2: coefficient of correlation; m is the slope of the regression line y = mx)

Table 4-12: Comparison of experimental values of Qe with values obtained from isotherm models at different doses of HAIX for phosphate removal (outliers have been removed)

Qe values	3 g/L	5 g/L	7 g/L	m	R^2
Experimental	12.58	11.61	10.52		
Langmuir	12.73	11.86	10.55	1.01	0.99
Freundlich	12.59	11.38	10.10	0.98	0.96
Sips	12.60	11.64	10.38	1.00	0.99

(R^2: coefficient of correlation; m is the slope of the regression line y = mx)

The kinetic data for the adsorption of both nitrate (Figure 4-18) and phosphate (Figure 4-19) were satisfactorily described by the Ho model. The Ho model parameters for the adsorption kinetics data are presented in Table 4-13. K_H value was found to decrease with increase HAIX dose showing that the rate of adsorption increased with HAIX dose.

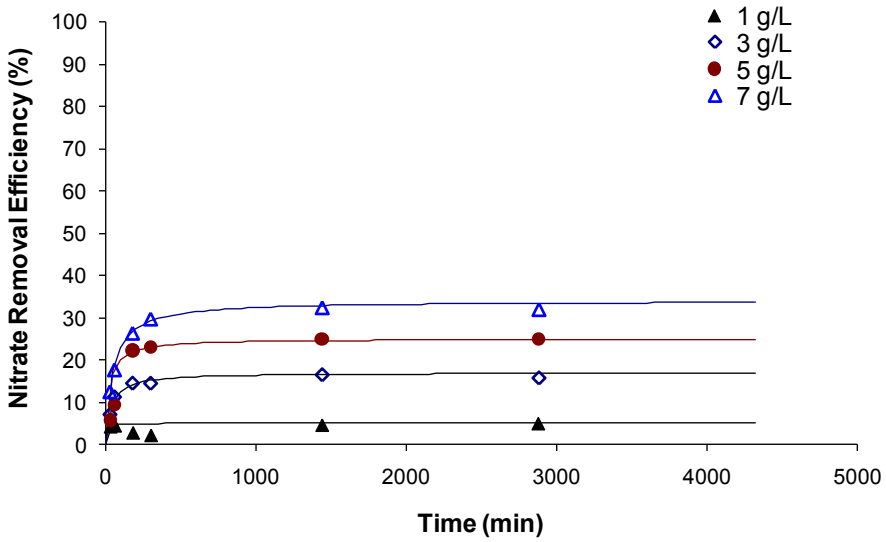

Figure 4-18: Kinetics modelling using Ho model for nitrate removal at varying dose of HAIX

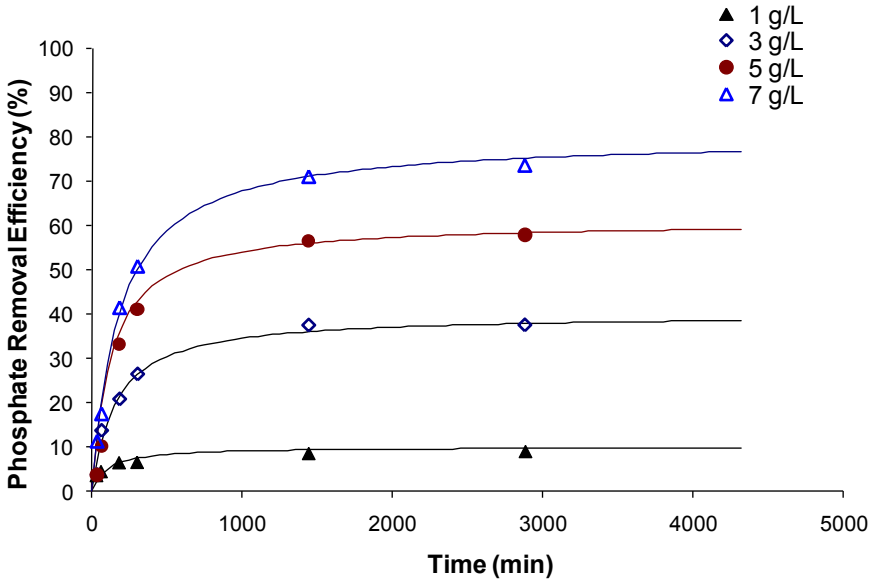

Figure 4-19: Kinetics modelling using Ho model for phosphate removal at varying dose of HAIX

Table 4-13: The values of the parameters in the Ho model for nitrate and phosphate removal at varying dose of HAIX

HAIX		1 g/L	3 g/L	5 g/L	7 g/L
Nitrate-N	q	5	17	25	34
	k_H	0.05	0.0008	0.0008	0.0003
Phosphate-P	q	10	40	61	80
	k_H	0.0005	0.00008	0.000065	0.000035

As for Purolite, another kinetics study was carried out but using a highly

concentrated synthetic feed of nitrate and phosphate (100 mg N/L and 50 mg P/L, respectively) with 5 g/L dose of HAIX. Figure 4-20 shows the trend of nitrate and phosphate removal during this kinetics study. The concentration of nitrate and phosphate at 360 min was 82.36 mg/L and 24.02 mg/L, respectively. This confirms that HAIX is phosphate selective as there was 52% removal efficiency for phosphate at 360 min, compared to 18% for nitrate.

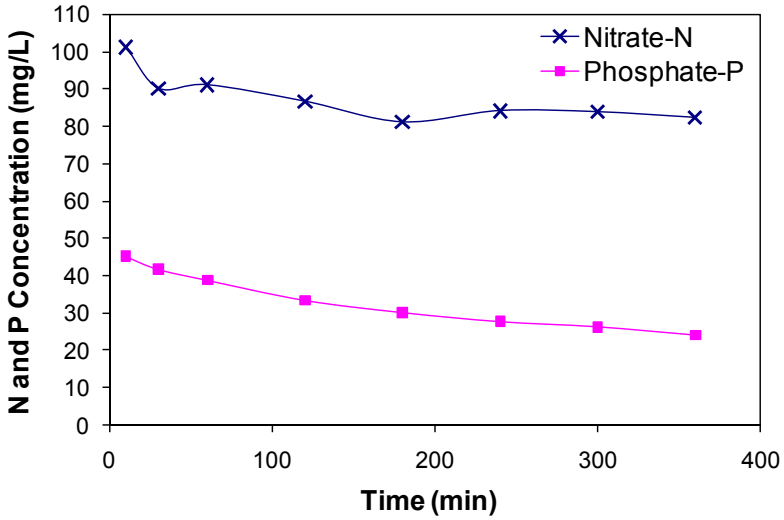

Figure 4-20: Adsorption kinetics with HAIX at 5g/L dose using a higher concentrated synthetic feed (initial concentrations of 100 mg/L nitrate and 50 mg/L phosphate)

As for Purolite, the Ho model was used to describe the adsorption kinetics with HAIX at 5 g/L using a higher concentrated synthetic feed of 100 mg N/L nitrate and 50 mg P/L phosphate. This model again satisfactorily explained the kinetics of adsorption of nitrate and phosphate on Purolite (Figure 4-21 and 4-22). The Ho model parameters for the data are presented in Table 4-14. The k_H values were lower than the values obtained for lower feed concentration of nitrate and phosphate presented in Table 4-13 for HAIX at the same dose of 5 g/L. This shows that an increase of feed concentration increased the rate of adsorption.

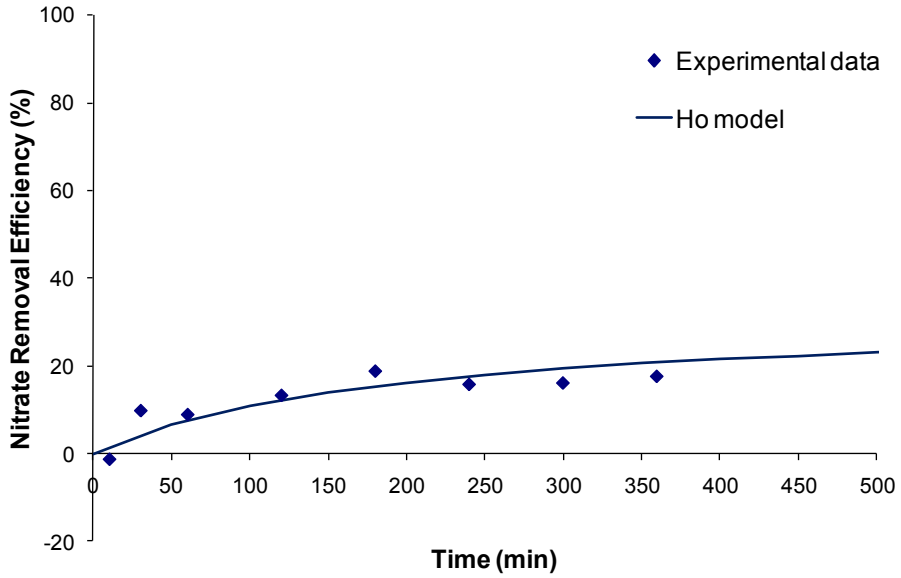

Figure 4-21: Kinetics modelling using Ho model for nitrate removal at 5 g/L of HAIX

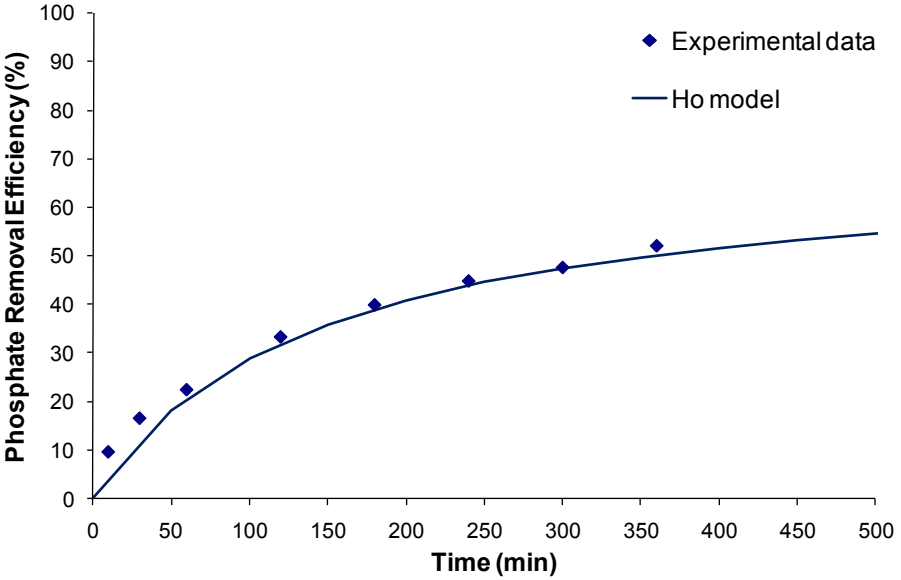

Figure 4-22: Kinetics modelling using Ho model for phosphate removal at 5 g/L of HAIX

Table 4-14: The values of the parameters in the Ho model for nitrate and phosphate removal at 5 g/L dose of HAIX

HAIX		5 g/L
Nitrate-N	q	32
	k_H	0.00008
Phosphate-P	q	70
	k_H	0.00005

4.1.3. HFO adsorbent

Batch studies were also conducted to observe the trend of adsorption of nitrate and phosphate in the synthetic feed on HFO. Varied doses of HFO at 0.5 g/L, 1 g/L, 3 g/L, 5 g/L and 10 g/L (0.075 g, 0.15 g, 0.45 g, 0.75 g and 1.5 g, respectively in 150 mL) with synthetic feed were used in the studies.

Figure 4-23 shows that very little (5 - 8%) nitrate was adsorbed on HFO at any of the doses of HFO. For phosphate, an increase in time up to approximately 1680 min for 0.5 g/L dose of HFO and up to 4320 min for 1, 3, and 5 g/L dose of HFO, the adsorption increased and beyond these times, they reached equilibrium. At the 10 g/L dose, almost all phosphate was adsorbed.

As the dose of HFO increased from 0.5 to 10 g/L, there was a significant increase in removal efficiency of phosphate (Figure 4-23). This is expected as a higher dose of HFO increases the number of adsorption sites. The nitrate and phosphate concentrations at equilibrium with 0.5 g/L HFO was 47.5 mg N/L and 9 mg P/L, respectively. These equilibrium concentrations decreased at 10 g/L dose (46.2 mg N/L and 0 mg P/L).

Nitrate did not adsorb on HFO because nitrate is non-specifically adsorbed on the positive charges on HFO and at the neutral pH of the feed, HFO has very small number of positive charges since HFO has a zero point of charge of around 7 (Streat, Hellgardt & Newton 2008b). In contrast to nitrate, phosphate is specifically adsorbed on both positive and neutral charged sites and therefore regardless of pH, it is adsorbed in large quantities.

Furthermore, this study confirmed that HFO is phosphate selective as found in Section 4.1.2 with HAIX, which contained HFO nanoparticles. Table 4-15 summarises the nitrate and phosphate removal efficiencies at equilibrium with the varied dose of HFO used. The results showed that at every dose of HFO used, the phosphate removal efficiency is much higher than the nitrate removal efficiency. At 5 and 10 g/L, the phosphate removal efficiency at equilibrium was 100%, signifying that HFO is phosphate selective.

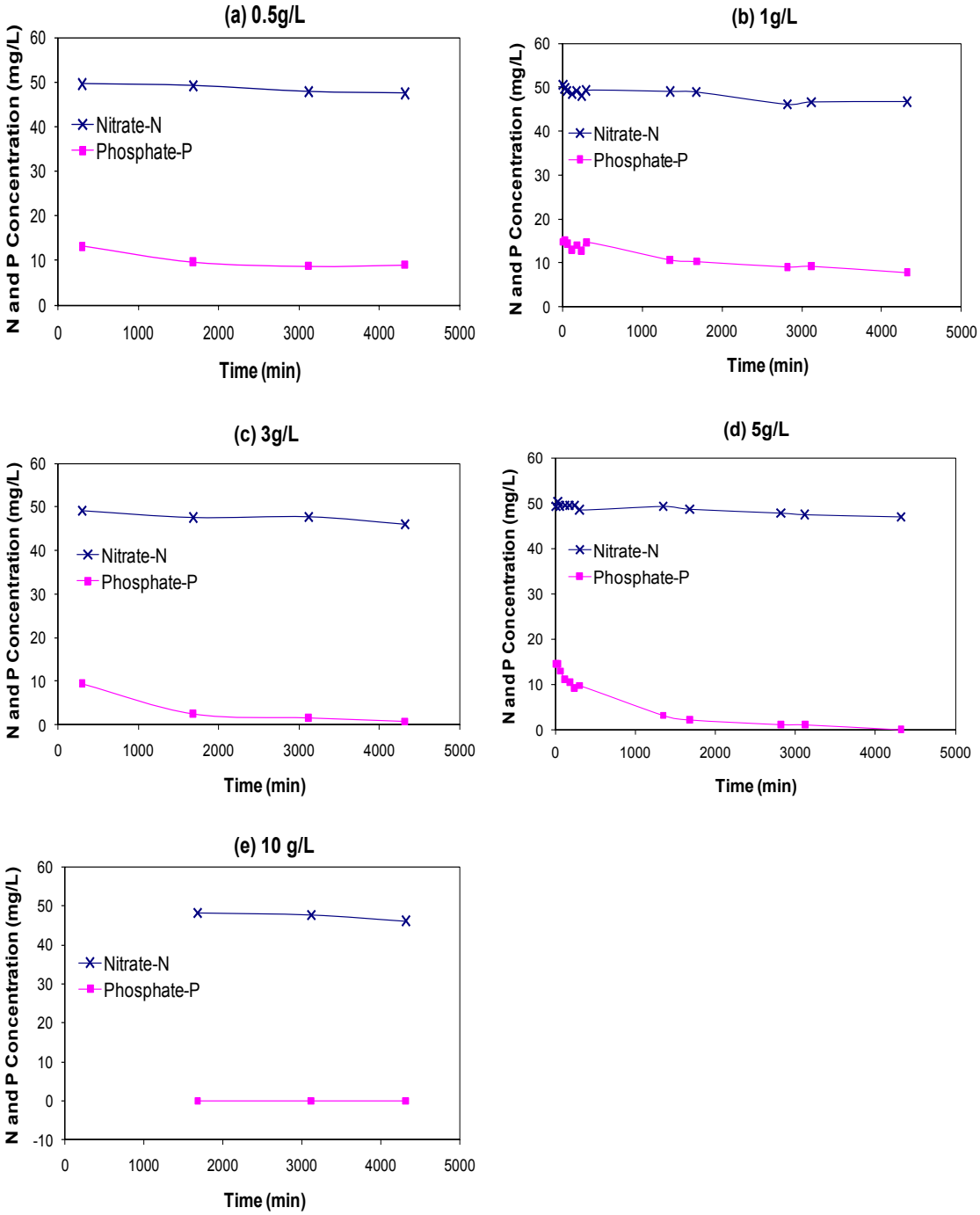

Figure 4-23: Kinetics of nitrate and phosphate adsorption on HFO at different doses of HFO (a) 0.5 g/L, (b) 1 g/L, (c) 3 g/L, (d) 5 g/L and (e) 10 g/L (feed concentration 50 mg N/L and 15 mg P/L)

Table 4-15: Nitrate and phosphate removal efficiencies (at equilibrium*) with varying dose of HFO

HFO dose (g/L)	Nitrate Removal Efficiency at Equilibrium (%)	Phosphate Removal Efficiency at Equilibrium (%)
0.5	5.1	39.7
1	6.5	48.1
3	8.0	94.9
5	5.8	100
10	7.7	100

* Equilibrium time used was 4320 min.

Modelling Experimental Data

The Langmuir, Freundlich and Sips isotherm models were used to model the equilibrium isotherm of phosphate removal by HFO as done for Purolite and HIAX adsorbents (Section 4.1.1 and 4.1.2). The results shown in Figure 4-24 indicate that the models fitted the data not so well as compared to the other adsorbents. This is confirmed by the relatively poor relationships between model predicted Qe and measured Qe (Figure 4-25 - 4.27).

The equilibrium data for phosphate was modelled only as HFO is phosphate selective and was not able to adsorb much nitrate during the batch equilibrium studies.

From the Langmuir isotherm model, the experimental results indicated the maximum adsorption capacity (q_m) of 14 mg P per g – dry resin and energy of adsorption value (b) of 0.6 L/mg. The value of r for the initial concentration of 15 mg P/L phosphate was found to be 0.1. Therefore, the ion exchanger HFO showed favourable adsorption of phosphate.

From the Freundlich isotherm model, the experimental results indicated the value of K_F was 5.7 and n was 3 for phosphate removal. From the Sips isotherm model, the experiment results indicated that the value of q_m was 15, b was 0.6 and 1/n was 0.8 for phosphate removal. The model parameters for the data are presented in Table 4-16 and Table 4-17.

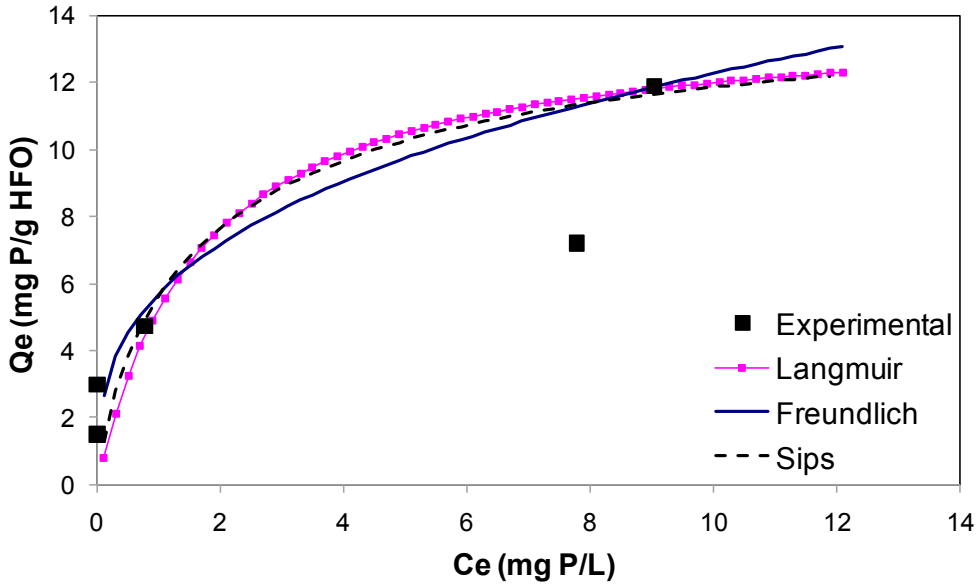

Figure 4-24: Equilibrium isotherm modelling plot for phosphate removal by HFO

Table 4-16: The values of the parameters in the Langmuir and Freundlich equation and r values for nitrate and phosphate removal

HFO	q_m (mg/g)	b (L/mg)	K_F (mg/g)	n	r
Phosphate-P	14	0.6	5.7	3	0.1

Table 4-17: The values of the parameters in the Sips equation for nitrate and phosphate removal

HFO	q_m (mg/g)	b (L/mg)	1/n
Phosphate-P	15	0.6	0.8

The results show that the experimental data satisfactorily fitted to all three models. The model predicted Qe and experimentally measured Qe were compared using the regression equation y = mx where y is the model predicted Qe, x is the experimentally measured Qe, and m is the slope (Figures 4-25 – 4-27, Tables 4-18).

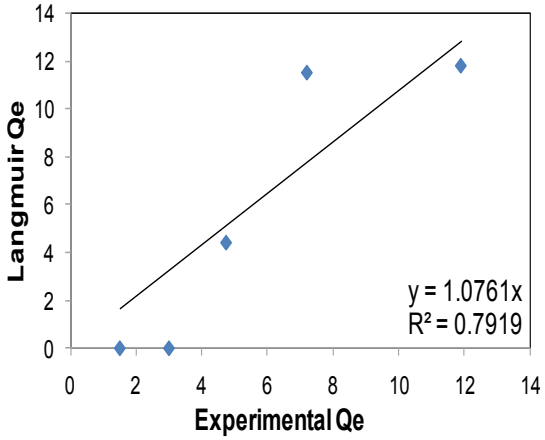

Figure 4-25: Langmuir model Qe compared with experimental Qe for phosphate removal at varying dose of HFO

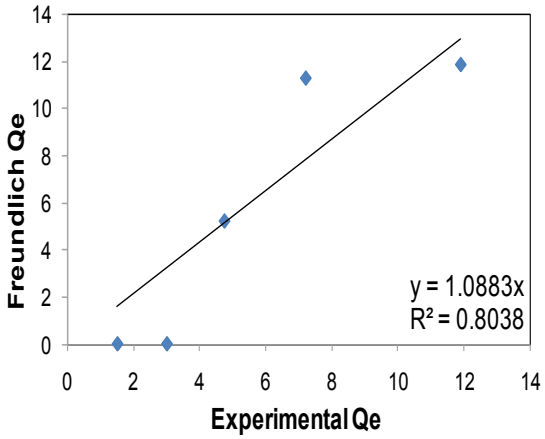

Figure 4-26: Freundlich model Qe compared with experimental Qe for phosphate removal at varying dose of HFO

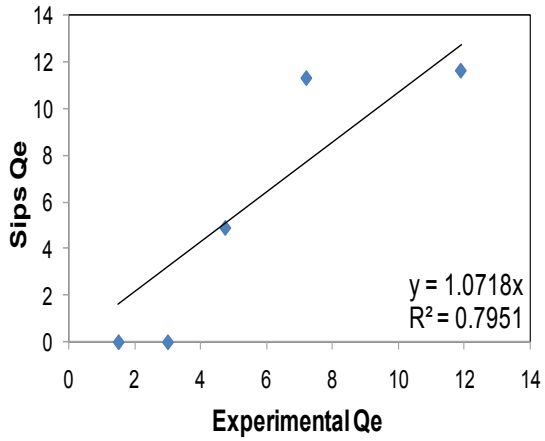

Figure 4-27: Sips model Qe compared with experimental Qe for phosphate removal at varying dose of HFO

Table 4-18: Comparison of experimental values of Qe with values obtained from isotherm models at different doses of HFO for phosphate removal

Qe values	0.5 g/L	1 g/L	3 g/L	5 g/L	10 g/L	m	R^2
Experimental	11.91	7.21	4.74	3.00	1.50		
Langmuir	11.82	11.53	4.42	0.00	0.00	1.08	0.792
Freundlich	11.88	11.30	5.22	0.00	0.00	0.80	0.804
Sips	11.66	11.34	4.91	0.00	0.00	1.07	0.795

(R^2: coefficient of correlation; m is the slope of the regression line y = mx)

The kinetic data for the adsorption of both nitrate (Figure 4-28) and phosphate (Figure 4-29) were satisfactorily described by the Ho model. The Ho model parameters for the adsorption kinetics data are presented in Table 4-19. K_H value was found to decrease with increase HFO dose showing that the rate of adsorption increased with HFO dose.

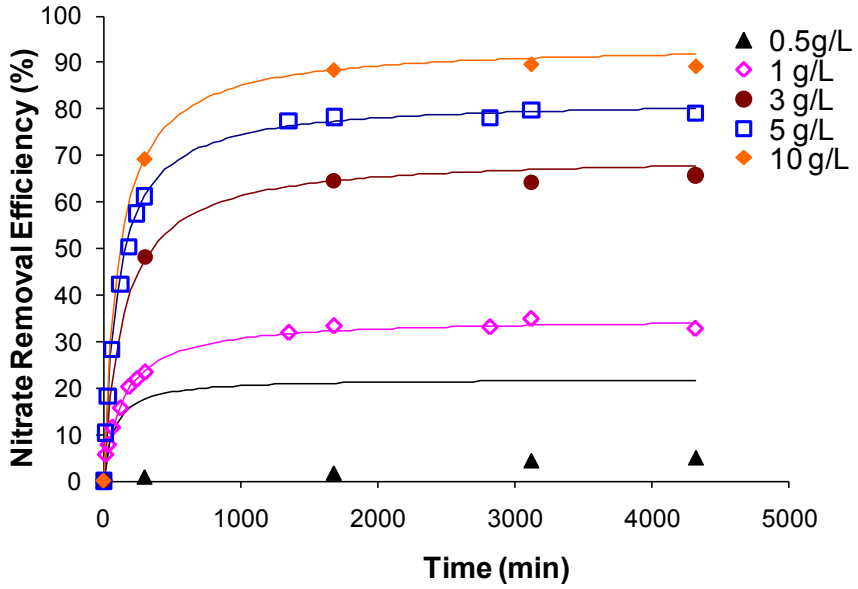

Figure 4-28: Kinetics modelling using Ho model for nitrate removal at varying dose of HFO

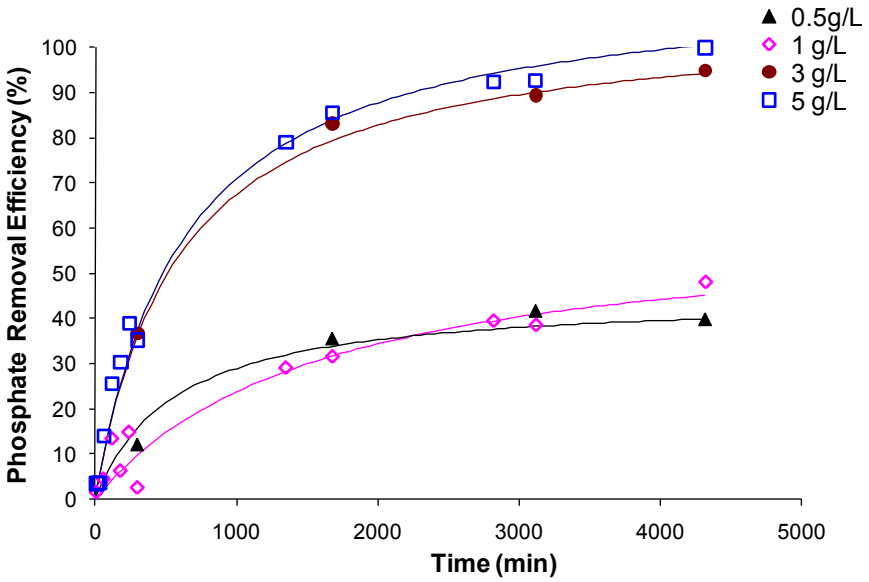

Figure 4-29: Kinetics modelling using Ho model for phosphate removal at varying dose of HFO

Table 4-19: The values of the parameters in the Ho model for nitrate and phosphate removal at varying dose of HFO

HFO		0.5 g/L	1 g/L	3 g/L	5 g/L	10 g/L
Nitrate-N	q	22	35	70	82	94
	k_H	0.0003	0.0001	0.00005	0.00006	0.00005
Phosphate-P	q	45	62	107	115	
	k_H	0.00002	0.000005	0.000008	0.000007	

4.2. Purolite - Anthracite Column as Adsorption Media for Nitrate and Phosphate Removal from Synthetic Water

The batch kinetics and equilibrium test results presented in the last section showed that Purolite had an affinity for nitrate removal. Purolite also had the ability to remove small quantity of phosphate simultaneously with nitrate. In the next phase of the study, these tests were repeated in column packed with Purolite and anthracite to determine the removal efficiencies of nitrate and phosphate from synthetic water

Columns were packed with anthracite and varied percentage by mass of Purolite (A500PS, 300 < p < 420 μm) at 1%, 3%, 5% and 10% to test the efficiency of Purolite to remove phosphate and nitrate. The mass of Purolite used was 1.4, 3.6, 6 and 12 g, respectively. The column height was 60 cm and the flow rate was 1 m/hr.

4.2.1. Breakthrough curves

The results showed that with varying percentage by mass of Purolite at 1, 3, 5, and 10%, the adsorption column achieved a breakthrough of nutrients at 15, 120, 240 and 600 min respectively as presented in Figure 4-30 and Table 4-20 for nitrate and at 15, 30, 90 and 180 min for phosphate, respectively.

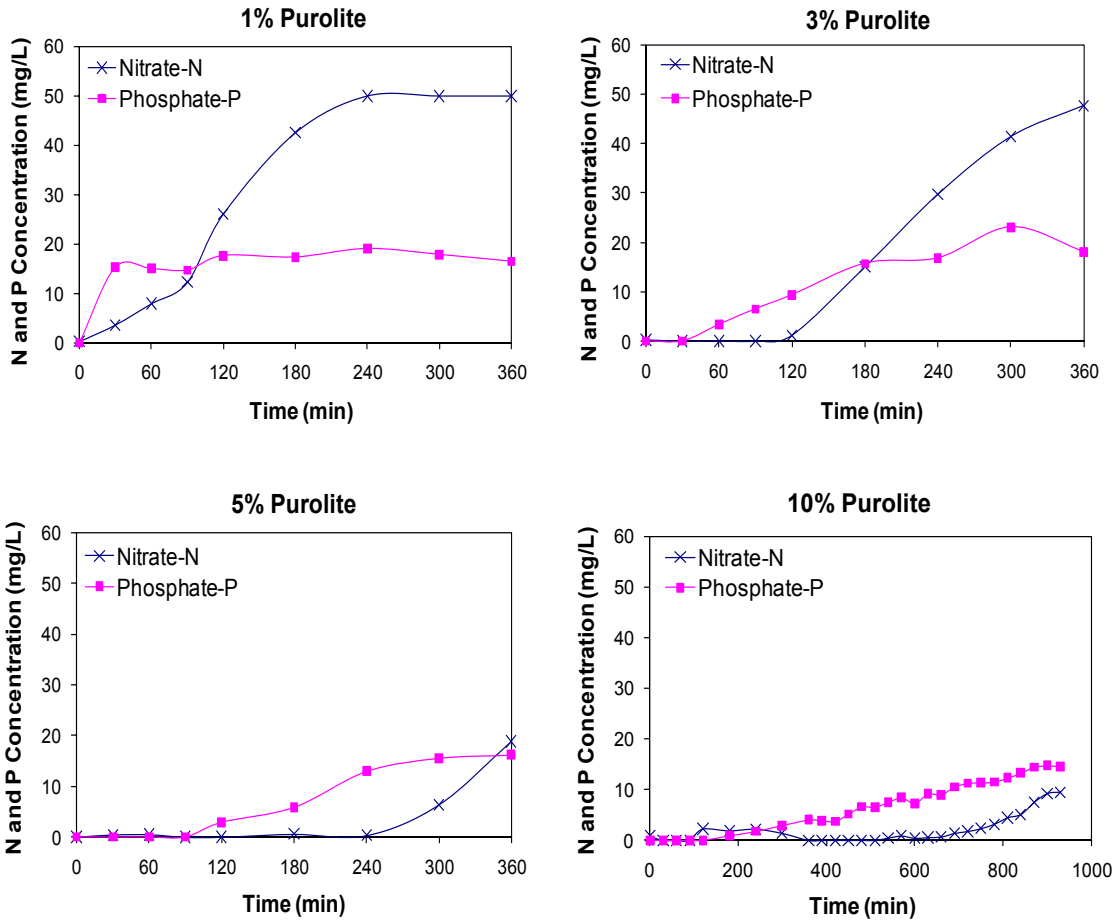

Figure 4-30: Nitrate and phosphate breakthrough curves with varied percentage by mass of Purolite (A500PS, 300 – 420 µm) (initial nitrate and phosphate concentrations were 50 mg N/L and 15 mg P/L, respectively)

Table 4-20: Breakthrough points from the column experiments using varied percentage by mass of Purolite

Purolite Mass (g)	Purolite (%)	Nitrate Breakthrough point (min)	Phosphate Breakthrough point (min)
1.4	1	15	15
3.6	3	120	30
6	5	240	90
12	10	600	180

After 30 min into the experiment of 1% Purolite, a build up of nutrients was observed in the effluent (Figure 4-30). This shows that 1% Purolite is not sufficient for the removal of nitrate and phosphate in the synthetic feed even at the very start of the experiment.

In the 3% Purolite experiment, the nitrate breakthrough occurred at 120 min in contrast to the phosphate breakthrough at 30 min into the run. There was a chromatographic peaking of phosphate towards the end of the experiment after 240 min into the run. This phenomenon is different from that in conventional anion exchange resins in which the nitrate breakthrough occurs earlier than the phosphate breakthrough (Blaney, Cinar & SenGupta 2007; Bae et al. 2002). At 240 min, the phosphate concentration in the effluent reached higher than the influent concentration found in the synthetic feed. When the phosphate ions reached the complete breakthrough point (effluent concentration equals influent concentration), the Purolite dumps the phosphate ions displaced by the nitrate ions, causing a chromatographic peaking of phosphate (Blaney, Cinar & SenGupta 2007; Pan et al. 2009; Bae et al. 2002). This is due to the higher affinity of nitrate than phosphate of this nitrate selective ion exchange resin.

Similar chromatograph peaking have been reported by Bae et al. (2002) when two anions of different affinity to the ion exchange resin were simultaneously adsorbed in the columns. The study reported chromatographic peaking of sulphate when both nitrate and sulphate were simultaneously adsorbed by nitrate-to-sulphate selective (NSS) resin. This resin was developed and successfully applied to groundwater with high sulphate concentrations. In the case of NSS resin, the sulphate breaks earlier than the nitrate in the column test due to the preference of NSS resin for nitrate. Thus when the sulphate ions reach the breakthrough point, the resin dumps sulphate ions displaced by nitrate ions, which cause a chromatographic peaking of sulphate (Blaney, Cinar & SenGupta 2007; Pan et al. 2009; Bae et al. 2002).

These observations clearly indicate the dynamic competitive adsorption and desorption processes as both nitrate and phosphate are passed through the Purolite resin column. Both nitrate and phosphate were adsorbed initially by the Purolite resin until the point at which phosphate starts to break through (15 min for 1% Purolite and 30 min for 3% Purolite). At this point, the Purolite resin continuously adsorbs nitrate by

competitively displacing previously adsorbed phosphate because of Purolite's relatively high selectivity for nitrate. This process results in a higher phosphate concentration in the effluent than in the influent. This phenomenon of chromatographic peaking is also referred as the "snow-plow" effect and has been described numerically by Barry et al. (1983) and Bajrachrya and Barry (1995).

In the 5% Purolite experiment, both the nitrate and phosphate breakthrough time increased compared to that at 1 and 3% Purolite. Breakthrough point for nitrate occurred at 240 min into the run and phosphate at 90 min. This shows that as the dose of Purolite increases, there are more adsorbing sites for both nitrate and phosphate and therefore these ions were removed from the synthetic feed for a longer period by Purolite.

After about 600 min into the experiment of 10% Purolite, the adsorption column achieved a breakthrough of nitrate. For phosphate, the breakthrough was observed at 180 min. These breakthrough times were longer than those for 5% Purolite column for the same reason given in the last paragraph (i.e. with increased % Purolite, more adsorption sites were available for adsorption of nitrate and phosphate).

Purolite exhibits a higher capacity for the removal of nitrate than for phosphate. Among the percentages of Purolite studied, 10% by mass of Purolite has shown to possess the highest efficiency in the removal of nitrate as compared to the other experiments using 1%, 3%, and 5% (Figure 4-30) as discussed in the batch adsorption study (Section 4.1.1).

The column adsorption by 1, 3, 5, and 10% Purolite (1.4, 3.6, 6 and 12 g, respectively) have been plotted in one graph against Bed Volume (BV) to illustrate the finding that increase dose of Purolite increases adsorption of nitrate and phosphate onto the media (Figure 4-31). When utilising 1% Purolite, the media became quickly exhausted within 6.67 BV for nitrate and as little as 0.83 BV for phosphate. This shows that 1% Purolite is not sufficient to remove 50 mg N/L nitrate and 15 mg P/L phosphate. However, once the amount of Purolite is increased to 3, 5 and 10% by mass, there was a higher efficiency of nitrate and phosphate removal.

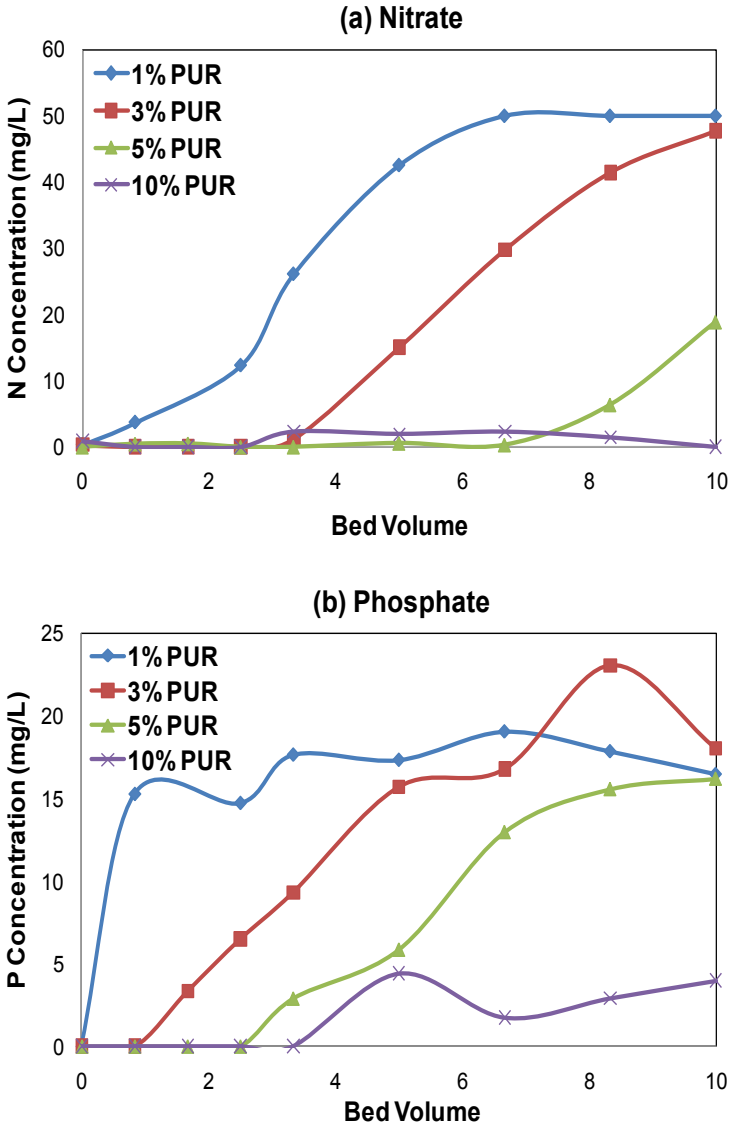

Figure 4-31: Effect of Purolite amount on (a) nitrate and (b) phosphate removal efficiency

Table 4-21 summarises the breakthrough points in terms of bed volume of the column adsorption experiments for 1, 3, 5, and 10% Purolite when C/Co = 0.2, C/Co = 0.5 and C/Co = 1. At C/Co = 0.2, the first breakthrough point occurs. At C/Co = 0.5, the effluent concentration was half the influent concentration. At C/Co = 1, the column was fully saturated and the influent and effluent's concentration are equal, which essentially means that Purolite is no longer removing any nitrate or phosphate and the exchange capacity of the media is exhausted.

The time required for the occurrence of the breakthrough points for nitrate was

longer than those observed for phosphate. This shows that Purolite has a high affinity for the removal of nitrate than for phosphate as observed in the batch study (Section 4.1.1). Purolite (A500PS) is nitrate selective and was very efficient in completely removing nitrate for over 25.83 BV in the 10% Purolite experiment in comparison to completely removing phosphate only up to 11 BV.

For 1% Purolite (Figure 4-32 and Table 4-21), the column reached a full breakthrough of C/Co = 1 at 6.67 BV for nitrate. On the other hand, the full breakthrough of phosphate occurred as early as 0.83 BV. After this point, the phosphate concentration in the effluent continued to increase and became much higher than that in the initial influent solution (C/Co ~ 1.54). The reason for this was explained earlier in Section 4.2.1 on page 70-71.

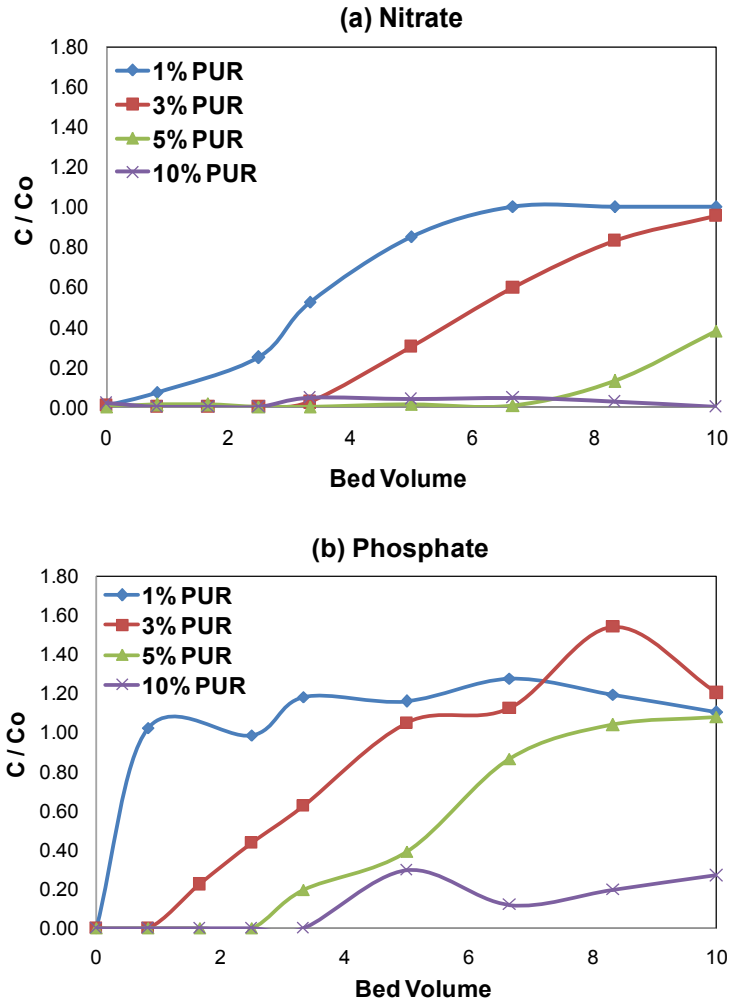

Figure 4-32: Breakthrough curve of (a) nitrate and (b) phosphate removal by different doses of Purolite

Table 4-21: Number of BV for the breakthrough curves of nitrate and phosphate removal by Purolite (shaded values were obtained from an experimental run over a longer period of time)

		Nitrate			Phosphate		
PUR Mass (g)	**% PUR**	**C/Co = 1 (BV)**	**C/Co = 0.5 (BV)**	**C/Co = 0.2 (BV)**	**C/Co = 1 (BV)**	**C/Co = 0.5 (BV)**	**C/Co = 0.2 (BV)**
1.4	1	6.67	3.33	2.6	0.83	0.415	0.5
3.6	3	10	6.67	4.5	5	2.5	1.8
6	5	>10	>10	9	8.33	5	3.33
12	10	>25.83	>25.83	25.83	25.83	12.5	11.67

4.2.2. Amount of nitrate and phosphate removed in Purolite column

Figure 4-33 and Figure 4-34 illustrate the effect of varied percentage by mass of Purolite on the amount of nitrate and phosphate removed. In Figure 4-33(a), both 5% and 10% Purolite data overlap one another up to 8 BV, which indicate that increasing the amount of Purolite beyond 5% has no additional effect in removing nitrate up to 8 BV. Under these experimental conditions using a synthetic feed of 50 mg N/L nitrate, 5% Purolite is sufficient for complete removal of nitrate at least up to 10.13 BV. After about 6.67 BV, 1% Purolite has reached saturation and did not adsorb anymore nitrate in the column. However, 5% and 10% Purolite continue to keep adsorbing nitrate in the column even after 10 BV because the total number of adsorption sites increased with increased amount of Purolite.

For phosphate removal, 1% Purolite reached maximum adsorption capacity by 0.83 BV, as shown in Figure 4-33(b). No phosphate was adsorbed by the Purolite media throughout the experimental run after 0.83 BV. For 3% Purolite, the media reached maximum adsorption capacity by 5 BV. After this point, no more phosphate was adsorbed in the column. For 5% Purolite, the media reached maximum adsorption capacity by 8.33 BV. For 10% Purolite, the media reached a maximum adsorption capacity at 25.83 BV (data not shown in Figure 4-33, refer to Appendix 6.1 p. 105). Under these experimental conditions using a synthetic feed of 15 mg P/L phosphate, 10% Purolite is required for the removal of phosphate up to 25.83 BV. Beyond this point, C/Co = 1, showing that the column cannot remove any phosphate. In contrast, 10% Purolite continued to remove nitrate even after 25.83 BV.

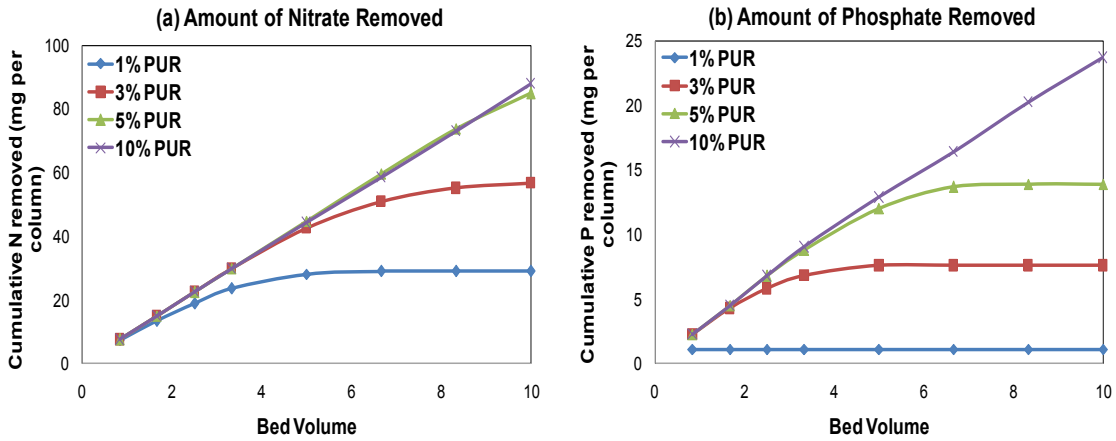

Figure 4-33: Effect of % Purolite on the cumulative amount of (a) nitrate and (b) phosphate removed

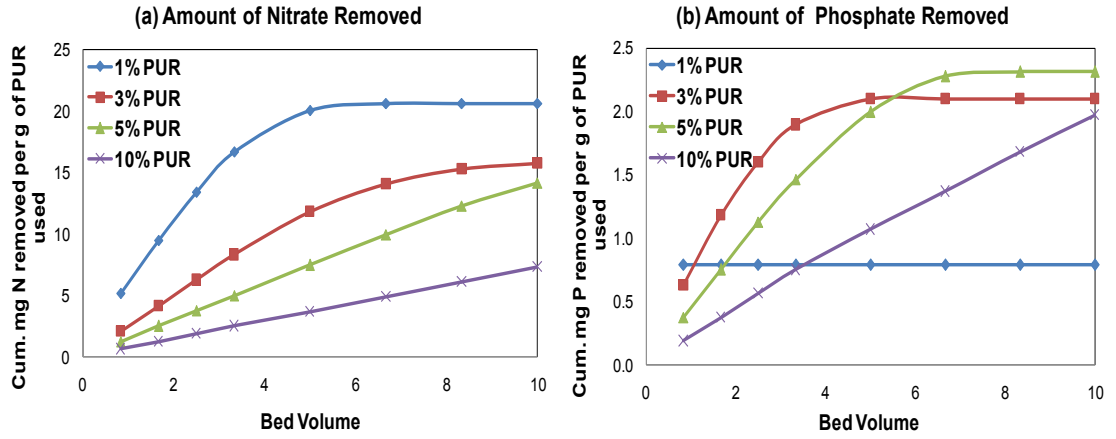

Figure 4-34: Effect of % Purolite on the cumulative amount of (a) nitrate and (b) phosphate removed per gram of Purolite used

4.3. Purolite Only as Adsorption Media for Nitrate and Phosphate Removal from Synthetic Water

In the previous study, varied percentage by mass of Purolite (A500PS) and anthracite were used as column adsorption media for nitrate and phosphate removal. The amount of Purolite used was small, between 1.4 - 12 g only per column. In this study, the column experiments were repeated with Purolite (A520E) alone as adsorption media instead of Purolite and anthracite media to determine whether Purolite alone, with weights much more than in Purolite and anthracite column, will increase the nutrient removal efficiency especially the phosphate removal efficiency. Varying bed heights of Purolite (3, 6 and 12 cm; corresponding weights of Purolite per column were

14, 28 and 56 g) was utilised as adsorption media for nitrate and phosphate removal at 2 m/hr flow rate. The following graphs illustrate C/Co for Purolite (A520E) as well as nitrate and phosphate removal efficiency.

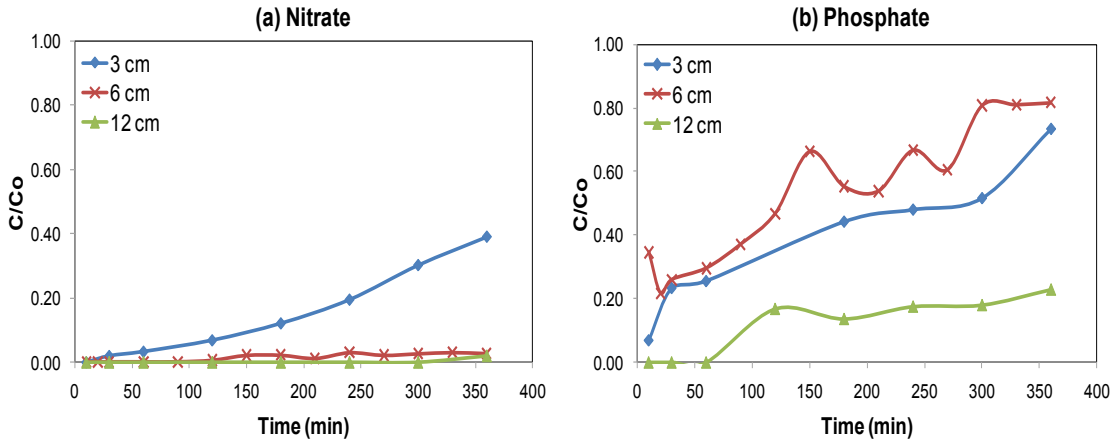

Figure 4-35: Effect of bed height on (a) nitrate and (b) phosphate removal for Purolite (A520E)

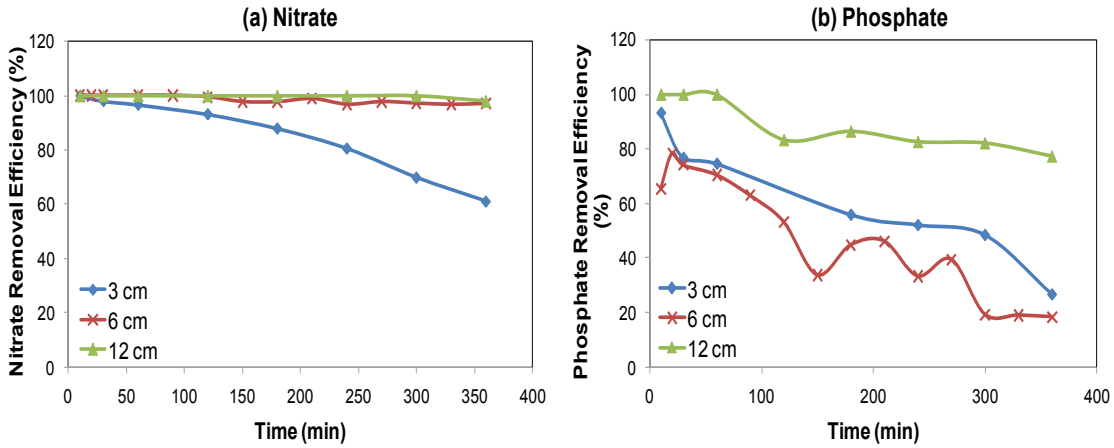

Figure 4-36: Effect of bed height on (a) nitrate and (b) phosphate removal efficiency for Purolite (A520E)

Figure 4-35(a) and Figure 4-36(a) shows that as the bed height increased, adsorption of nitrate onto the medium also increased. Both 6 cm and 12 cm bed height completely removed nitrate up to 360 min. For phosphate removal, although the 12 cm bed height performed better than the 3 cm and 6 cm bed height (Figure 4-35b and Figure 4-36b), the removal was complete only up to 60 min. These results again showed that Purolite is selective for nitrate removal and even by having only Purolite with weights more than in the Purolite and anthracite column, phosphate removal efficiency

was poor.

Figure 4-37(a) below illustrates the cumulative amount of nitrate removed (mg per column) by Purolite (A520E) at 2 m/hr flow rate. The 6 cm and 12 cm bed height overlap each other up to 360 min, which indicate that under these experimental conditions using a synthetic feed of 50 mg/L nitrate, 6 cm Purolite is sufficient for the complete removal of nitrate up to 360 min. For phosphate removal, at least a 12 cm bed height is required as Purolite is nitrate selective and therefore more medium is required for the removal of 15 mg P/L phosphate in the synthetic feed. As shown in Figure 4-36(b), even with 12 cm bed height, the removal efficiency of phosphate is lower than for nitrate beyond 60 min.

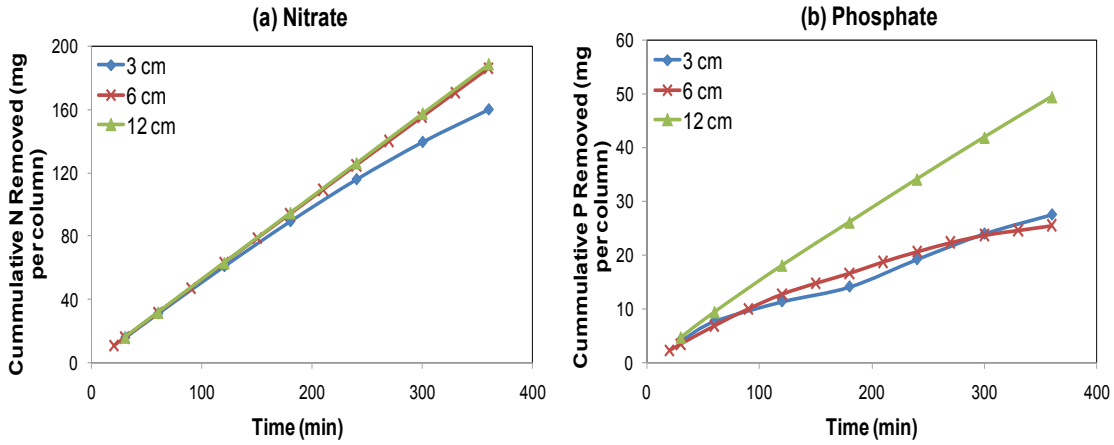

Figure 4-37: Effect of bed height on cumulative amount of (a) nitrate and (b) phosphate removed for Purolite (A520E) at 2m/hr flow rate

4.3.1. Purolite column adsorption with highly concentrated synthetic feed

A column adsorption study was carried out using a highly concentrated synthetic feed of nitrate and phosphate (100 mg N/L and 50 mg P/L, respectively) with 6 cm bed height (24 g) of Purolite (A500PS) at 2 m/hr (10.5 mL/min). Figure 4-38 shows the trend of nitrate and phosphate removal during this study. Nitrate was successfully removed throughout the experiment up to 480 min. Phosphate was only removed up to 360 min and after which, the phosphate concentration in the effluent was higher than the influent.

The breakthrough curve, given in Figure 4-39, shows that nitrate was

successfully removed throughout the experiment reaching C/Co = 0.6 at 267 BV (480 min). However, the full breakthrough of phosphate occurred as early as 200 BV (360 min). After this point, the phosphate concentration in the effluent continued to increase and became much higher than that in the initial influent solution (C/Co ~ 1.21), confirming a chromatographic peaking of phosphate. This phenomenon was described earlier in Section 4.2.1 on page 70-71. Table 4-22 summarises the breakthrough points in bed volume for this study when C/Co = 0.2, C/Co = 0.5 and C/Co = 1.

Furthermore, this study confirmed that Purolite (A500PS) is nitrate selective. The partial breakthrough of nitrate (C/Co = 0.5) occurred at 250 BV whereas the partial breakthrough for phosphate occurred as early as 33 BV (given in Table 4-22). Purolite was able to remove nitrate for up to 267 BV and was still not exhausted by the end of the experimental run.

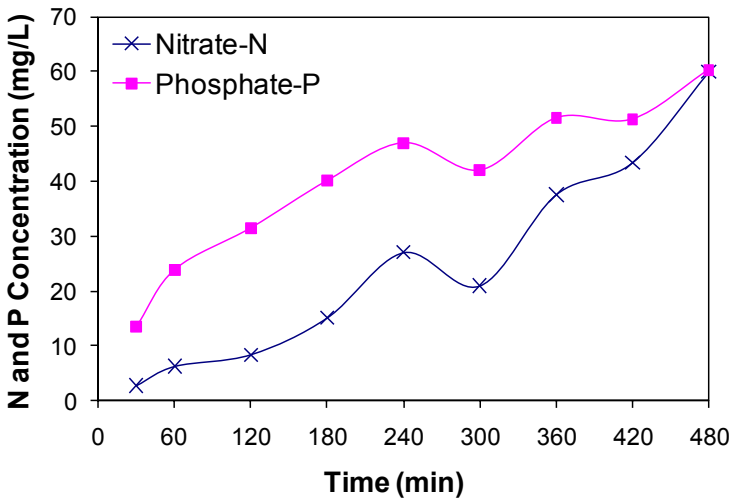

Figure 4-38: Column adsorption study with Purolite (A500PS) at 6 cm bed height and 2 m/hr using a higher concentrated synthetic feed (initial concentrations of 100 mg N/L nitrate and 50 mg P/L phosphate)

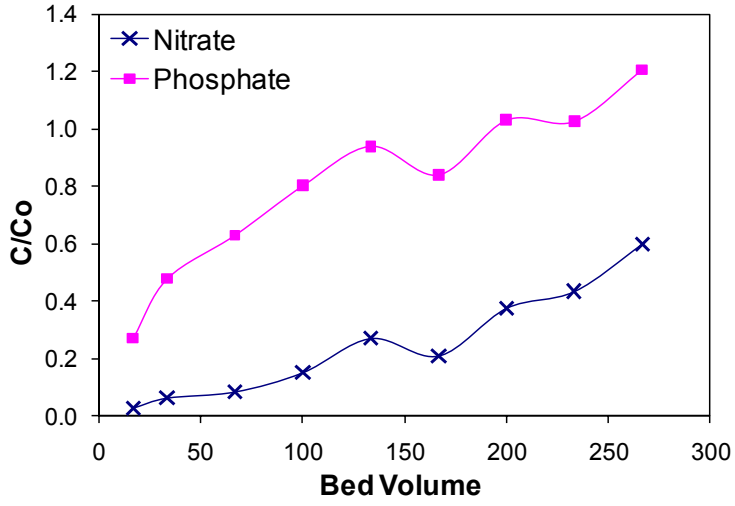

Figure 4-39: Breakthrough curve of Purolite (A500PS) at 6 cm bed height and 2 m/hr using a higher concentrated synthetic feed (initial concentrations of 100 mg N/L nitrate and 50 mg P/L phosphate)

Table 4-22: Number of BV for the breakthrough curve of nitrate and phosphate removal by Purolite (A500PS) at 2 m/hr using a higher concentrated synthetic feed

		Nitrate			Phosphate		
Bed Height	**Purolite Mass (g)**	**C/Co = 1 (BV)**	**C/Co = 0.5 (BV)**	**C/Co = 0.2 (BV)**	**C/Co = 1 (BV)**	**C/Co = 0.5 (BV)**	**C/Co = 0.2 (BV)**
6 cm	24	>267	250	100	200	33	17

4.4. HAIX as Adsorption Media for Nitrate and Phosphate Removal from Synthetic Water

The column experiments were repeated with HAIX alone as adsorption media instead of Purolite media to determine whether HAIX alone will increase the nutrient removal efficiency because of the presence of the phosphate selective HFO in HIAX. Bed height of 6 cm and 2 m/hr flow rate was utilised for nitrate and phosphate removal with synthetic feed (50 mg N/L nitrate and 15 mg P/L phosphate). Figure 4-40 illustrates the breakthrough curve for nitrate and phosphate removal with HAIX.

Figure 4-40 shows that HAIX completely removed phosphate up to 360 min and did not reach saturation (C/Co = 1) during the experimental run of 1420 min. However, HAIX did not completely removal nitrate at any time and saturation occurred at 1420 min. This confirmed the results obtained in batch study that HIAX was phosphate selective.

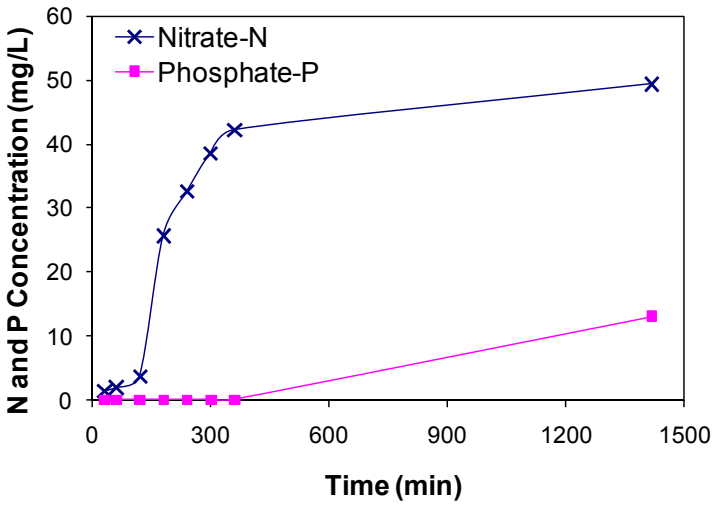

Figure 4-40: Nitrate and phosphate breakthrough curve with HAIX at 6 cm bed height and 2 m/hr flow rate

4.4.1. HAIX column adsorption with highly concentrated synthetic feed

A column adsorption study was carried out using a highly concentrated synthetic feed of nitrate and phosphate (100 mg N/L and 50 mg P/L, respectively) with 6 cm bed height (24 g) of HAIX at 2 m/hr (10.5 mL/min), as carried out for Purolite (Section 4.3.1). Figure 4-41 shows the trend of nitrate and phosphate removal during this study. Phosphate was completely removed for up to 180 min. Nitrate was only removed up to 60 min and after 420 min, the nitrate concentration in the effluent was higher than the influent.

The breakthrough curve, given in Figure 4-42, shows that phosphate was completely removed up to 100 BV (180 min). The partial breakthrough of phosphate (C/Co = 0.5) occurred at 167 BV whereas the partial breakthrough for nitrate occurred as early as 83 BV (given in Table 4-23). After this point, HAIX continued to remove phosphate reaching a full breakthrough of C/Co = 1 at 267 BV (480 min). However, the full breakthrough of nitrate occurred as early as 167 BV (300 min). After this point, the nitrate concentration in the effluent continued to increase and became much higher than that in the initial influent solution (C/Co ~ 1.08), confirming a chromatographic peaking of nitrate. This phenomenon was described earlier in Section 4.2.1 on page 70-71. In earlier section, the peaking was observed for phosphate in Purolite adsorbent whereas

here the peaking was for nitrate in HAIX. This difference is due to the difference in the selectivity for the two ions for adsorption in the two adsorbents.

This study again confirmed the results of the batch study (Section 4.1.2) that HAIX is phosphate selective.

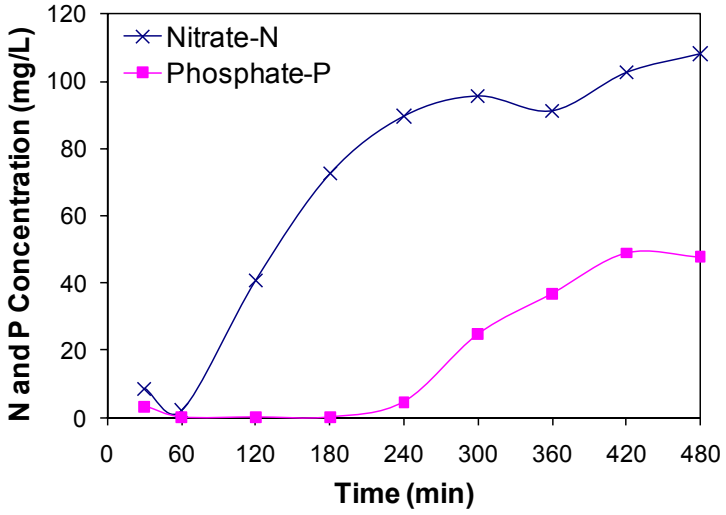

Figure 4-41: Column adsorption study with HAIX at 6 cm bed height and 2 m/hr using a higher concentrated synthetic feed (initial concentrations of 100 mg N/L nitrate and 50 mg P/L phosphate)

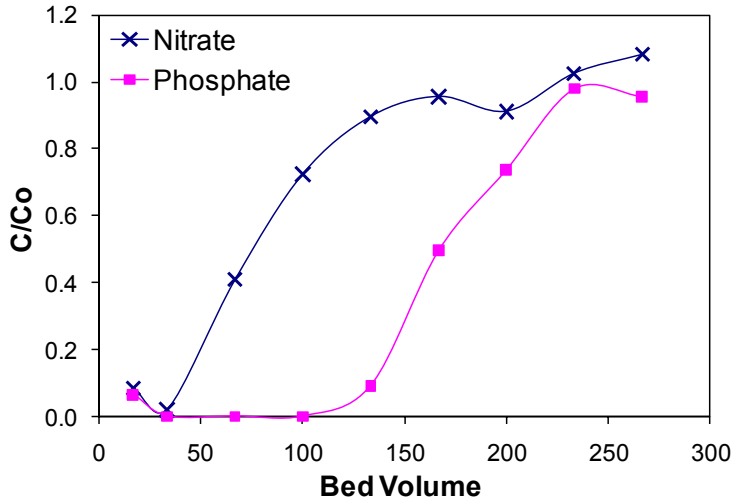

Figure 4-42: Breakthrough curve of HAIX at 6 cm bed height and 2 m/hr using a higher concentrated synthetic feed (initial concentrations of 100 mg N/L nitrate and 50 mg P/L phosphate)

Table 4-23: Number of BV for the breakthrough curve of nitrate and phosphate removal by HAIX at 2 m/hr using a higher concentrated synthetic feed

		Nitrate			Phosphate		
Bed Height	**HAIX Mass (g)**	**C/Co = 1 (BV)**	**C/Co = 0.5 (BV)**	**C/Co = 0.2 (BV)**	**C/Co = 1 (BV)**	**C/Co = 0.5 (BV)**	**C/Co = 0.2 (BV)**
6 cm	24	167	83	50	267	167	150

4.5. Purolite and Hydrated Ferric Oxide (HFO) with Anthracite in Series as Adsorption Media for Nitrate and Phosphate Removal from Synthetic Water

The experiments conducted with Purolite only showed that Purolite can successfully be used to remove nitrate but not phosphate. Therefore an HFO column was added to the Purolite column to remove phosphate. HFO has a high affinity for the removal of phosphate than nitrate (Blaney, Cinar & SenGupta 2007). This is because phosphate is specifically adsorbed to HFO in the positively charged sites and neutral sites whereas nitrate is non-specifically adsorbed only on positively charged sites. This was confirmed in the experiments with HAIX, which consisted of HFO and ion exchange resin. In these experiments (Section 4.4), HAIX was shown to have selectivity for phosphate over nitrate.

Purolite (A500PS) and HFO were used in series to simultaneously remove nitrate and phosphate. These experimental runs were carried out with synthetic feed, through the Purolite column first and then through the HFO column. The nitrate and phosphate removal data for the Purolite column was presented earlier in Section 4.2. In this section, the nutrient removal data for HFO is presented. The influent concentration of nitrate and phosphate to HFO column were different because different amounts of nitrate and phosphate were removed by Purolite from the synthetic feed influent to Purolite.

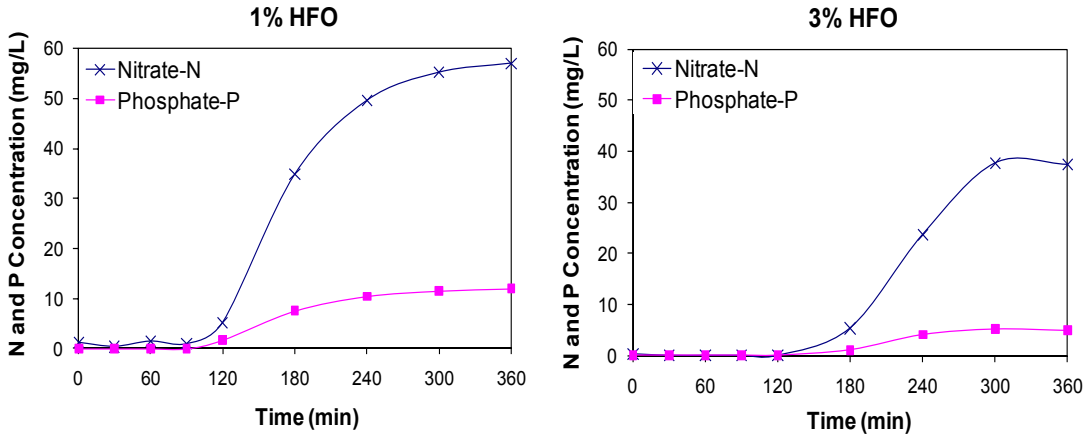

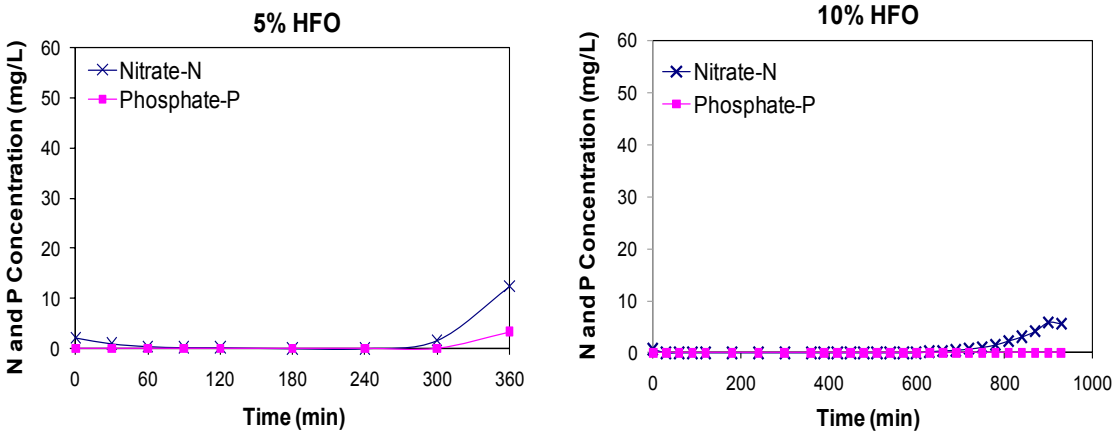

Figure 4-43: Nitrate and phosphate breakthrough curves with varied percentage by mass of HFO (nitrate and phosphate concentrations in the influent feed to HFO were different)

Table 4-24: Breakthrough points from the column experiments using varied percentage by mass of HFO

Mass of HFO (g)	HFO (%)	Nitrate breakthrough point (min)	Phosphate breakthrough point (min)
1.4	1	90	120
3.6	3	120	180
6	5	270	300
12	10	700	> 960

With varying percentage by mass of HFO at 1, 3, 5, and 10%, the adsorption column achieved a breakthrough of nutrients at 90, 120, 270 and 700 min respectively for nitrate as shown in Table 4-24 and 120, 180, 300 and >960 min respectively for phosphate. During the period of observation for 1% and 3% HFO, the phosphate concentrations reached steady state after about 240 min (6.67 BV). However, for 1% HFO, the phosphate concentration reached steady state at about 12 mg/L and for 3% HFO, the phosphate concentration at steady state was about 5 mg/L.

After about 700 min into the experiment of 10% HFO, the breakthrough for nitrate was observed whereas phosphate was completely removed for up to 960 min. This confirms that HFO is phosphate selective and is very efficient in removing phosphate for up to several hours.

Because the synthetic feed was passed through the Purolite column, the concentration of nitrate and phosphate in the influent to HFO column had decreased to different levels. Therefore the breakthrough curves for HFO were plotted in Figure 4-44, as the ratio of concentration of nutrients in the effluent of the HFO to the concentration in the influent to the HFO column. This is considered to provide a

realistic assessment of the efficiency of HFO column in removing nitrate and phosphate.

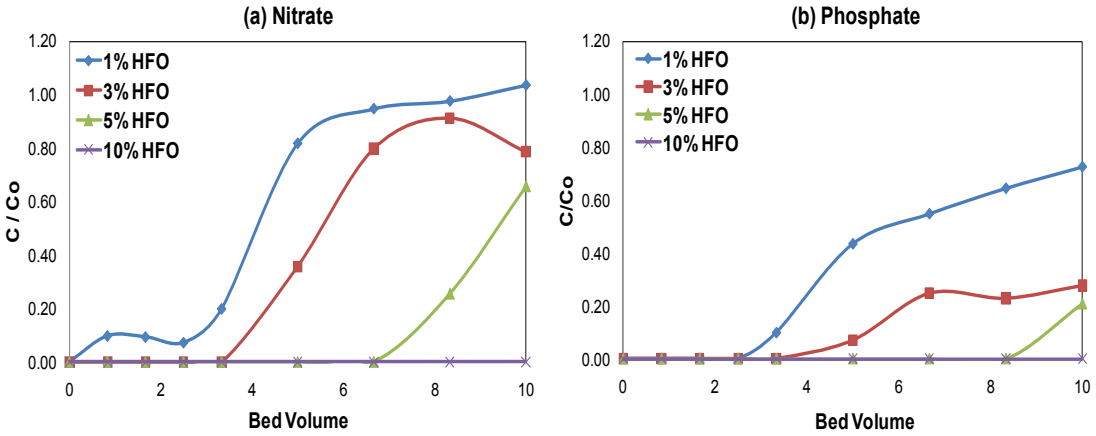

Figure 4-44: Breakthrough curve for (a) nitrate and (b) phosphate removal by HFO

Table 4-25: C/Co values for the breakthrough curves of nitrate and phosphate removal by HFO (Shaded values were obtained from an experimental run over a longer period of time)

		Nitrate			Phosphate		
HFO Mass (g)	**% HFO**	**C/Co = 1 (BV)**	**C/Co = 0.5 (BV)**	**C/Co = 0.2 (BV)**	**C/Co = 1 (BV)**	**C/Co = 0.5 (BV)**	**C/Co = 0.2 (BV)**
1.4	1	6.67	4.17	3.33	>10	6.67	3.8
3.6	3	8.33	5.84	4.5	>10	>10	6.2
6	5	>10	9.17	8	>10	>10	10
12	10	>25.83	22.50	17	>25.83	>25.83	>25.83

Table 4-25 summarises the breakthrough points in bed volume of the column adsorption experiments for 1, 3, 5, 10% HFO when C/Co = 0.2, C/Co = 0.5 and C/Co = 1. At C/Co = 0.2, the first breakthrough point occurs. At C/Co = 0.5, half the nutrients in the influent were removed. At C/Co = 1, the column was saturated and the influent and effluent's concentration were equal, which essentially means that HFO was no longer removing any nitrate or phosphate and was exhausted. The breakthrough points observed for phosphate were higher than those observed for nitrate. This shows that HFO had a high affinity for the removal of phosphate than for nitrate. 10% HFO was very efficient in removing 80% of the influent phosphate (C/Co = 0.2) for over 25.83 BV in comparison to the 17 BV in removing 80% of the influent nitrate.

For 1% HFO (Figure 4-44 and Table 4-25), the column reached a full breakthrough (C/Co = 1) at over 10 BV for phosphate. On the other hand, the full breakthrough of nitrate occurred as early as 6.67 BV. After this point, the nitrate concentration in the effluent continued to increase and became higher than that in the initial influent solution (C/Co ~ 1.04). These observations clearly indicate the dynamic

competitive sorption and desorption processes as both nitrate and phosphate were passed through the HFO column. Both nitrate and phosphate were adsorbed initially by the HFO until the point at which nitrate starts to break through (6.67 BV for 1% HFO and 8.33 BV for 3% HFO). In the Purolite column, the C/Co for phosphate reached values greater than 1 because Purolite is selective for nitrate but in the HFO column, C/Co values for nitrate reached values greater than 1 because HFO is selective to phosphate. This phenomenon is often referred as the "snow-plow" effect or chromatographic peaking and has been explained in Section 4.2.1 (pg. 70-71) in detail. This phenomenon is observed for 1% HFO column only and not for higher percentage of HFO because at low percentage adsorbent the adsorption sites were limited and this results in higher competition for adsorption between nitrate and phosphate.

Table 4-25 shows that 1%, 3% and 5% HFO were all very efficient in removing phosphate for over 10 BV. For 10% HFO, phosphate was successfully removed from the influent for over 25.83 BV. Under these experimental conditions using a synthetic feed of 15 mg P/L, 1% HFO is sufficient for removal of phosphate at least for 10 BV after the feed was passed through 1% Purolite column.

4.5.1. Cumulative amounts of nitrate and phosphate removed by HFO

Figure 4-45 and Figure 4-46 illustrates the effect of varied percentage by mass of HFO on the amount of nitrate and phosphate removed. An increase in the percentage by mass of HFO increased the number of adsorption sites and therefore removed increased amount of both nitrate and phosphate. This happens despite lower concentrations of nitrate and phosphate in the influent entering HFO column at higher percentage HFO as a result of higher removal of these nutrients at high percentage Purolite in the Purolite column. For the higher % HFO (3%, 5%, and 10%), the amounts of phosphate removed were higher than nitrate. This is because in most cases, the influent concentration of phosphate was higher than nitrate because the Purolite column removed relatively less phosphate than nitrate before the synthetic feed reached the HFO column. Moreover, the results also reflected that the HFO affinity for phosphate is higher than nitrate.

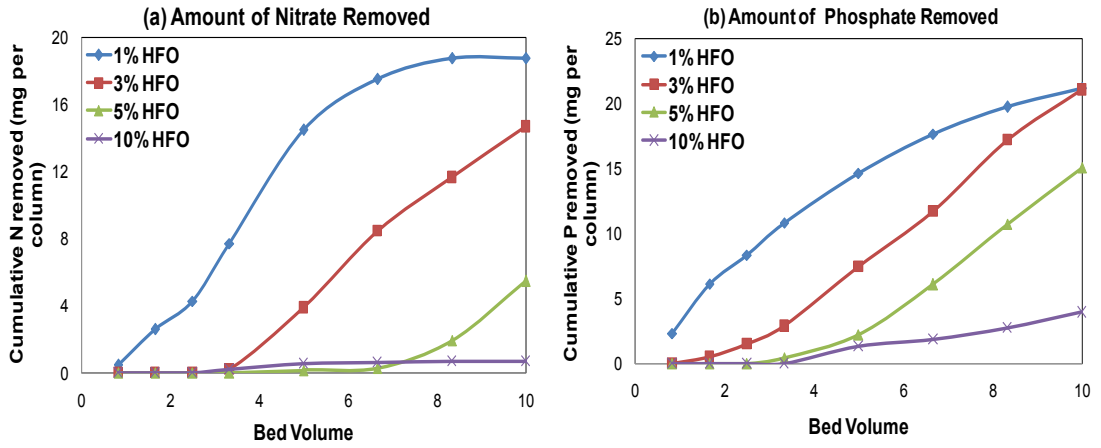

Figure 4-45: Effect of % HFO on the cumulative amount of (a) nitrate and (b) phosphate removed

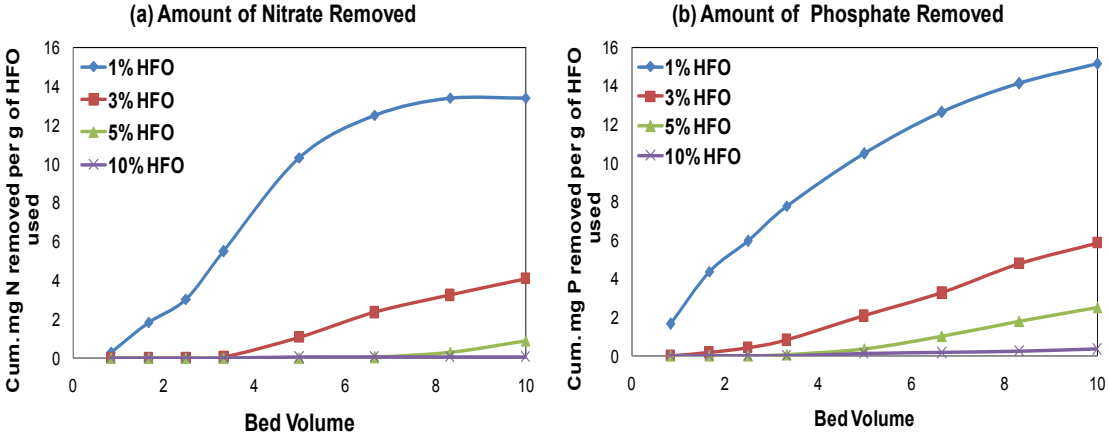

Figure 4-46: Effect of % HFO on the cumulative amount of (a) nitrate and (b) phosphate removed per gram of HFO used

After about 6.67 BV, 1% HFO reached saturation and did not adsorb anymore nitrate in the column. After 8.33 BV, 3% HFO reached saturation (C/Co = 1) and did not adsorb anymore nitrate in the column. However, 5% and 10% HFO continued to keep adsorbing nitrate in the column for over 10 BV and 25.83 BV, respectively. Under these experimental conditions using a synthetic feed of 50 mg N/L, 5% and 10% HFO were more successful in removing nitrate for at least 10 BV and 25.83 BV after the synthetic feed was passed through 5 and 10% Purolite columns, respectively.

4.5.2. Selectivity of adsorption media

In order to confirm the selectivity of Purolite and HFO utilised in series for nitrate and phosphate removal, the removal efficiencies of nitrate and phosphate were

calculated for each medium. A plot of %phosphate / %nitrate removal efficiency ratio was plotted against %Purolite and %HFO used in the experiments (Figure 4-47). The removal efficiencies for nitrate and phosphate were calculated using Equation 4-1 and Equation 4-2, respectively.

$$\%\ \boldsymbol{N\ removal\ efficiency} = \frac{\boldsymbol{Conc.of\ N\ in\ influent - Conc.of\ N\ in\ effluent}}{\boldsymbol{Conc.of\ N\ in\ influent}}\ \boldsymbol{x\ 100} \qquad \textbf{Equation 4-1}$$

$$\%\ \boldsymbol{P\ removal\ efficiency} = \frac{\boldsymbol{Conc.of\ P\ in\ influent - Conc.of\ P\ in\ effluent}}{\boldsymbol{Conc.of\ P\ in\ influent}}\ \boldsymbol{x\ 100} \qquad \textbf{Equation 4-2}$$

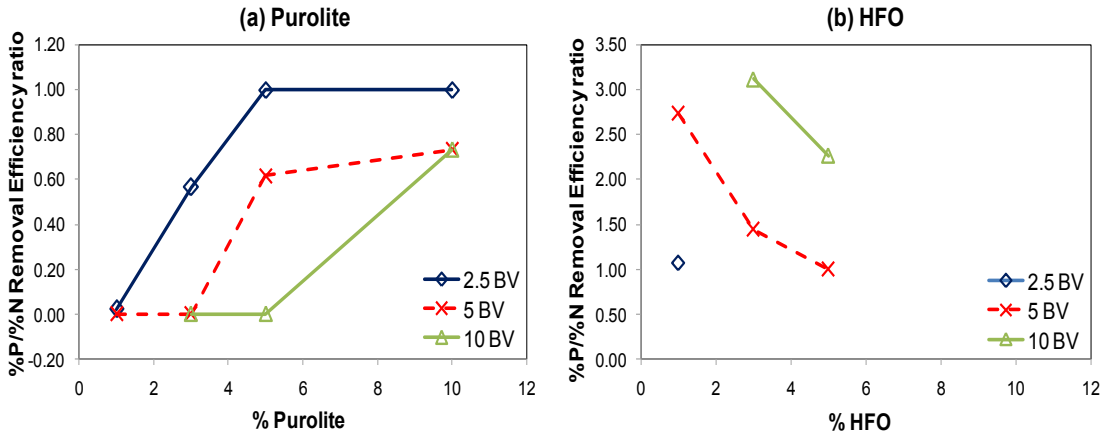

Figure 4-47: Phosphate and nitrate removal efficiency ratio for (a) Purolite and (b) HFO

Figure 4-47(a) shows that P/N removal efficiency ratios for all percentages of Purolite were between 0 to 1 confirming that Purolite is nitrate selective. An increase in %Purolite used, increased P/N values, which indicated that nitrate selectivity decreased as the dose of Purolite increased. As the amount of Purolite used in the column increased, there were more sites for adsorption of anions therefore there was less competition between nitrate and phosphate and thus the nitrate selectivity decreased. At high % Purolite and low bed volume, P/N ratio approached 1, which indicated no selectivity. This was found in the 5% and 10% Purolite adsorption column studies for the 2.5 BV. At low BV, the total amount of nitrate and phosphate that had passed through the column was lower than the amount of adsorption sites in Purolite and hence the competition for adsorption was low.

The selectivity of Purolite for nitrate increased as the bed volume increased

because of the cumulative effect of excess nitrate over phosphate adsorbed with continued passage of the synthetic feed through the column.

There was limited data available for the HFO column because the concentrations of nitrate and phosphate in the influent were very small, sometimes 0 mg/L after passing through the Purolite column (i.e. Purolite has removed most of the nitrate and phosphate from the synthetic feed) (Figure 4-47(b)). When calculating removal efficiencies for HFO, this sometimes gave unrealistic values (for example, sometimes values had to be divided by 0 mg/L) and therefore removal efficiencies were not able to be calculated for all the bed volumes of the HFO experiment.

Unlike the case with Purolite, the P/N ratios for HFO were higher than 1 suggesting that HFO is phosphate selective. However, an increase in %HFO used in the adsorption column decreased P/N ratio, showing that the HFO selectivity for phosphate decreased when the number of sites available for adsorption increased. The P/N values reached 1 for 5 BV as the %HFO increased, suggesting that beyond 5% HFO, the medium was not selective for phosphate at 5 BV. At low bed volume such as 2.5 BV, it appears that even 1% HFO was not phosphate selective. At constant %HFO used in adsorption column, an increase in bed volumes, increased the P/N ratio, indicating higher selectivity for phosphate.

4.6. Regeneration Study

4.6.1. Distilled water wash for the regeneration of used Purolite and HFO

Regeneration tests were conducted to investigate how long the media can be used for nutrient removal and recovery. Purolite (A500PS, 10%, 12 g) and 90% anthracite was used to run a 6 hr experiment using water containing 50 mg N/L of nitrate and 15 mg P/L of phosphate and then the column was cleaned with distilled water for 5 min and left to stand with distilled water overnight for 16 hr. The next day, the same column was utilised for another 6 hour experiment. This was continued until the Purolite became ineffective for further adsorptions of nutrients.

Figure 4-48 illustrates the regeneration study with 10% Purolite and 90% anthracite over 5 days. These observations are plotted together as Stage I, Stage II, Stage III, Stage IV and Stage V, representing each day of experiment. In Stage I, the

Purolite removed nitrate and phosphate effectively for 6 hr. At the end of Stage I, the nitrate and phosphate concentrations in the effluent were at 12 mg N/L and 16 mg P/L. At the beginning of Stage II, the nitrate concentration after cleaning with distilled water was about 5 mg N/L and phosphate concentration was about 4 mg P/L. This shows that the cleaning has helped to slightly regenerate the used Purolite for reuse. Similar patterns were observed for Stage III and Stage IV. Nitrate and phosphate concentrations in the sampling over the 5 days increased with time, showing that the capacity of the Purolite column to remove nitrate and phosphate decreased with time and the washing with water did not significantly regenerate the column to continue a sustained removal of these nutrients.

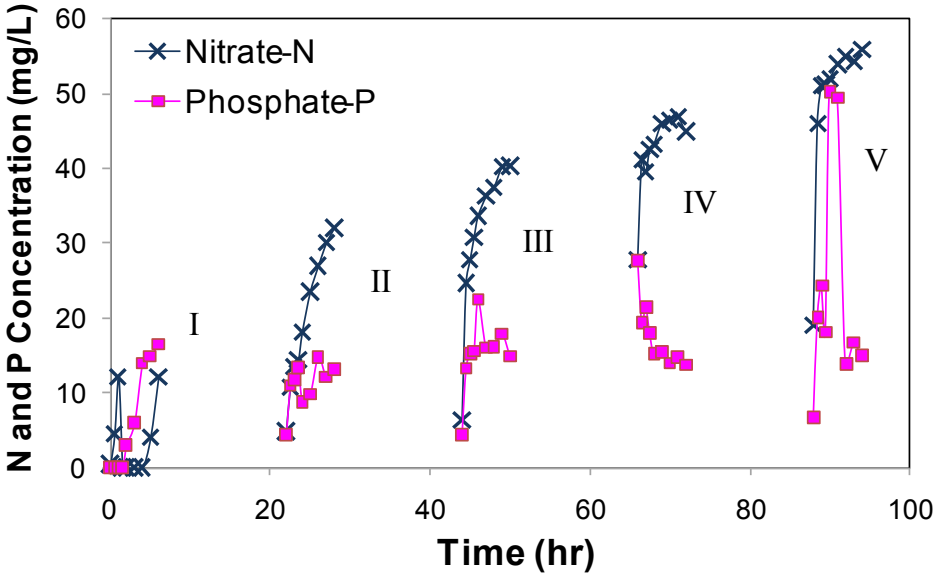

Figure 4-48: Regeneration of 10% Purolite with distilled water

As reported earlier, Purolite and HFO columns were run in series to remove nitrate and phosphate. HFO was used to run a 6 hr experiment and then the column was cleaned with distilled water for 5 min. The next day, the same column was utilised for another 6 hr experiment. This was continued for 5 days.

Figure 4-49 illustrates the regeneration study with 10% HFO and anthracite over 5 days. These observations are plotted together as Stage I, Stage II, Stage III, Stage IV and Stage V, as done for Purolite in Figure 4-48. In Stage I, the HFO removed nitrate and phosphate efficiently for 6 hr. At the end of Stage I, the nitrate and phosphate concentrations were down to 7 mg N/L and 0 mg P/L. At the beginning of Stage II, the

nitrate concentration after cleaning was about 3 mg N/L and phosphate concentration was about 0 mg P/L. This shows that the cleaning has slightly helped regenerate the exhausted HFO for reuse for nitrate removal. Similar results were observed for Stage III. However, there was a build up of nitrate in the sampling over the 5 days, as obtained for Purolite (Figure 4-48). Therefore, the distilled water wash was not effective in the regeneration of HFO column. Phosphate was removed entirely for the duration of 5 days.

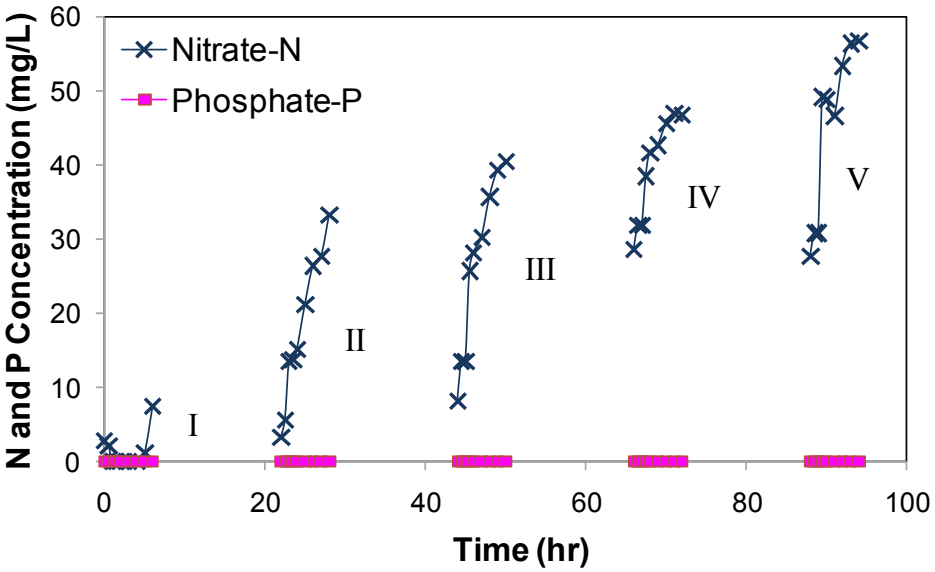

Figure 4-49: Regeneration of 10% HFO with distilled water

Table 4-26 and Table 4-27 summarise the amount of nitrate and phosphate washed after each run as a percentage of the amount of nitrate and phosphate adsorbed in the preceding run. The data shows that the distilled water wash was not sufficient in regenerating the exhausted Purolite and HFO. The wash only removed the synthetic feed trapped in the column but did not desorb the ions that had been adsorbed by the media in the preceding run. This is expected because the distilled water that was used for the wash had no anions to exchange with the nitrate and phosphate adsorbed in the column media.

Table 4-26: Amount of nitrate-N and phosphate-P washed (A) as a percentage of amount adsorbed in the preceding run (B) for distilled water wash in the Purolite column

	Nitrate-N		
	A (mg)	B (mg)	A/B x 100%
Wash 1	0.27	85	0.3
Wash 2	0.54	216	0.3
Wash 3	0.55	402	0.1
Wash 4	0.89	533	0.2
Wash 5	0.91	752	0.1

	Phosphate-P		
	A (mg)	B (mg)	A/B x 100%
Wash 1	0.18	14	1.3
Wash 2	0.25	39	0.7
Wash 3	0.21	77	0.3
Wash 4	0.29	78	0.4
Wash 5	0.28	137	0.2

Table 4-27: Amount of nitrate-N and phosphate-P washed (A) as a percentage of amount adsorbed in the preceding run (B) for distilled water wash in the HFO column

	Nitrate-N		
	A (mg)	B (mg)	A/B x 100%
Wash 1	0.14	5.35	2.6
Wash 2	0.70	14.19	4.9
Wash 3	0.70	24.78	2.8
Wash 4	1.04	30.44	3.4
Wash 5	1.05	40.41	2.6

	Phosphate-P		
	A (mg)	B (mg)	A/B x 100%
Wash 1	0	16	0
Wash 2	0	44	0
Wash 3	0	90	0
Wash 4	0	268	0
Wash 5	0	362	0

4.6.2. NaCl wash for regeneration of used Purolite

This experiment was conducted with Purolite only column (without anthracite

and HFO). Used Purolite (A500PS) was regenerated using 3% NaCl solution for 4 experimental runs. The following experimental conditions were used in this experiment: 6 cm bed height, 6 m/hr flow rate. After each run of 27 hr, the column was washed using 3% NaCl solution for 40 min at 10 m/hr flow rate. The high flow rate was used to ensure that the NaCl solution will effectively desorb the nitrate and phosphate in the column media.

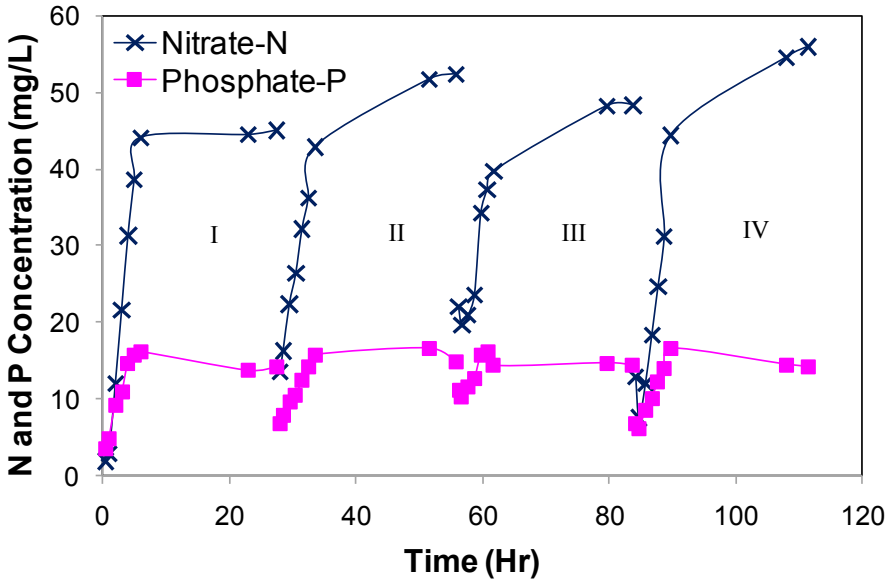

Figure 4-50: Purolite (A500PS) regeneration with 3% NaCl solution

As in distilled water wash, the amounts of nitrate and phosphate desorbed by NaCl as a percentage of the amount of these ions adsorbed in the media prior to the NaCl wash was calculated and presented in Table 4-28. Because chloride interferes with the nitrate and phosphate measured in the ion chromatography, it was not possible to measure the nitrate and phosphate concentration. Instead, both nitrate and phosphate concentrations in the NaCl wash were estimated from the amount of nitrate and phosphate adsorbed in the subsequent runs. Here it was assumed that the amount of nitrate and phosphate desorbed by NaCl created vacant adsorption sites for nitrate and phosphate adsorption in the subsequent runs. For nitrate, 6 hr of sampling data was utilised to estimate the amount of nitrate desorbed by the NaCl wash. For phosphate, 4 hr of sampling data was used to estimate the amount of phosphate desorbed by the NaCl wash. These values were indicative of the amount of nutrients being adsorbed by the column during each run (denoted in the table as 'A'). The third column in Table 4-28 is

the cumulative amount of nitrate and phosphate adsorbed in the preceding run (denoted in the table as 'B'). These values (A and B) were compared to get the amount of nitrate and phosphate washed as a percentage of the amount adsorbed in the preceding run.

Table 4-28: Amount of nitrate-N and phosphate-P washed (A; estimated values) as a percentage of amount adsorbed in the preceding run (B) for NaCl wash in regenerating used Purolite (A500PS)

	Nitrate-N		
	A (mg)	B (mg)	A/B x 100%
Wash 1	263	552	48
Wash 2	251	908	28
Wash 3	334	1376	24

	Phosphate-P		
	A (mg)	B (mg)	A/B x 100%
Wash 1	43	63	69
Wash 2	23	110	21
Wash 3	49	152	32

From the results (fourth column in Table 4-28), it can be concluded that the NaCl wash has regenerated 21-69% of the used Purolite. The NaCl wash was able to desorb the nitrate and phosphate by ion exchange with the chloride ions in NaCl.

4.6.3. NaCl wash for regeneration of used HAIX

Used HAIX was regenerated using 3% NaCl solution in 2 experimental runs. The following conditions were used in this experiment: 12 cm bed height, 6 m/hr flow rate, feed concentration was 50 mg N/L and 15 mg P/L. After each run of 28 hr, the column was washed using 3% NaCl solution for 40 min at 10 m/hr flow rate. The high flow rate was used to ensure that the NaCl solution will effectively desorb the nitrate and phosphate in the column media.

Both nitrate and phosphate concentrations in the NaCl wash were estimated from the amount of nitrate and phosphate adsorbed in the subsequent runs, as in Section 4.6.2.

From the results (fourth column in Table 4-29), it can be concluded that the NaCl wash has fully regenerated the used HAIX after the first run for nitrate. However,

the extent of regeneration for phosphate was low. This is probably because the chloride anion in the NaCl wash was able to exchange completely with the weakly adsorbed nitrate but not with the strongly adsorbed phosphate.

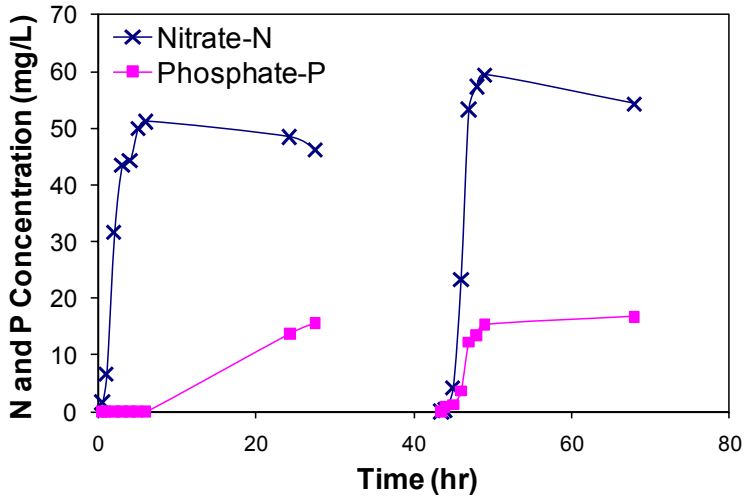

Figure 4-51: HAIX regeneration with 3% NaCl solution

Table 4-29: Amount of nitrate-N and phosphate-P washed (A; estimated values) as a percentage of amount adsorbed in the preceding run (B) for NaCl wash in regenerating used HAIX

	Nitrate-N		
	A (mg)	B (mg)	A/B x 100%
Wash 1	253	210	121

	Phosphate-P		
	A (mg)	B (mg)	A/B x 100%
Wash 1	96	452	21

4.7. Use of Adsorption Columns to Remove Nitrate and Phosphate from MBR Effluent

A detailed experiment was also conducted to investigate the possibility of removing the nitrate and phosphate in MBR effluent. This will help in obtaining a high quality water for reuse.

4.7.1. Purolite only as adsorption media

Figure 4-52 shows the removal trend of nitrate and phosphate using MBR effluent as feed. This experiment ran for 48.5 hr at 3 cm bed height (12 g of Purolite) and 2 m/hr flow rate. The feed concentration varied over time thus the feed sample was collected on each day and presented in Figure 4-52 as Feed N (for nitrate) and Feed P (for phosphate). The results showed that nitrate was successfully removed throughout the experiment with the final eluent having only 1 mg N/L, which is approximately 30% of the feed nitrate concentration. Phosphate was successfully removed throughout the experiment as well and only minute concentrations were found in the last sampling (0.24 mg P/L).

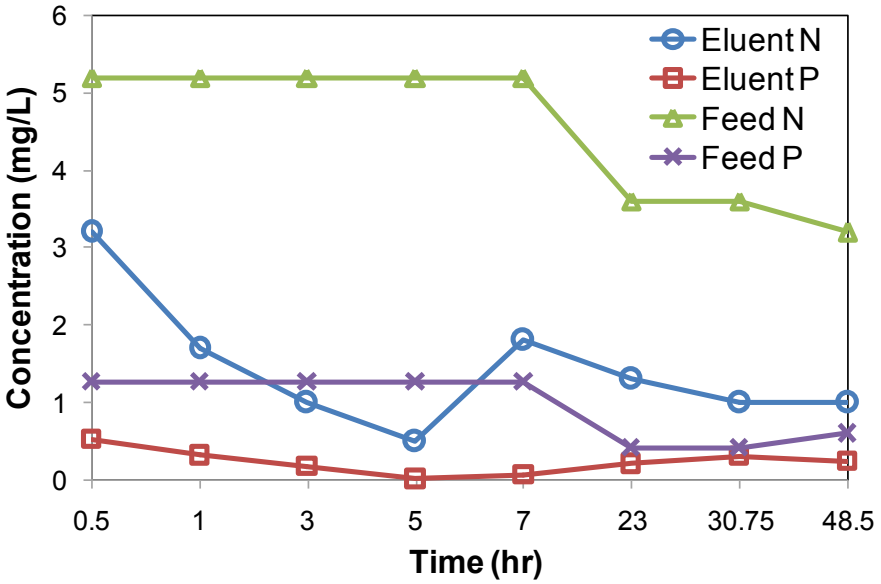

Figure 4-52: Removal of nitrate and phosphate in MBR Effluent by Purolite A500PS (3 cm bed height, 2 m/hr flow rate)

The experiment was repeated with a 6 cm bed height (24 g) of Purolite and at 2 flow rates (2 m/hr and 6 m/hr) for a period of 72 hr to determine the effect of increased bed height and flow rate on nitrate and phosphate removal. Figure 4-53 shows the trends of nitrate and phosphate removal in these 2 experimental runs. The feed concentration is presented in Figure 4-53 as Feed N (for nitrate) and Feed P (for phosphate).

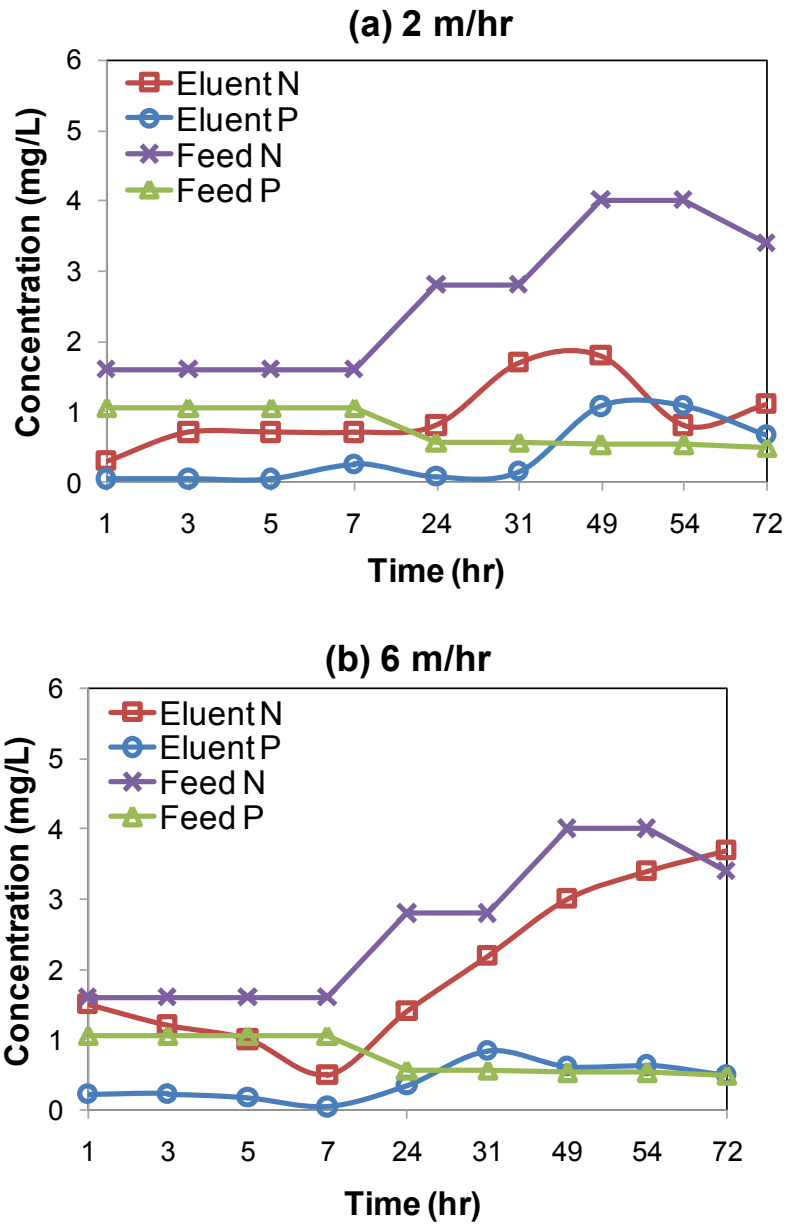

Figure 4-53: Removal of nitrate and phosphate in MBR effluent by 6 cm bed height Purolite (A500PS) at (a) 2 m/hr and (b) 6 m/hr

In Figure 4-53(a), the nitrate concentration in the feed reached a peak of 4 mg N/L at 49 hr of experimentation and the nitrate concentration in the column eluent reached a peak of 1.8 mg N/L at the same time with flow rate of 2 m/hr. The Purolite has successfully removed the nitrate to about 1 mg N/L, which is a 30% reduction from the nitrate concentration of the feed. Similar to nitrate, the phosphate concentration peaked at 49 hr into the experiment. At this point, the effluent concentration is higher than the influent concentration. This confirms that Purolite (A500PS) is nitrate selective

and the competition for phosphate and nitrate adsorption is fairly high after 30 hr into the experiment. The peaking of phosphate is the same phenomenon of chromatographic peaking that was observed with experiments in the synthetic feed (see Section 4.2.1, pg. 70-71).

At 6 m/hr flow rate, the nitrate concentration continually increased after 7 hr of experimentation (Figure 4-53(b)). This signifies that, with a higher flow rate of 6 m/hr, the column media reaches a breakthrough faster than with 2 m/hr. At 6 m/hr, complete breakthrough (C/Co > 1) was observed at 72 hr for nitrate and at 27 hr for phosphate. Whereas, at the low flow rate of 2 m/hr, there was no complete breakthrough for nitrate up to 75 hr but breakthrough of phosphate occurred at 35 hr. In both flow rates, a breakthrough of phosphate was observed (C/Co > 1). These results show that at low flow rate, the removal efficiency of nitrate and phosphate is higher. This is due to longer contact between the adsorbate and adsorbent at lower flow rate as suggested by Han et al. (2006).

4.7.2. Purolite and HFO column in series

By having Purolite and HFO in series, it was investigated if the removal of nitrate and phosphate can be improved further. In this experiment, effluent from a MBR experiment was collected and then subjected to ion exchange column as post treatment to remove nutrients (nitrate and phosphate). The details of the MBR effluent are given in Section 3.2.7 (pg. 37-39).

This experiment was run at 1 m/hr flow rate using columns, one packed with 2.5% or 5% percentage by mass of Purolite and 97.5% or 95% anthracite, respectively, and the second one also packed with the same percentage by mass of HFO and anthracite. A lower flow rate than the earlier experiment was used to maintain a stable column mixture of Purolite and anthracite during the experimental run, and also because earlier experiments (Section 4.7.1) showed that at low flow rate, the nutrient removal efficiency is better.

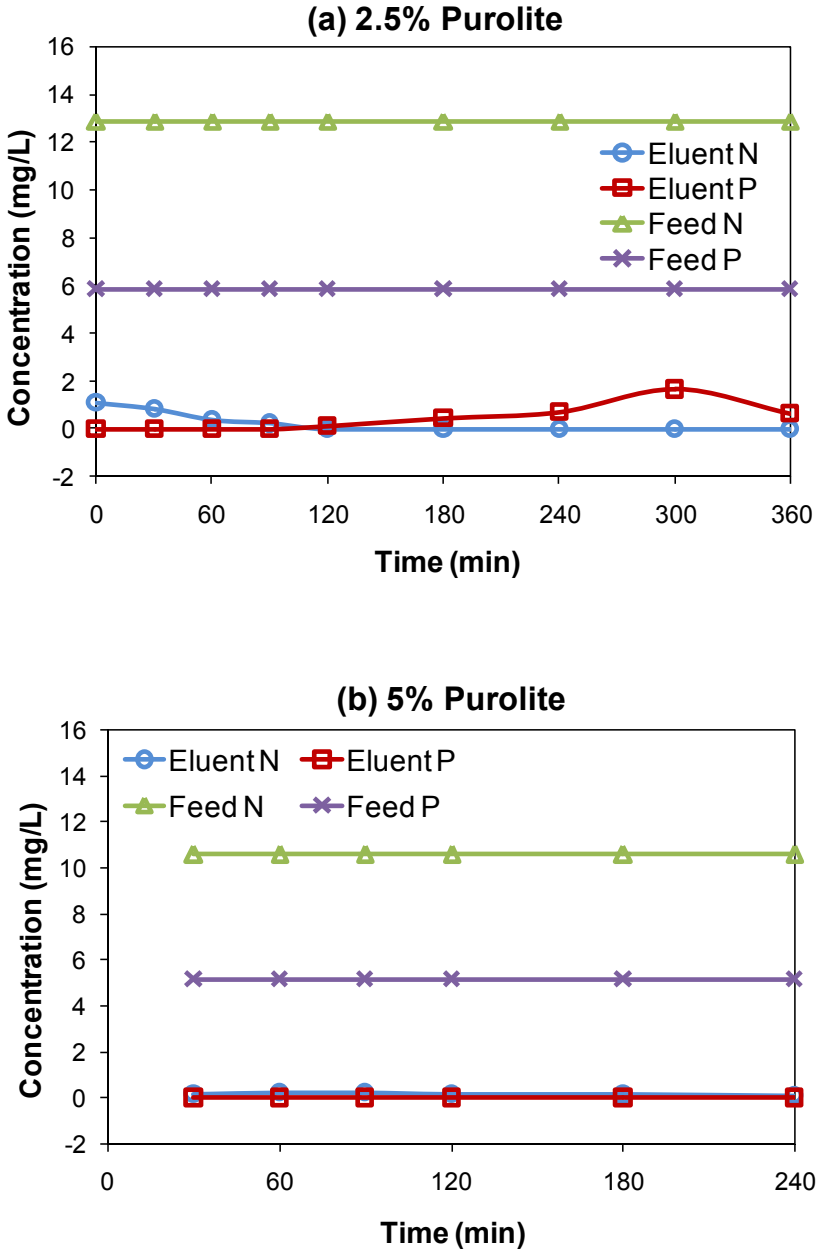

Figure 4-54: Removal of nitrate and phosphate in MBR effluent by (a) 2.5% and (b) 5% Purolite

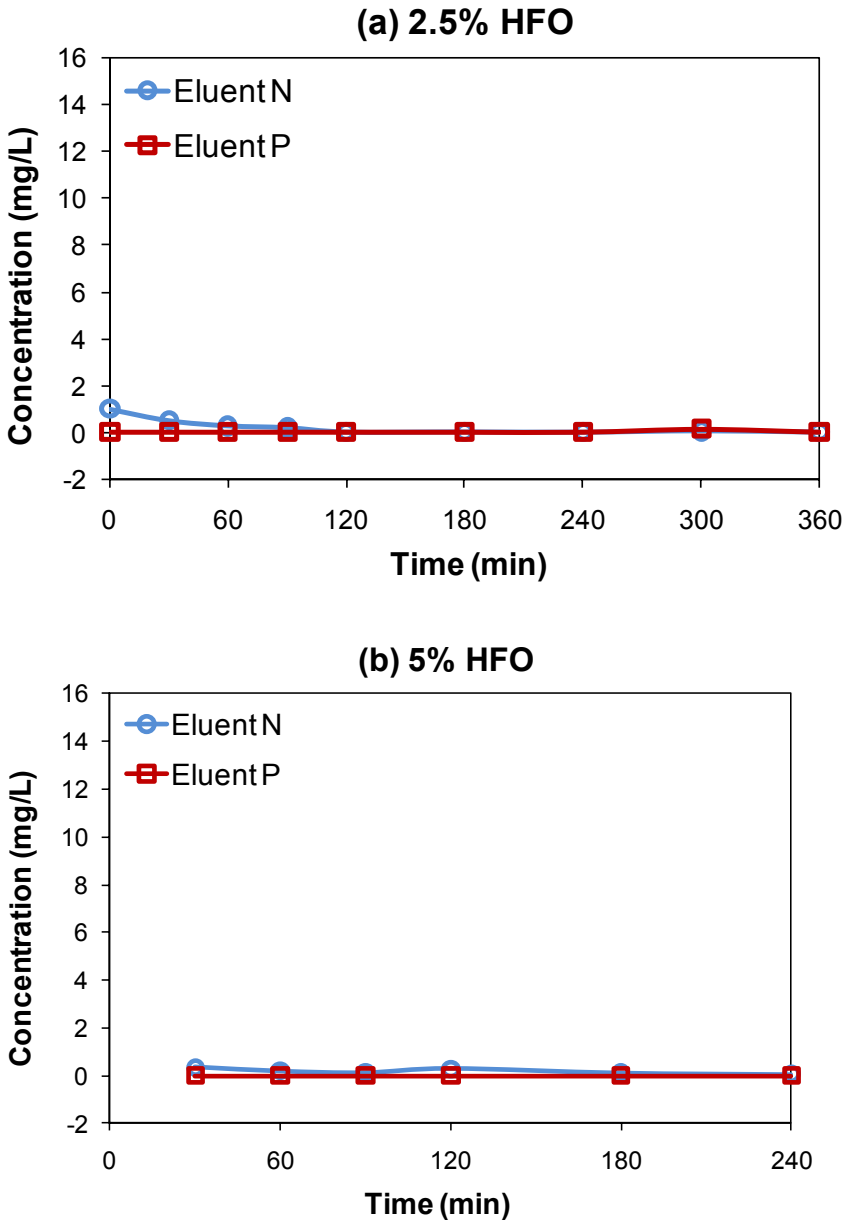

Figure 4-55: Removal of nitrate and phosphate in MBR effluent by (a) 2.5% and (b) 5% HFO

The respective concentration of nitrate and phosphate in the feed were constant throughout the experiment, similar to the synthetic feed experiment in Section 4.5 (pg. 82). However, the feed consisted of a lower concentration of nitrate and phosphate as compared to the synthetic feed (50 mg N/L and 15 mg P/L). Therefore, as seen in Figure 4-54, the adsorption trend for Purolite is quite different as compared to the experiments ran previously with the synthetic feed. For 2.5% Purolite in Figure 4-54(a), phosphate was completely removed throughout the experiment until about 90 min when there was

a sudden increase of phosphate in the sampling reaching a peak of about 1.7 mg P/L (at 300 min). Very minute concentrations of nitrate were present in the sampling at the beginning of the experiment, starting at 1.1 mg N/L and then nitrate was almost completely removed throughout the rest of the experiment.

Phosphate was completely removed throughout the 5% Purolite experiment (Figure 4-54b). Very minute concentration of nitrate (less than 0.1 mg N/L) was present in the sampling at the end of the experiment.

As seen in Figure 4-55, the adsorption trend for HFO is quite different as compared to the experiments ran previously with the synthetic feed (50 mg N/L and 15 mg P/L). After passing through the 2.5% Purolite column, there was still phosphate present in the influent to the 2.5% HFO column. Phosphate was then completely removed by the 2.5% HFO column (Figure 4-55a). Very minute concentrations of nitrate (1.0 mg N/L) were present in the effluent at the beginning of the experiment and then nitrate was successfully removed throughout the rest of the experiment.

Phosphate was also completely removed throughout the 5% HFO experiment (Figure 4-55b). Very minute concentrations of nitrate (less than 0.1 mg N/L) were present in the effluent at the end of the experiment.

Furthermore, both N and P in the MBR effluent were found in different forms (as NH_4 – N, organic N, inorganic and organic phosphorus). Other competing anions like Cl^- and SO_4^{2-} were also present in the feed. Despite the competing anions, the system still had a removal efficiency of 87-100%.

These experiments dealt with minute concentrations of nitrate and phosphate in the feed as well as in the sampling. The concentrations of nitrate and phosphate present in the eluent at the end of the experimental run at 240 min in both 2.5% and 5% Purolite and HFO columns were very low (below 0.1 mg N/L and 0.1 mg P/L) and thus it can be concluded that the Purolite and HFO in series were successful in removing both nitrate and phosphate up to 240 min (6.67 BV) and 2.5% Purolite and HFO was sufficient. However, for longer time of removal, higher percentage of Purolite and HFO is required.

5. Conclusions

From the batch equilibrium and kinetics adsorption study, it was concluded that Purolite exhibits a higher capacity for the removal of nitrate than for phosphate. As the dose of Purolite increased from 0.5 to 10 g/L, there was a significant increase in removal efficiency of both nitrate and phosphate. This is expected as a higher dose of Purolite increases the number of adsorptions sites. The study showed that as the Purolite dose increased the equilibrium concentration of nitrate and phosphate decreased confirming that at higher doses of the media, there was better removal efficiency. The results showed that at every dose of Purolite used, the nitrate removal efficiency is higher than the phosphate removal efficiency. The removal efficiency difference became narrow as the dose of Purolite increased because there were more sites for adsorption at high doses and this decreased the competition for adsorption.

Batch equilibrium and kinetics adsorption study showed that HAIX is phosphate selective unlike Purolite which was nitrate selective. As the dose of HAIX increased, the removal efficiency of nitrate and phosphate significantly increased as observed for Purolite. The results showed that at every dose of HAIX used, the phosphate removal efficiency is higher than the nitrate removal efficiency. At 10, 15 and 20 g/L, the phosphate removal efficiency at equilibrium was 100%, signifying that HAIX is phosphate selective.

Batch equilibrium and kinetics adsorption study indicated that HFO is phosphate selective. As the dose of HFO increased from 0.5 to 10 g/L, there was a significant increase in removal efficiency of phosphate. Nitrate did not adsorb on HFO because nitrate is non-specifically adsorbed on the positive charges on HFO and at the neutral pH of the feed, HFO has very small number of positive charges since HFO has a zero point of charge of around 7. In contrast to nitrate, phosphate is specifically adsorbed on both positive and neutral charged sites and therefore regardless of pH, it is adsorbed in large quantities.

The Langmuir, Freundlich and Sips isotherm models were used to model the equilibrium isotherm of nitrate and phosphate removal by Purolite (A500PS), HAIX and HFO. The results show that the experimental data satisfactorily fitted to all three models. The kinetic data for the adsorption of both nitrate and phosphate were

satisfactorily described by the Ho model. The fit for phosphate on HFO was less satisfactory than the other adsorbents.

In column adsorption study with Purolite only, among the different doses studied, 10% by mass of Purolite has shown to possess the highest efficiency in the removal of nitrate as compared to the other experiments using 1%, 3%, and 5%. In the 3% Purolite experiment, the nitrate breakthrough occurred at 120 min in contrast to the phosphate breakthrough at 30 min into the run. There was a chromatographic peaking of phosphate towards the end of the experiment after 240 min into the run. At 240 min, the phosphate concentration in the effluent reached higher than the influent concentration found in the synthetic feed. When the phosphate ions reached the complete breakthrough point (effluent concentration equals influent concentration), the Purolite dumps the phosphate ions displaced by the nitrate ions, causing a chromatographic peaking of phosphate. This is due to the higher affinity of nitrate than phosphate of this nitrate selective ion exchange resin.

In column adsorption study, it was found that HAIX exhibits a higher affinity for the removal of phosphate than for nitrate. In a study with higher concentrated feed (100 mg N/L and 50 mg P/L), phosphate was completely removed for up to 180 min. Nitrate was only removed up to 60 min and after 420 min, the nitrate concentration in the effluent was higher than the influent indicating a chromatographic peaking of nitrate.

The experiments conducted with Purolite only showed that Purolite can successfully be used to remove nitrate but not phosphate. Therefore an HFO column was added to the Purolite column to remove phosphate. HFO has a high affinity for the removal of phosphate than nitrate. This is because phosphate is specifically adsorbed to HFO in the positively charged sites and neutral sites whereas nitrate is non-specifically adsorbed only on positively charged sites. This was confirmed in the experiments with HAIX, which consisted of HFO and ion exchange resin. In these experiments, HAIX was shown to have selectivity for phosphate over nitrate.

1%, 3% and 5% HFO were all very efficient in removing phosphate for over 360 min. For 10% HFO, phosphate was successfully removed from the influent for over 960 min. Under these experimental conditions using a synthetic feed of 15 mg P/L, 1% HFO

is sufficient for removal of phosphate at least for 360 min.

Hydrated ferric oxide exhibits a higher capacity for the removal of phosphate than for nitrate. Among the different doses studied, 10% by mass of hydrated ferric oxide has shown to possess the highest efficiency in the removal of phosphate as compared to the other experiments using 1%, 3%, and 5%. For about 10 hr, it has successfully removed both nitrate and phosphate.

Regeneration tests with distilled water were carried out on both Purolite and HFO in series. Tests with 10% of each media were undertaken. The data showed that the distilled water wash was not sufficient in regenerating the exhausted Purolite and HFO. The wash may have only removed the synthetic feed trapped in the column but did not desorb the ions that had been adsorbed by the media in the preceding run. This is expected because the distilled water that was used for the wash had no anions to exchange with the nitrate and phosphate adsorbed in the column media.

3% NaCl wash was also investigated for the regeneration of used Purolite and HAIX. It can be concluded that the NaCl wash has regenerated 21-69% of the used Purolite. The NaCl wash was able to desorb the nitrate and phosphate by ion exchange with the chloride ions in NaCl. It can be concluded that the NaCl wash has fully regenerated the used HAIX after the first run for nitrate. However, the extent of regeneration for phosphate was low. This is probably because the chloride anion in the NaCl wash was able to exchange completely with the weakly adsorbed nitrate but not with the strongly adsorbed phosphate.

A column experiment was also conducted with MBR effluent to investigate the possibility of removing the nitrate and phosphate for obtaining a high quality water for reuse. Purolite only was used in column adsorption studies to determine whether it is a viable media for nitrate and phosphate removal from MBR effluent. The results showed that nitrate was successfully removed throughout the experiment (3 cm bed height and 2 m/hr flow rate) with the final sample having only 1 mg N/L, which is approximately 30% of the feed nitrate-N concentration. Phosphate was successfully removed throughout the experiment as well and only minute concentrations were found in the last sampling (0.24 mg P/L).

The experiment was repeated with a 6 cm bed height (24 g) of Purolite and at 2

flow rates (2 m/hr and 6 m/hr) for a period of 72 hr to determine the effect of increased bed height and flow rate on nitrate and phosphate removal. The results signify that, with a higher flow rate of 6 m/hr, the column media reaches a breakthrough faster than with 2 m/hr. At 6 m/hr, complete breakthrough (C/Co > 1) was observed at 72 hr for nitrate and at 27 hr for phosphate. Whereas, at the low flow rate of 2 m/hr, there was no complete breakthrough for nitrate up to 75 hr but breakthrough of phosphate occurred at 35 hr. These results show that at low flow rate, the removal efficiency of nitrate and phosphate is higher. This is due to longer contact between the adsorbate and adsorbent at lower flow rate.

By having Purolite and HFO in series, it was investigated if the removal of nitrate and phosphate from MBR effluent can be improved further. This experiment was run at 1 m/hr flow rate using columns, one packed with 2.5% and 5% percentage by mass of Purolite and anthracite and the second one also packed with the same percentage by mass of HFO and anthracite. A lower flow rate than the earlier experiment was used to maintain a stable column mixture of Purolite and anthracite during the experimental run, and also because earlier experiment showed that at low flow rate, the nutrient removal efficiency is better. Both N and P in the MBR effluent were found in different forms (as NH_4 – N, organic N, inorganic and organic phosphorus). Other competing anions like Cl^- and SO_4^{2-} were also present in the feed. Despite the competing anions, the system still had a removal efficiency of 87-100%.

6. Bibliography

Ayoub, G.M., Koopman, B. & Pandya, N. 2001, 'Iron and aluminum hydroxy (oxide) coated filter media for low-concentration phosphorus removal', *Water Environment Research,* vol. 73, no. 4, pp. 478.

Ayyasamy, P.M., Shanthi, K., Lakshmanaperumalsamy, P., Lee, S., Choi, N. & Kim, D. 2007, 'Two-stage removal of nitrate from groundwater using biological and chemical treatments', *Journal of Bioscience and Bioengineering,* vol. 104, no. 2, pp. 129-34.

Azizian, S. 2004, 'Kinetic models of sorption: a theoretical analysis', *Journal of colloid and interface science,* vol. 276, no. 1, pp. 47-52.

Bae, B., Jung, Y., Han, W. & Shin, H. 2002, 'Improved brine recycling during nitrate removal using ion exchange', *Water research,* vol. 36, no. 13, pp. 3330-40.

Bajracharya, K. & Barry, D.A. 1995, 'Analysis of one-dimensional multispecies transport experiments in laboratory soil columns', *Environment international,* vol. 21, no. 5, pp. 687-91.

Barry, D.A., Starr, J.L., Parlange, J.Y. & Braddock, R.D. 1983, 'Numerical analysis of the snow-plow effect', *Soil Science Society of America Journal,* vol. 47, no. 5, pp. 862-8.

Baykal, B.B. & Guven, D.A. 1997, 'Performance of clinoptilolite alone and in combination with sand filters for the removal of ammonia peaks from domestic wastewater', *Water Science and Technology,* vol. 35, no. 7, pp. 47-54.

Beler-Baykal, B., Oldenburg, M. & Sekoulov, I. 1996, 'The use of ion exchange in ammonia removal under constant and variable loads', *Environmental technology,* vol. 17, no. 7, pp. 717-26.

Blaney, L.M., Cinar, S. & SenGupta, A.K. 2007, 'Hybrid anion exchanger for trace phosphate removal from water and wastewater', *Water research,* vol. 41, no. 7, pp. 1603-13.

Bohart, G. & Adams, E.Q. 1920, 'Some aspects of the behaviour of charcoal with respect to chlorine', *Journal of the American Chemical Society,* vol. 42, pp. 523-44.

Cambardella, C.A., Moorman, T.B., Jaynes, D.B., Hatfield, J.L., Parkin, T.B., Simpkins, W.W. & Karlen, D.L. 1999, 'Water quality in Walnut Creek watershed: nitrate–nitrogen in soils, subsurface drainage water, and shallow groundwater', *Journal of Environmental Quality,* vol. 28, no. 1, pp. 25-34.

Carucci, A., Ramadori, R., Rossetti, S. & Tomei, M.C. 1996, 'Kinetics of denitrification reactions in single sludge systems', *Water research,* vol. 30, no. 1, pp. 51-6.

Chabani, M., Amrane, A. & Bensmaili, A. 2009, 'Equilibrium sorption isotherms for nitrate on resin Amberlite IRA 400', *Journal of hazardous materials,* vol. 165, no. 1-3, pp. 27-33.

Chiu, Y. & Chung, M. 2003, 'Determination of optimal COD/nitrate ratio for biological denitrification', *International Biodeterioration & Biodegradation,* vol. 51, no. 1, pp. 43-9.

Clark, T., Stephenson, T. & Pearce, P.A. 1997, 'Phosphorus removal by chemical precipitation in a biological aerated filter', *Water research,* vol. 31, no. 10, pp. 2557-63.

Clifford, D.A. & Liu, X. 1993, 'Ion exchange for nitrate removal', *AWWA,* vol. 85, no. 4, pp. 135-43.

Conley, D.J., Paerl, H.W., Howarth, R.W., Boesch, D.F., Seitzinger, S.P., Havens, K.E., Lancelot, C. & Likens, G.E. 2009, 'ECOLOGY: Controlling Eutrophication: Nitrogen and Phosphorus', *Science,* vol. 323, no. 5917, pp. 1014-5.

Cooney, D.O. 1999, *Adsorption Design for Wastewater Treatment,* Lewis Publishers, Boca Raton, Florida.

Crittenden, J.C., Luft, P., Hand, D.W., Oravitz, J.L., Loper, S.W. & Ari, M. 1985, 'Prediction of multicomponent adsorption equilibria using ideal adsorbed solution theory', *Environmental Science & Technology,* vol. 19, no. 11, pp. 1037-43.

Cumbal, L. & SenGupta, A.K. 2005, 'Arsenic Removal Using Polymer-Supported Hydrated Iron(III) Oxide Nanoparticles: Role of Donnan Membrane Effect', *Environmental Science & Technology,* vol. 39, no. 17, pp. 6508-15.

Davis, J.A. & Leckie, J.O. 1978, 'Surface ionization and complexation at the oxide/water interface II. Surface properties of amorphous iron oxyhydroxide and adsorption of metal ions', *Journal of colloid and interface science,* vol. 67, no. 1, pp. 90-107.

de Vicente, I., Huang, P., Andersen, F. & Jensen, H.S. 2008, 'Phosphate adsorption by fresh and aged aluminum hydroxide: consequences for lake restoration', *Environmental Science and Technology,* vol. 42, no. 17, pp. 6650-5.

Della Rocca, C., Belgiorno, V. & Meriç, S. 2007, 'Overview of in-situ applicable nitrate removal processes', *Desalination,* vol. 204, no. 1-3, pp. 46-62.

Dutta, P.K., Ray, A.K., Sharma, V.K. & Millero, F.J. 2004, 'Adsorption of arsenate and arsenite on titanium dioxide suspensions', *Journal of colloid and interface science,* vol. 278, no. 2, pp. 270-5.

Faust, S.D. & Aly, O.M. 1987, *Adsorption processes for water treatment,* Butterworths, Boston.

Fewtrell, L. 2004, 'Drinking-water nitrate, methemoglobinemia, and global burden of disease: a discussion', *Environmental Health Perspectives,* vol. 112, no. 14, pp. 1371-4.

Fytianos, K., Voudrias, E. & Raikos, N. 1998, 'Modelling of phosphorus removal from aqueous and wastewater samples using ferric iron', *Environmental Pollution,* vol. 101, no. 1, pp. 123-30.

Genz, A., Kornmüller, A. & Jekel, M. 2004, 'Advanced phosphorus removal from membrane filtrates by adsorption on activated aluminium oxide and granulated ferric hydroxide', *Water research,* vol. 38, no. 16, pp. 3523-30.

Gimenez, D. 2006, *Macroporosity* , Encyclopedia of Soil Science, USA, viewed December/04 2010, <http://www.informaworld.com.ezproxy.lib.uts.edu.au/smpp/content~content=a740186660~db=all~jumptype=rss>.

Goh, K., Lim, T. & Dong, Z. 2008, 'Application of layered double hydroxides for removal of oxyanions: A review', *Water research,* vol. 42, no. 6-7, pp. 1343-68.

Greenan, C.M., Moorman, T.B., Kaspar, T.C., Parkin, T.B. & Jaynes, D.B. 2006, 'Comparing carbon substrates for denitrification of subsurface drainage water ', *Journal of Environmental Quality,* vol. 35, no. 3, pp. 824-9.

Gu, B., Brown, G.M., Bonnesen, P.V., Liang, L., Moyer, B.A., Ober, R. & Alexandratos, S.D. 2000, 'Development of Novel Bifunctional Anion-Exchange Resins with Improved Selectivity for Pertechnetate Sorption from Contaminated Groundwater', *Environmental Science & Technology,* vol. 34, no. 6, pp. 1075-80.

Gu, B., Ku, Y. & Jardine, P.M. 2004, 'Sorption and Binary Exchange of Nitrate, Sulfate, and Uranium on an Anion-Exchange Resin', *Environmental Science & Technology,* vol. 38, no. 11, pp. 3184-8.

Han, R., Zou, W., Li, H., Li, Y. & Shi, J. 2006, 'Copper(II) and lead(II) removal from aqueous solution in fixed-bed columns by manganese oxide coated zeolite', *Journal of hazardous materials,* vol. 137, no. 2, pp. 934-42.

Hascoet, M.C. & Florentz, M. 1985, 'Influence of nitrates on biological phosphorus removal of wastewater', *Water SA,* vol. 11, pp. 1-8.

Healy, M.G., Rodgers, M. & Mulqueen, J. 2006, 'Denitrification of a nitrate-rich synthetic wastewater using various wood-based media materials', *Journal of Environmental Science and Health,* vol. 41, no. 5, pp. 779-88.

Ho, Y.S., Wase, D.A.J. & Forster, C.F. 1996, 'Kinetic Studies of Competitive Heavy Metal Adsorption by Sphagnum Moss Peat
', *Environmental Technology,* vol. 17, no. 1, pp. 71-77.

Hutchins, R.A. 1973, 'New method simplifies design of activated carbon system', *Chem. Eng.,* vol. 80, no. 19, pp. 133-8.

Jorgensen, T.C. & Weatherley, L.R. 2003, 'Ammonia removal from wastewater by ion exchange in the presence of organic contaminants', *Water research,* vol. 37, no. 8, pp. 1723-8.

Jung, Y., Koh, H., Shin, W. & Sung, N. 2006, 'A novel approach to an advanced tertiary wastewater treatment: Combination of a membrane bioreactor and an oyster-zeolite column', *Desalination,* vol. 190, no. 1-3, pp. 243-55.

Killingstad, M.W., Widdowson, M.A. & Smith, R.L. 2002, 'Modeling Enhanced In Situ Denitrification in Groundwater', *Journal of Environmental Engineering,* vol. 128, no. 6, pp. 491-504.

Kim, Y., Nakano, K., Lee, T., Kanchanatawee, S. & Matsumura, M. 2002, 'On-site nitrate removal of groundwater by an immobilized psychrophilic denitrifier using soluble starch as a carbon source', *Journal of Bioscience and Bioengineering,* vol. 93, no. 3, pp. 303-8.

Kumar, K.V. & Sivanesan, S. 2006, 'Pseudo second order kinetic models for safranin onto rice husk: Comparison of linear and non-linear regression analysis', *Process Biochemistry,* vol. 41, no. 5, pp. 1198-202.

Lee, S.H., Lee, B.C., Lee, S.H., Choi, Y.S., Park, K.Y. & Iwamoto, M. 2007, 'Phosphorus recovery by mesoporous structure materials from wastewater', *Water Science and Technology,* vol. 55, no. 1-2, pp. 169-76.

Liang, S., Mann, M.A., Guter, G.A., Kim, O. & Hardan, D.L. 1999, 'Nitrate removal from contaminated ground water', *AWWA,* vol. 91, no. 2, pp. 79-91.

Lohumi, N., Gosain, S., Jain, A., Gupta, V.K. & Verma, K.K. 2004, 'Determination of nitrate in environmental water samples by conversion into nitrophenols and solid phase extraction−spectrophotometry, liquid chromatography or gas chromatography–mass spectrometry', *Analytica Chimica Acta,* vol. 505, no. 2, pp. 231-7.

Lv, L., Sun, P., Wang, Y., Du, H. & Gu, T. 2008, 'Phosphate removal and recovery with calcined layered double hydroxides as an adsorbent', *Phosphorus, Sulfur, and Silicon and the Related Elements,* vol. 183, no. 2-3, pp. 519-26.

Marais, G.v.R., Loewenthal, R.E. & Siebritz, I.P. 1983, 'Review: observations supporting phosphate removal by biological excess uptake.', *Water Science Technology,* vol. 15, pp. 15-41.

Martin, B.D., Parsons, S.A. & Jefferson, B. 2009, 'Removal and recovery of phosphate from municipal wastewaters using a polymeric anion exchanger bound with hydrated ferric oxide nanoparticles', *Water Science and Technology,* vol. 60, no. 10, pp. 2637-45.

Matsui, Y., Yuasa, A. & Li, F. 1998, 'Overall Adsorption Isotherm of Natural Organic Matter', *Journal of Environmental Engineering,* vol. 124, no. 11, pp. 1099-107.

Menasveta, P., Panritdam, T., Sihanonth, P., Powtongsook, S., Chuntapa, B. & Lee, P. 2001, 'Design and function of a closed, recirculating seawater system with denitrification for the culture of black tiger shrimp broodstock', *Aquacultural Engineering,* vol. 25, no. 1, pp. 35-49.

Morse, G.K., Brett, S.W., Guy, J.A. & Lester, J.N. 1998, 'Review: Phosphorus removal and recovery technologies', *The Science of the total environment,* vol. 212, no. 1, pp. 69-81.

National Health and Medical Research Council, Australian Government 2009, *Australian Drinking Water Guidelines (ADWG),* Australian Government, Australia, viewed December/04 2010, <http://www.nhmrc.gov.au/publications/synopses/eh19syn.htm#comp>.

Oehmen, A., Lemos, P.C., Carvalho, G., Yuan, Z., Keller, J., Blackall, L.L. & Reis, M.A.M. 2007, 'Advances in enhanced biological phosphorus removal: From micro to macro scale', *Water research,* vol. 41, no. 11, pp. 2271-300.

Onyango, M.S., Kuchar, D., Kubota, M. & Matsuda, H. 2007, 'Adsorptive removal of phosphate ions from aqueous solution using synthetic zeolite', *Industrial and Engineering Chemistry Research,* vol. 46, no. 3, pp. 894-900.

OzCoasts 2010, *Coastal Eutrophication,* Australian Online Coastal Information, Australia, viewed December/05 2010, <http://www.ozcoasts.org.au/indicators/coastal_eutrophication.jsp>.

Pan, B., Wu, J., Pan, B., Lv, L., Zhang, W., Xiao, L., Wang, X., Tao, X. & Zheng, S. 2009, 'Development of polymer-based nanosized hydrated ferric oxides (HFOs) for enhanced phosphate removal from waste effluents', *Water research,* vol. 43, no. 17, pp. 4421-9.

Park, J.B.K., Craggs, R.J. & Sukias, J.P.S. 2008, 'Treatment of hydroponic wastewater by denitrification filters using plant prunings as the organic carbon source', *Bioresource technology,* vol. 99, no. 8, pp. 2711-6.

Pradhan, J., Das, J., Das, S. & Thakur, R.S. 1998, 'Adsorption of Phosphate from Aqueous Solution Using Activated Red Mud', *Journal of colloid and interface science,* vol. 204, no. 1, pp. 169-72.

Prosnansky, M., Sakakibara, Y. & Kuroda, M. 2002, 'High-rate denitrification and SS rejection by biofilm-electrode reactor (BER) combined with microfiltration', *Water research,* vol. 36, no. 19, pp. 4801-10.

Purolite 2010a, *A-500PS Technical Data,* The Purolite Company, USA, viewed December/07 2010, <http://www.purolite.com/Customized/CustomizedControls/Products/PDSFiles/ProductInfo_212_512010212935612.pdf>.

Purolite 2010b, *A-520E Technical Data,* The Purolite Company, USA, viewed December/05 2010, <http://www.purolite.com/Customized/CustomizedControls/Products/Resources/rid_55.pdf>.

Sage, M., Daufin, G. & Gésan-Guiziou, G. 2006, 'Denitrification potential and rates of complex carbon source from dairy effluents in activated sludge system', *Water research,* vol. 40, no. 14, pp. 2747-55.

Samatya, S., Kabay, N., Yuksel, U., Arda, M. & Yuksel, M. 2006a, 'Removal of nitrate from aqueous solution by nitrate selective ion exchange resins', *Reactive and Functional Polymers.vol,* vol. 66, no. 11, pp. 1206-14.

Samatya, S., Yuksel, U., Arda, M., Kabay, N. & Yuksel, M. 2006b, 'Investigation of selectivity and kinetic behavior of strong-base ion exchange resin Purolite A 520E for nitrate removal from aqueous solution', *Separation Science and Technology,* vol. 41, no. 13, pp. 2973-88.

Seida, Y. & Nakano, Y. 2002, 'Removal of phosphate by layered double hydroxides containing iron', *Water research,* vol. 36, no. 5, pp. 1306-12.

Sherwood, L.J. & Qualls, R.G. 2001, 'Stability of phosphorus within a wetland soil following ferric chloride treatment to control eutrophication', *Environmental Science and Technology,* vol. 35, no. 20, pp. 4126-31.

Shon, H.K., Vigneswaran, S., Kim, I.S., Cho, J., Kim, G.J., Kim, J.B. & Kim, J.H. 2007, 'Preparation of Titanium Dioxide (TiO_2) from Sludge Produced by Titanium Tetrachloride ($TiCl_4$) Flocculation of Wastewater', *Environmental Science and Technology,* vol. 41, no. 4, pp. 1372-7.

Srivastava, V.C., Prasad, B., Mishra, I.M., Mall, I.D. & Swamy, M.M. 2008, 'Prediction of Breakthrough Curves for Sorptive Removal of Phenol by Bagasse Fly Ash Packed Bed', *Industrial & Engineering Chemistry Research,* vol. 47, no. 5, pp. 1603-13.

Streat, M., Hellgardt, K. & Newton, N.L.R. 2008a, 'Hydrous ferric oxide as an adsorbent in water treatment: Part 1. Preparation and physical characterization', *Process Safety and Environmental Protection,* vol. 86, no. 1, pp. 1-9.

Streat, M., Hellgardt, K. & Newton, N.L.R. 2008b, 'Hydrous ferric oxide as an adsorbent in water treatment: Part 3: Batch and mini-column adsorption of arsenic, phosphorus, fluorine and cadmium ions', *Process Safety and Environmental Protection,* vol. 86, no. 1, pp. 21-30.

Suzuki, T. 1990, *Adsorption engineering,* Kodansha, Tokyo, Japan.

Suzuki, Y., Maruyama, T., Numata, H., Sato, H. & Asakawa, M. 2003, 'Performance of a closed recirculating system with foam separation, nitrification and denitrification units for intensive culture of eel: towards zero emission', *Aquacultural Engineering,* vol. 29, no. 3-4, pp. 165-82.

Sydney Water 2010, *Penrith Wastewater Treatment Plant,* viewed 01/05 2010, <http://210.247.145.33/Education/Tours/virtualtour/fact_sheets/treatment_processes_factsheet_FINAL.pdf>.

Tam, N.F.Y., Leung, G.L.W. & Wong, Y.S. 1994, 'The effect of external carbon loading on nitrogen removal in sequencing batch reactors', *Water Science and Technology,* vol. 30, pp. 73-81.

Tan, T.W. & Ng, H.Y. 2008, 'Influence of mixed liquor recycle ratio and dissolved oxygen on performance of pre-denitrification submerged membrane bioreactors', *Water research,* vol. 42, no. 4-5, pp. 1122-32.

Terry, P.A. 2009, 'Removal of nitrates and phosphates by ion exchange with hydrotalcite', *Environmental Engineering Science,* vol. 26, no. 3, pp. 691-6.

Thomas, H.C. 1944, 'Heterogeneous ion exchange in a flowing system', *Journal of the American Chemical Society,* vol. 66, pp. 1664-6.

Trivedi, P. & Axe, L. 2000, 'Modeling Cd and Zn Sorption to Hydrous Metal Oxides', *Environmental Science & Technology,* vol. 34, no. 11, pp. 2215-23.

Tseng, C., Potter, T.G. & Koopman, B. 1998, 'Effect of influent chemical oxygen demand to nitrogen ration on a partial nitrification/complete denitrification process', *Water research,* vol. 32, no. 1, pp. 165-73.

Van Loosdrecht, M.C.M., Hooijmans, C.M., Brdjanovic, D. & Heijnen, J.J. 1997, 'Biological phosphate removal processes', *Applied Microbiology and Biotechnology,* vol. 48, no. 3, pp. 289-96.

van Rijn, J., Tal, Y. & Schreier, H.J. 2006, 'Denitrification in recirculating systems: Theory and applications', *Aquacultural Engineering,* vol. 34, no. 3, pp. 364-76.

Wang, Y., Kmiya, Y. & Okuhara, T. 2007, 'Removal of low-concentration ammonia in water by ion-exchange using Na-mordenite', *Water research,* vol. 41, no. 2, pp. 269-76.

Wang, Y., Han, T., Xu, Z., Bao, G. & Zhu, T. 2005, 'Optimization of phosphorus removal from secondary effluent using simplex method in Tianjin, China', *Journal of hazardous materials,* vol. 121, no. 1-3, pp. 183-6.

Water Quality Products April 2003, *Nitrate Removal by Ion Exchange,* Scranton Gillette Communications, USA, viewed December/04 2010, <http://www.wwdmag.com/Nitrate-Removal-by-Ion-Exchange-article3906>.

Weber, W.J. 1972, 'Physicochemical processes for water quality control', *Adsorption,* In: Weber W.J. edn, Wiley, New York, pp. 199-259.

Yamaguchi, T., Harada, H., Hisano, T., Yamazaki, S. & Tseng, I. 1999, 'Process behavior of UASB reactor treating a wastewater containing high strength sulfate', *Water research,* vol. 33, no. 14, pp. 3182-90.

Yoon, Y.H. & Nelson, J.H. 1984, 'Application of gas adsorption kinetics I, A theoretical model for respirator cartridge service time', *American Industrial Hygiene Association Journal,* vol. 45, pp. 509-16.

Zeng, L., Li, X. & Liu, J. 2004, 'Adsorptive removal of phosphate from aqueous solutions using iron oxide tailings', *Water research,* vol. 38, no. 5, pp. 1318-26.

Zhao, D. & Sengupta, A.K. 1998, 'Ultimate removal of phosphate from wastewater using a new class of polymeric ion exchangers', *Water research,* vol. 32, no. 5, pp. 1613-25.

7. Appendices

7.1. 10% Purolite and HFO Columns in Series Data

The following figures show the data obtained on the lengthy experimental run using 10% Purolite and 10% HFO with anthracite in series to remove nitrate and phosphate from synthetic water (50 mg N/L and 15 mg P/L). The feed passed through the Purolite column first, then through the HFO column. The data has been plotted as the ratio of effluent concentration to influent concentration against bed volume to show a realistic assessment of the breakthrough curve for both columns.

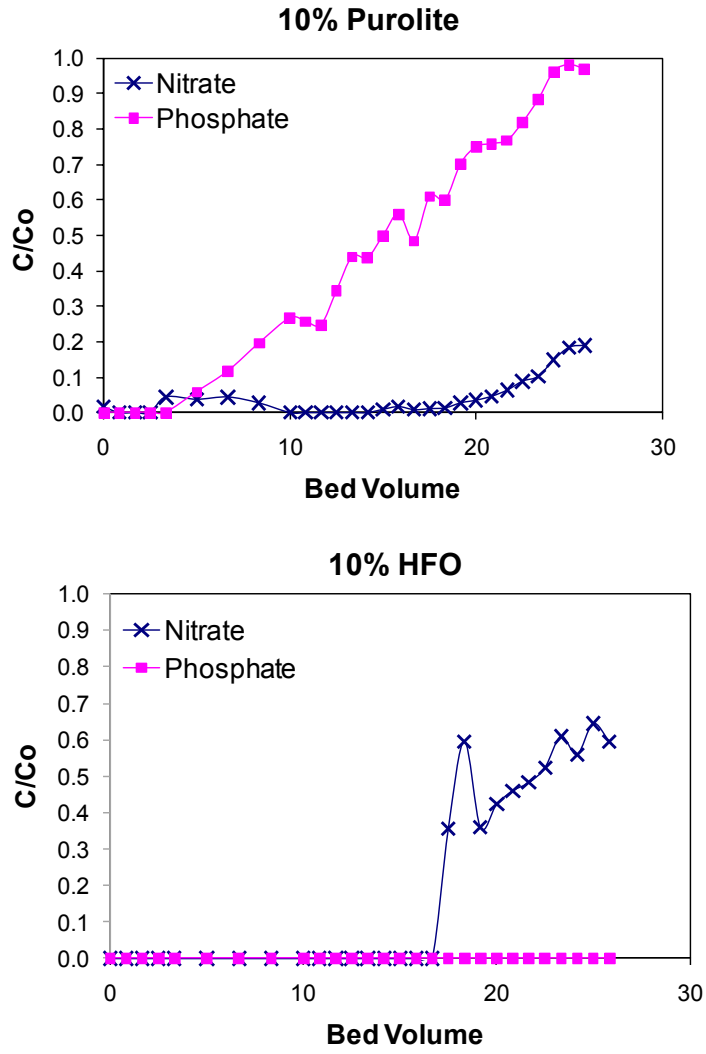

Figure 7-1: Breakthrough curve of 10% Purolite and % HFO (used in series)

7.2. Extended Modelling Results

Srivastava et al (2008) (Srivastava et al. 2008) have discussed the theory associated with several empirical models that have been used for the prediction of breakthrough time in fixed bed adsorption. The Bohart-Adams model (BDST) is used for the description of the initial part of the breakthrough curve in the fixed bed, Bohart et al. (1920) (Bohart & Adams 1920).

$$\ln\left(\frac{C_o}{C}-1\right)=\ln\left[\exp\left(kN_o\frac{L}{U}\right)-1\right]-kC_o t \qquad (1)$$

where, k is adsorption rate constant for a fixed bed (l/min mg), N_0 is the adsorptive capacity of adsorbent (mg/l), L is the height of the column bed (cm), and U is the linear flow velocity of the feed to the bed (m/min). Hutchins (1973) (Hutchins 1973) linearized this equation to give bed depth service time (BDST).

$$t=\frac{N_o}{C_o U_o}L-\frac{1}{kC_o}\ln\left(\frac{C_o}{C}-1\right) \qquad (2)$$

Thomas model assumes plug flow behavior in the bed, and uses the Langmuir isotherm for equilibrium, and second-order reversible reaction kinetics. This model is suitable for adsorption processes where the external and internal diffusion limitations are absent, Thomas (1944) (Thomas 1944).

$$\ln\left(\frac{C_o}{C}-1\right)=\frac{k_T q_o m_c}{Q}-k_T C_o t \qquad (3)$$

where k_T is the Thomas rate constant (l/min mg), q_0 is the maximum solid-phase concentration of the solute (mg/g), m_C is the mass of adsorbent in the column (g) and Q is the volumetric flow rate (l/min).

Yoon and Nelson (1984) (Yoon & Nelson 1984) developed a model based on the assumption that the rate of decrease in the probability of adsorption of adsorbate molecule is proportional to the probability of the adsorbate adsorption and the adsorbate

breakthrough on the adsorbent.

$$\ln\left(\frac{C_o}{C}-1\right)=k_{YN}t-t_{0.5}k_{YN} \tag{4}$$

where k_{YN} is the Yoon–Nelson rate constant (min^{-1}).

7.2.1. 1% Purolite and HFO in series Modelling Experimental Data

The following graphs illustrate the modelling data for 1% Purolite and 1% HFO in series with anthracite experiment.

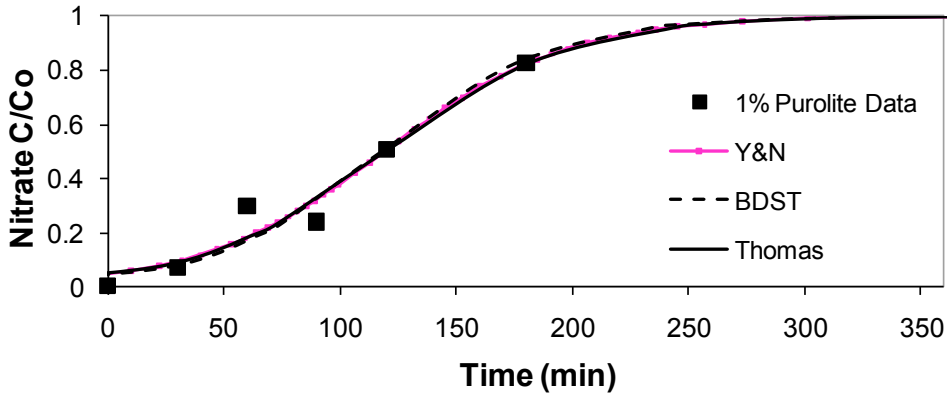

Figure 7-2: Modelling plot for nitrate removal by 1% Purolite (A500PS)

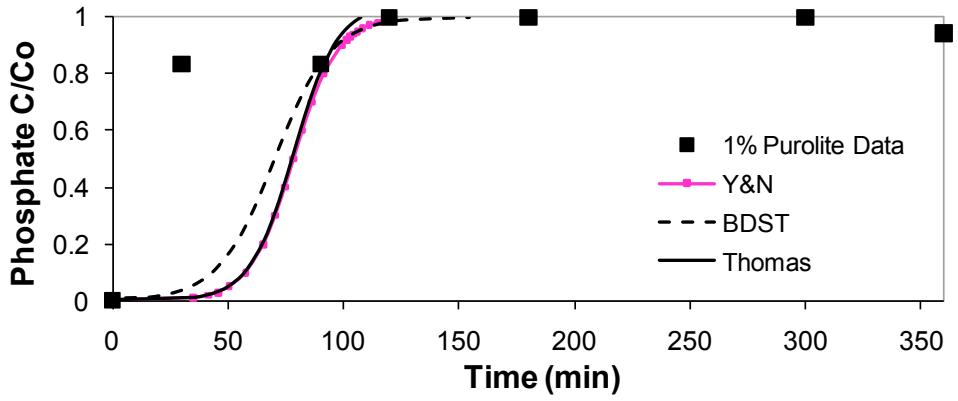

Figure 7-3: Modelling plot for phosphate removal by 1% Purolite (A500PS)

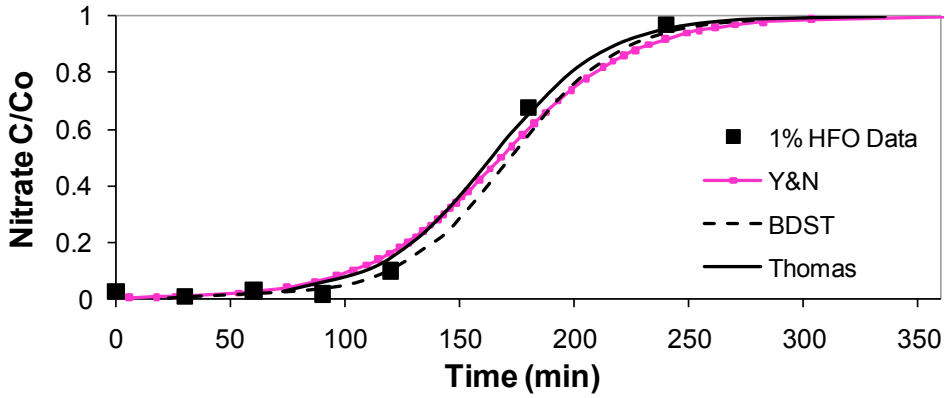

Figure 7-4: Modelling plot for nitrate removal by 1% HFO

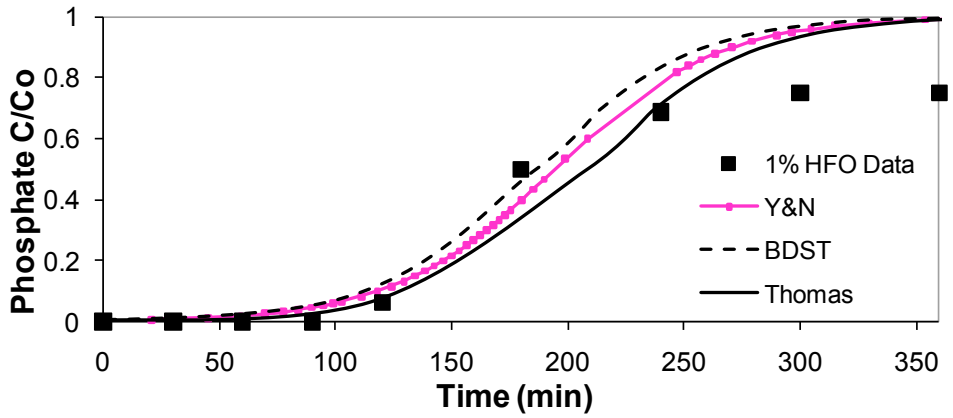

Figure 7-5: Modelling plot for phosphate removal by 1% HFO

Table 7-1: Estimated parameters for semi-empirical models for the fixed bed adsorption of nitrate and phosphate by 1% Purolite (A500PS) and HFO

	Media	Nitrate/ Phosphate	Co	k	$t_{0.5}$
Y&N	HFO	N	50	3.40E-02	1.68E+02
	HFO	P	15	2.88E-02	1.94E+02
	PUR	N	50	2.52E-02	1.19E+02
	PUR	P	15	1.06E-01	7.83E+01
BDST	HFO	N	50	8.33E-04	
	HFO	P	15	2.00E-03	
	PUR	N	50	5.42E-04	
	PUR	P	15	4.85E-03	
Thomas	HFO	N	50	1.34E-03	
	HFO	P	15	1.92E-03	
	PUR	N	50	8.40E-04	
	PUR	P	15	7.07E-03	

7.2.2. 3% Purolite and HFO in series Modelling Experimental Data

The following graphs illustrate the modelling data for 3% Purolite and 3% HFO in series with anthracite experiment.

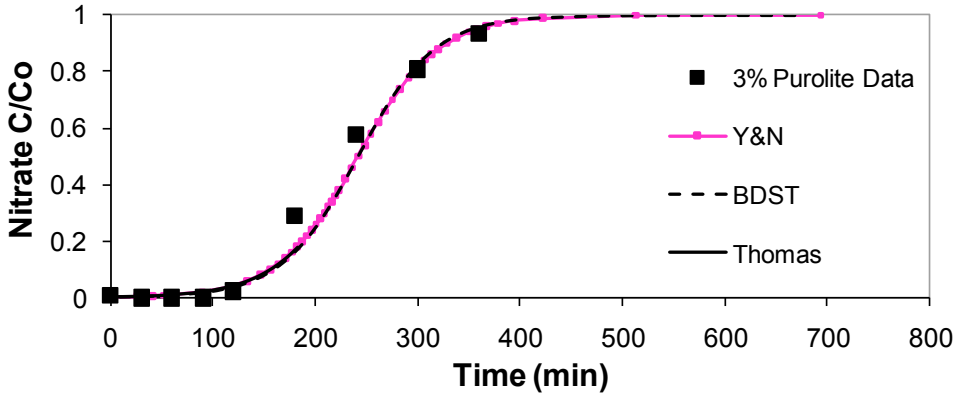

Figure 7-6: Modelling plot for nitrate removal by 3% Purolite (A500PS)

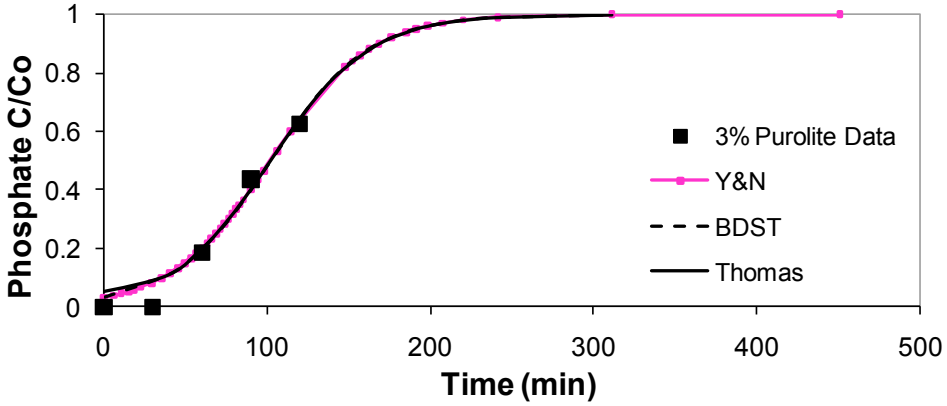

Figure 7-7: Modelling plot for phosphate removal by 3% Purolite (A500PS)

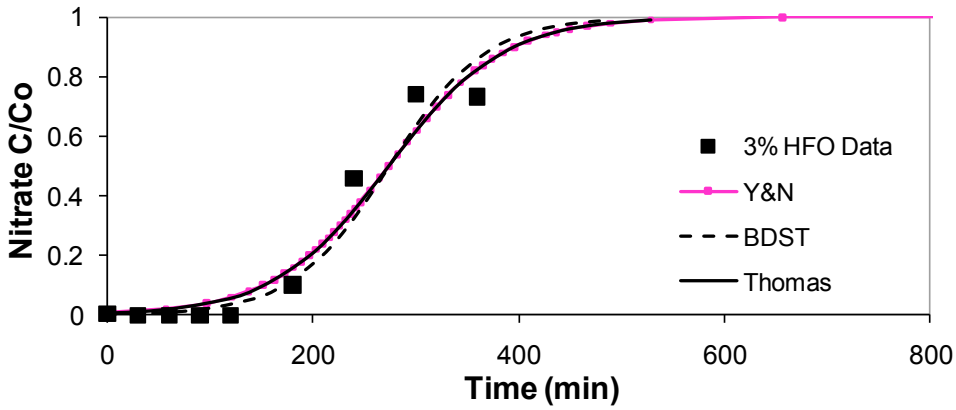

Figure 7-8: Modelling plot for nitrate removal by 3% HFO

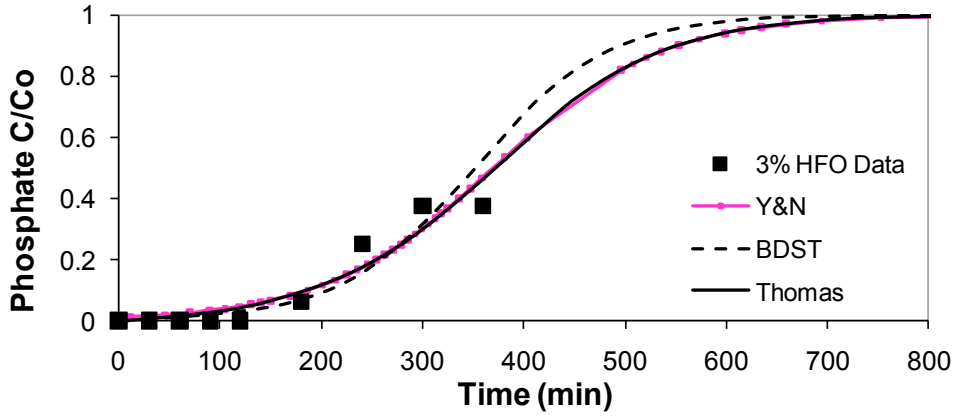

Figure 7-9: Modelling plot for phosphate removal by 3% HFO

Table 7-2: Estimated parameters for semi-empirical models for the fixed bed adsorption of nitrate and phosphate by 3% Purolite (A500PS) and HFO

	Media	Nitrate/ Phosphate	Co	k	$t_{0.5}$
Y&N	HFO	N	50	1.80E-02	2.73E+02
	HFO	P	15	1.20E-02	3.70E+02
	PUR	N	50	2.55E-02	2.42E+02
	PUR	P	15	3.30E-02	1.02E+02
BDST	HFO	N	50	4.25E-04	
	HFO	P	15	1.00E-03	
	PUR	N	50	5.35E-04	
	PUR	P	15	2.24E-03	
Thomas	HFO	N	50	6.00E-04	
	HFO	P	15	8.00E-04	
	PUR	N	50	8.50E-04	
	PUR	P	15	2.20E-03	

7.2.3. 5% Purolite and HFO in series Modelling Experimental Data

The following graphs illustrate the modelling data for 5% Purolite and 5% HFO in series with anthracite experiment.

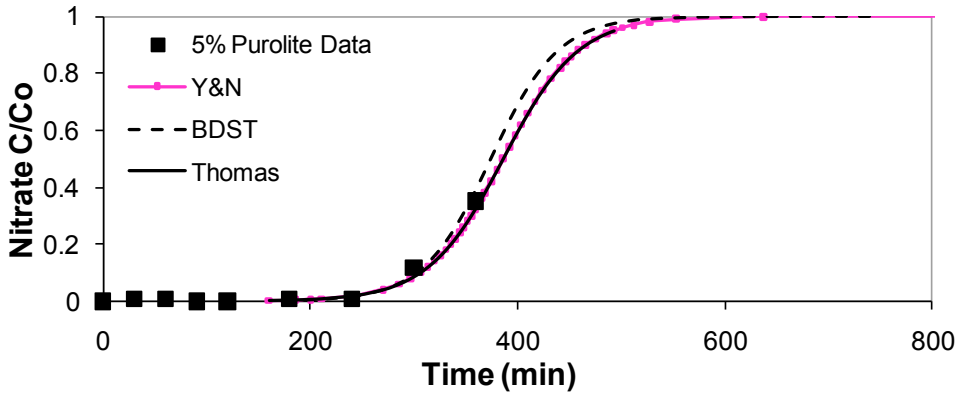

Figure 7-10: Modelling plot for nitrate removal by 5% Purolite (A500PS)

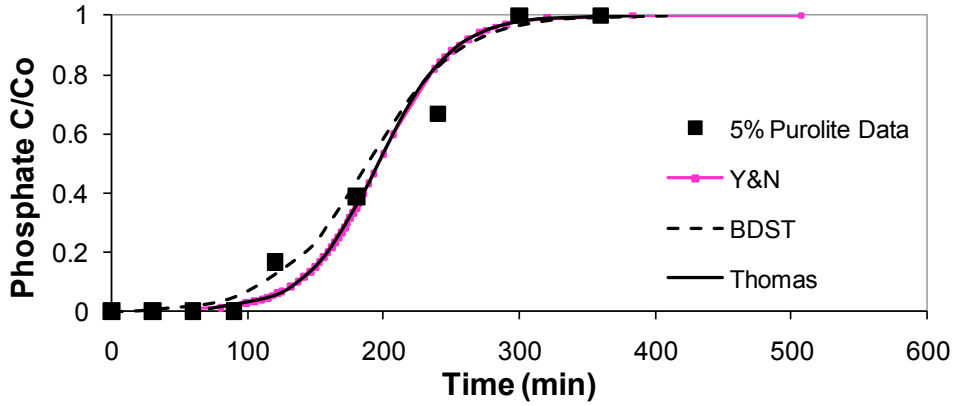

Figure 7-11: Modelling plot for phosphate removal by 5% Purolite (A500PS)

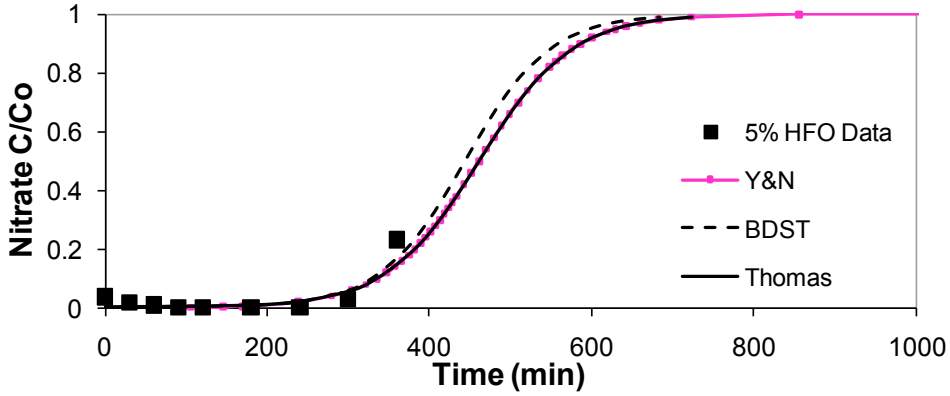

Figure 7-12: Modelling plot for nitrate removal by 5% HFO

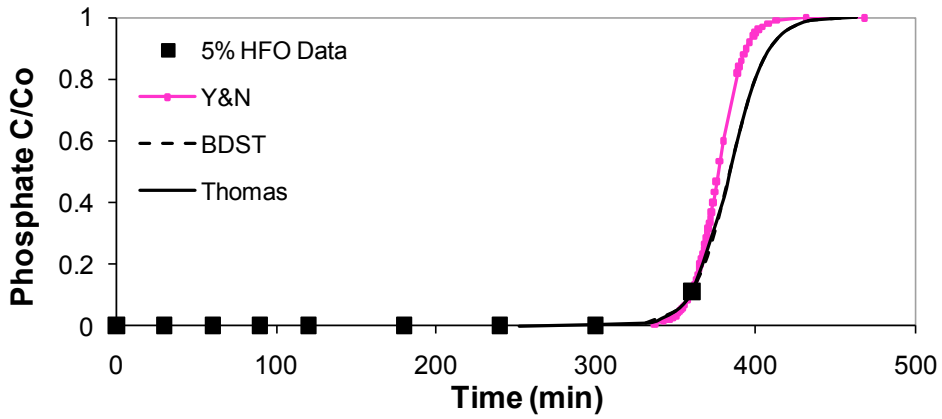

Figure 7-13: Modelling plot for phosphate removal by 5% HFO

Table 7-3: Estimated parameters for semi-empirical models for the fixed bed adsorption of nitrate and phosphate by 5% Purolite (A500PS) and HFO

	Media	Nitrate/ Phosphate	Co	k	$t_{0.5}$
Y&N	HFO	N	50	1.75E-02	4.61E+02
	HFO	P	15	1.26E-01	3.77E+02
	PUR	N	50	2.75E-02	3.86E+02
	PUR	P	15	3.70E-02	1.96E+02
BDST	HFO	N	50	3.83E-04	
	HFO	P	15	5.81E-03	
	PUR	N	50	6.14E-04	
	PUR	P	15	2.00E-03	
Thomas	HFO	N	50	5.83E-04	
	HFO	P	15	5.81E-03	
	PUR	N	50	9.17E-04	
	PUR	P	15	2.47E-03	